Applied Geochemistry

Trace element and Pb and Sr isotope investigation of tooth enamel from archaeological remains at El-Kurru, Sudan: Evaluating the role of groundwater-related diagenetic alteration

--Manuscript Draft--

Manuscript Number:	APGEO-D-21-00121R1
Article Type:	Research Paper
Keywords:	tooth enamel; Pb and Sr isotope ratios; El-Kurru; ICP-MS; groundwater alteration; provenance
Corresponding Author:	Antonio Simonetti, PhD University of Notre Dame Notre Dame, Indiana UNITED STATES
First Author:	Antonio Simonetti, PhD
Order of Authors:	Antonio Simonetti, PhD
	Michele R. Buzon, PhD
	Loretta Corcoran, PhD
	Abagail M. Breidenstein, PhD
	Geoff Emberling, PhD
Abstract:	This study reports new trace element and Pb and Sr isotope compositions of tooth enamel from archaeological remains at a Medieval (Christian) cemetery located adjacent to the Kushite royal cemetery of El-Kurru, Sudan. The archaeological site of El-Kurru is located along the Nile River on the southern edge of the Nubian Plateau; the bedrock geology consists of Neoproterozoic crystalline basement and is overlain by fluvial sandstones and mudstones of Cretaceous age. El-Kurru is situated between two well-developed drainage basins, and in the past has been subjected to periodic (wadi-related) flooding as a result of intense local precipitation events. Enamel samples were taken from 18 individuals of varying ages and both sexes. Trace element abundances for a significant number of samples record elevated concentrations relative to modern ("in-vivo") enamel, including Pb and U; however, the abundances for both elements do not correlate significantly with the contents of the remaining trace elements (Ba, Fe, Mg, Mn, Nd, Sr) investigated here. The calculated enrichment factors for all trace elements studied here relative to average crustal values are not consistent with exposure to Pb ores for human purposes, which is corroborated by the Pb isotope results. The Sr isotope compositions define 2 main groups that yield 87Sr/86Sr ratios that are either higher or lower than 0.7072 with similar Sr abundances (range between ~100 and ~400 ppm). The Pb isotope compositions are extremely variable and correlate well with their corresponding U/Pb ratios; the former overlap Pb isotope ratios for proximal Neoproterozoic rocks belonging to the Saharan Metacraton and Arabian Nubian Shield tectonic provinces. The combined trace element abundances and Sr and Pb isotope compositions for the enamel samples located within the Christian cemetery at El-Kurru are best interpreted to record interaction with groundwater that occurred post-mortem during flooding events. As reported in previous anthropological studies of a similar nature, the Pb isotope results reported here are particularly sensitive to monitoring post mortem diagenetic alteration given their extremely low abundances in non-altered tooth enamel. In contrast, the 87Sr/86Sr ratios have been minimally perturbed by post mortem alteration, and therefore most likely represent individuals with distinct Sr isotopic signatures inherited from different geographic regions.

UNIVERSITY OF NOTRE DAME
College of Engineering
DEPARTMENT OF CIVIL AND ENVIRONMENTAL ENGINEERING AND EARTH SCIENCES

156 Fitzpatrick Hall Notre Dame, Indiana 46556
tel (574) 631-6710 *fax* (574) 631-9236 *email* simonetti.3@nd.edu
web ceees.nd.edu

July 25, 2021

Dear Dr. Romain Millot,

As requested, I am submitting our revised manuscript entitled, "*Trace element and Pb and Sr isotope investigation of tooth enamel from archaeological remains at El-Kurru, Sudan: Evaluating the role of groundwater-related diagenetic alteration*". The revised manuscript has taken into careful consideration all of the points and queries reported by the two reviewers. Below, we provide detailed responses to their comments. I believe we have adequately responded to all of their queries.

Our detailed responses to each of the reviewers' comments are listed in *blue, italicized* font.

Reviewer #1:

The analytical work in the paper is well presented and described and I have no criticism of the data production, however, I found the paper difficult to follow and somewhat convoluted in its presentation. My main issue is the focus of the paper, which presents itself as an assessment of diagenetic alteration of tooth enamel and the use of Pb isotopes as a measure of such alteration rather than focussing on the source and timing of the alteration as ground water, which is the more interesting conclusion.

The revised manuscript focuses more on the groundwater alteration aspect of our study rather than the anthropological implications; although, we still believe that the latter are extremely significant for the community at-large. Of importance, the groundwater alteration aspect of this study was not 'self-evident' as stated by the reviewer given the 'good' or 'satisfactory' state of preservation of the enamel samples. As requested by the reviewer, we now provide more details on the state of preservation of the enamel samples on the basis of Montgomery (2002) classification – please see pertinent reply below.
Additional revisions carried out that emphasize the groundwater alteration aspect are the following:
- The first paragraph of the introduction section 1.1 of the original manuscript, which emphasized the anthropological aspects of the study, has been deleted and section rename accordingly;

- We now discuss in detail Kamenov et al.'s (2018) MTC (maximum threshold concentration) index for anthropological samples, which highlights the preferential behavior of the trace elements analyzed here (lines 82 to 88, lines 330-335, and lines 444-446).
- We have included a new Figure 3, which illustrates the Kamenov et al. (2018) C/MTC normalized patterns for the samples investigated here; the diagram clearly shows that the contents of U, Fe, and Nd are elevated compared to modern-day (in vivo) human enamel samples, and these are consistent with groundwater alteration (now discussed in lines 330 to 335).
- The timing of the groundwater alteration has to clearly be post mortem (i.e., within the last 600 years), especially given the radiogenic signatures of the Pb isotope ratios for several samples; i.e., time is required to accrue radiogenic Pb from the decay of U). This is now clearly stated in lines 449 to 451.

The paper starts with a discussion of evidence for post mortem diagenetic alteration in tooth enamel. Cautioning against the problems of such alteration of Sr in ancient skeletal remains and noting the use of Sr ppm range of 100-250 as guidance for un-altered enamel. Such generalization should be treated with caution as diet and climate can affect Sr concentrations (Evans et al 2012).

- Reference to the Evans et al. (2012) study in relation to Sr abundances in relation to diet and climate is now made in lines 72 to 75. However, low C/MTC values (<<1) for Sr (new Figure 3) clearly show that Sr has not been perturbed by groundwater alteration; this is now stated in lines 368-369.

Sr isotopes have been used in tooth enamel for many years now and Pb is increasing used eg Samulsen and Potra 2020. Where Pb is present, at low concentrations, it is obvious that it is more susceptible to contamination via the laws of mixing and there are several papers, as noted by the authors, warning of this. Of course, in the spectrum of preservation between modern teeth and fossilized teeth, diagenesis will occur.

- The Samulsen and Potra (2020) study is now cited in line 137.

The important question for archaeological studies is how to detect and monitor this and the most important starting point is to use robust samples: A good guide to sample preservation is given in Montgomery 2002. Table 5.1, p120. It is essential that the method of preparation and sampling to the materials for analysis need to be described.

- Agreed – As requested, we provide more details in relation to the nature and state of the samples investigated here in lines 221 to 233. We now refer to Montgomery's (2002) Enamel Preservation Classification Score, and scores for our enamel samples rank between 3 and 4 indicating that all tooth preservation was graded as 'good' or 'satisfactory' in lines 223-224.

This study makes it clear that it has chosen poor quality skeletal material in order to study this process of diagenesis so why then try to discuss this with respect to preserved biogenic signatures of Sr?

The skeletal material may have been poor, but this was not the material analyzed and reported here. As stated above, the preservation state of our enamel samples was good to satisfactory. As we point out in lines 226 to 229, "Despite the presence of such damages and moderate to severe occlusal attrition in almost all adult teeth, the enamel of the selected teeth was generally hard, glossy, and milky-white with only some small areas of discoloration. Some teeth were previously harvested of dentine for ancient DNA analysis in a clean lab." Thus, this is the main reason why we discuss the preserved biogenic signatures of Sr in the manuscript.

Why did the authors not use Kamenov geochemical index of alteration as it clear picks up the elevated REE content of their samples- a good sign of geogenic alteration.

- As stated and detailed above, the Kamenov et al. (2018) MTC index for sample preservation is now discussed in detail and presented in new Figure 3.

The definition of anthropogenic expose is unclear to me. The authors contrast geogenic (exposure to soil bedrock) to anthropogenic (exposure to ores used in making Kohl and glazes). I would argue that anthropogenic exposure is related to exposure of EXTRACTED ore used for human purposes. So this need clarifying. Neolithic populations, living close to an orebody, but predating mining activity, would not have anthropogenic exposure to the ore.

- Agreed- we have clarified the meaning of anthropogenic exposure in lines 14, 261 and lines 393-394.

Why would you expect Pb ppm to correlate with 87Sr/86Sr ratios? (P20)

- The reviewer admits in one of their preceding comments that because of the low Pb abundances in human enamel, then it is obviously more susceptible to contamination via the laws of mixing. Therefore, the reviewer's question is somewhat odd; i.e., one would expect a correlation between Pb concentrations (ppm) and 87Sr/86Sr ratios if indeed the latter were also impacted by the groundwater alteration, which they are not……

Reviewer #2 (numbered points are from reviewer):

The authors measured Sr and Pb stable isotope ratios of human tooth enamel for 18 individuals, recovered from a Christian cemetery near the Nile River in Sudan. They used the two isotope systems to investigate diagenetic changes in the teeth. Samples with "acceptable" Sr concentrations but unusual 87Sr/86Sr ratios were interpreted as individuals originating from other regions. Prior flooding of the cemetery likely impacted Pb isotopic compositions.

The text was concise and clear. With that said, I would suggest minor revisions to the text. In addition, I believe some sample labels have been mismatched with data in the tables and figures as patterns described in the text do not fit what I can "see" in my review of numbers; more details are given in #10 below. This potential problem must be addressed before the paper is accepted for publication.

I hope the authors find the following questions and recommendations useful:

I would suggest using the term "ratios" as opposed to "values" when presenting Sr or Pb results (i.e., Line 37, 382, etc.).

- Agreed – we have made this change throughout the text.

In Section 1.3, what are "incompatible elements" (Line 116) and how does this impact Pb concentrations/isotope ratios?

- The definition of an incompatible element is now provided in lines 118-120, and it is pertinent given that both Pb and U belong to this group of elements; obviously, the U/Pb ratio is one parameter that controls the Pb isotope compositions of samples.

In Section 2.3, the standard notation for "radiocarbon" is 14C, not C14. Please correct.

- *Corrected as requested (lines 210 and 212).*

In Line 213, the authors note that "not all 27 individuals uncovered were examined/sampled" but the reader must look at Table 1 to see how many WERE examined/sampled. As part of Section 2.3, I would recommend specifying that teeth from 18 of 27 individuals are included in the current study.

- As requested, this information has been added to the revised manuscript (line 204).

In Section 3.1, I believe the references to Table 1 should instead be references to Table 2.

- References to Table 2 have been made in Section 3.1.

Please be consistent in the shorthand used to describe solutions. The terminology is not currently standardized – for example: DD (16N) HNO3 (Line 226) 2.5N DD HCl (Line 244) 0.8 N DD HBr (Line 261)

- As requested, the shorthand is now consistent throughout this section.

Check the solutions listed for separation and purification of Sr in Section 3.2. It appears the same solution of 2.5N HCl was used to load the columns and also elute the Sr? I do not believe that's correct.

- We are slightly confused here by the reviewer's query. It is standard procedure to use the same high quality, double-distilled 2.5N HCl throughout the ion exchange chromatography in order to ensure lowest blank levels. Obviously, it is not exactly the same solution that is used, i.e., different aliquots are involved, one contains the sample, the other is simply acid. We have tried to clarify this point (lines 278 - 280).

[8] How many "analytical sessions" (Line 253) were used for measuring Sr isotope ratios? If SRM 987 was analyzed 4 times, does that represent the number of analytical sessions? Similarly, how many analytical sessions were used for measuring Pb isotope ratios? Line 277 mentions "the analytical session" although 2□ for SRM 981 was apparently calculated from 3 measurements.

- Data was collected during 2 analytical sessions; this information has now been added in line 288 for Sr isotope measurements and line 314 for Pb isotope analyses.

[9] Check the "certified value" of SRM 987 (Line 254) and the 2005 citation for the number given in the text. The certificate available online from NIST.gov is dated 19 June 2007 and gives the following: 87Sr/86Sr = 0.710 34 ± 0.000 26

- This is somewhat of an odd query and it's the first time I've been asked this question during the past 30 years of isotope geochemistry research. It is a well-known and established fact that the accepted value for the NIST SRM 987 Sr standard is 0.71025; one has to merely type in this number with the standard name in a Google search and you will be inundated with scholarly papers that cite this isotope ratio. In any event, we now provide a citation to Faure and Mensing's (2005) Principles of Isotope Geology textbook (line 290) since in Chapter 5, page 78, it states that the NBS 987 Sr isotope standard has a certified value of 0.71025.

In addition, please add a source for the "certified values" of SRM 981. The certificate available online from NIST.gov only provides numbers for 204Pb/206Pb, 207Pb/206Pb, and 208Pb/206Pb.

- We have inserted the paper by Baker et al. (2004) in line 317, which provides a robust compilation and comparison of NIST SRM 981 values, including values obtained by triple-spike method.

[10] In Section 4, the authors note 6 samples (3, 7, 12, 14, 15, and 16) had "elevated Sr abundances" (Lines 288-289). However, it appears that KUR-9 also falls outside the shaded box in Figure 3. Yet KUR-9 has a Sr concentration of 106 ppm in Table 2, which would place the sample inside the shaded box. In fact, the samples noted as having elevated abundances in the text and Figure 3 aren't all supported by the data in Table 2. For example –

KUR-3 = 343 ppm (Table 2), outside shaded box in Figure 3 KUR-4 = 398 ppm (Table 2), inside shaded box in Figure 3
Am I not correctly reading the data in the table and cross-referencing it to the figure? Were some lines in the table sorted incorrectly? Were some the labels in the figure jumbled?
If there has been a mismatch in data and sample identifiers (as I suspect there has been), it would explain why the only sample with an EF >20 is KUR-11… and not KUR-6 as currently stated in the text (Line 318). Please check the sample identifiers are correctly aligned with results and address this potential mismatch.

- Agreed – the mismatch issue was related to the concentrations solely listed in Table 2 and not in the figures; the data in the latter were accurately illustrated. We have now fixed the elemental concentrations in Table 2 so that they accurately record the data shown in the various trace element and isotope plots.

[11] If correlations are mentioned (Line 292), I would suggest providing the Pearson's r (or other statistic).

- R2 value for this regression is now provided in line 328.

[12] Is the content of both U and Pb expected to be in vivo <1 ppm? It's unclear in Line 296. What is the "expected" content for Mn (Line 299)? In other words, how did the authors know Mn content was elevated in the study samples?

- Yes, the elevated contents of Mn and other elements are in relation to 'in vivo' samples. This is now discussed in more detail in lines 330 to 335.

[13] How exactly were the 7 samples flagged in red in Figure 3 identified? It appears to be a combination of elevated Sr concentration (i.e., the shaded box) with higher 87Sr/86Sr ratio (>0.7072?) – but why was that ratio limit selected/used? Did the authors simply look for a natural "break" in the measured ratios of the samples? Please clarify.

- Based on the distribution of the data in now Figure 4 (old figure 3), it is clear that there are 2 groups of 87Sr/86Sr ratios given a similar range of Sr contents, which are considered non-altered or overlap in vivo modern-day human enamel (100 to 250 ppm; shaded region).

On a related note, it would be useful if the authors could provide 87Sr/86Sr ratios of the local El- Kurru geology. Although the local geology is described in Section 2.1, I did not find a measurements of soil/rocks from the region. (In contrast, some geologic references were provided for Pb isotope ratios – i.e., green symbols in Figure 6.)

- Agreed – Although we had reported a range of Sr isotope compositions for metamorphic rocks belonging to the SMC and ANS in the discussion section of the original version of the manuscript

(now again in lines 477 to 482), we have now nonetheless included a new paragraph with this information (lines 339 to 343).

[14] Please label KUR-4 in Figure 6 if it's called out in the text as being a distinctive endmember (Line 374). Likewise, KUR-3, -12, -16, and -18 (Line 421) should be labeled in the appropriate figures if they are called out as plotting "closest to the natural Pb endmember component."

- Labels for samples KUR-3, -12, -16, and -18 have been inserted in new Fig. 7 (old Fig. 6). However, the Pb isotope composition for sample KUR-4 is not illustrated for scaling reasons; i.e., its ratios are extremely radiogenic and would significantly compress all of the data if added. This exclusion is now stated in the accompanying figure caption.

[15] This study did not demonstrate that analysis of "small amounts of sample material" was reliable… unless there was a method validation component to Section 3 that was not emphasized enough for me to recognize the effort? For example, were samples or reference measured repeatedly at a variety of starting weights/concentration?
At present, I would recommend deleting the 3rd concluding point.

- Agreed, although not entirely an accurate statement, this conclusion point has been deleted

Finally, please check that the samples called out in the last concluding point are the correct samples based on the potential mismatch in data and sample identifiers (see #10).

- Again and as stated above, the sample numbers listed are the correct ones since the mismatch issue was related to Table 2 and not in any of the figures.

Tables:
Please use consistent sample identifiers between tables and text. Should it be KUR-# or Kur-#?
- Agreed- These have been made consistent throughout the text and tables.

Table 1 – The Methods text should be referenced for the explanation of EF (enrichment factors).
- Agreed – this description was previously in the Discussion section of the original manuscript, and is now in the Methods section (lines 258 to 274).

Table 2 – What exactly is different about KUR-4? It's not the only sample with two digits provided for uncertainty (see also KUR-1, KUR-15).

- The reason for the lesser significant figures is because of the significantly higher, absolute ratios associated with sample KUR-4; i.e., it doesn't make sense to list additional significant figures after the decimal place when the uncertainty is already significant in the first decimal place!

Figures:
Figure 1 – Please include an overview map of northern Africa, for orientation.
- As requested, an inset map of Africa has been added to Figure 1 for orientation purposes.

Figure 3 – The shaded box is very faint when printed.
- Shading of box has been made less transparent (now Figure 4).

Figure 4 – Use the shorthand from Figure 1 (SMC, ANS). The shaded regions are very faint when printed.
- As requested, acronyms have been added to Figure 4 (now Figure 5) and shaded regions have been made less transparent.

Figure 6 – Consider using gray dots for El-Kurru enamel (this study) as red dots were used in previous figures to "flag" samples. Also, "el" should be capitalized in the legend.
- As suggested, dots have been made gray and "el" has been capitalized in the legend (now Figure 7).

References:
The Geologic Map of Sudan cited in Line 171 is not included in the list of References. Also check the format of that in-text citation.
- Reference has been added to citation list.

Grammatical –
Line 40: Sentence subject "use of…" is singular and "have" should be "has" - *corrected*
Line 72: Closing parenthesis missing – "…(e.g., brushite…" - *corrected*
Line 76: "… is the predominant process" of diagenesis? *- corrected*
Line 86: REE is not defined – *now defined*
Line 131: Sentence subject "reporting" is singular and "are" should be "is" in Line 134 - *corrected*
Line 239: Check formatting of standard solution concentration – *this had been verified*
Line 325: Abbreviate Stacey and Kramers evolution curve as S/K to match figure Line 364: Capitalize 87sr – *S/K abbreviation has been inserted and Sr capitalized as requested.*

Should you require additional information, then please don't hesitate to contact me.

We look forward to hearing from you soon with a final decision on the publication of our manuscript in Applied Geochemistry.

Best regards,

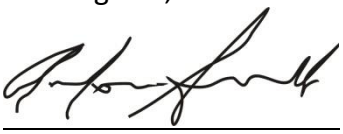

Dr. Antonio Simonetti

UNIVERSITY OF NOTRE DAME
College of Engineering
DEPARTMENT OF CIVIL AND ENVIRONMENTAL ENGINEERING AND EARTH SCIENCES

156 Fitzpatrick Hall Notre Dame, Indiana 46556
tel (574) 631-6710 *fax* (574) 631-9236 *email* simonetti.3@nd.edu
web ceees.nd.edu

July 25, 2021

Dear Dr. Romain Millot,

As requested, I am submitting our revised manuscript entitled, "*Trace element and Pb and Sr isotope investigation of tooth enamel from archaeological remains at El-Kurru, Sudan: Evaluating the role of groundwater-related diagenetic alteration*". The revised manuscript has taken into careful consideration all of the points and queries reported by the two reviewers. Below, we provide detailed responses to their comments. I believe we have adequately responded to all of their queries.

Our detailed responses to each of the reviewers' comments are listed in *blue, italicized* font.

Reviewer #1:

The analytical work in the paper is well presented and described and I have no criticism of the data production, however, I found the paper difficult to follow and somewhat convoluted in its presentation. My main issue is the focus of the paper, which presents itself as an assessment of diagenetic alteration of tooth enamel and the use of Pb isotopes as a measure of such alteration rather than focussing on the source and timing of the alteration as ground water, which is the more interesting conclusion.

The revised manuscript focuses more on the groundwater alteration aspect of our study rather than the anthropological implications; although, we still believe that the latter are extremely significant for the community at-large. Of importance, the groundwater alteration aspect of this study was not 'self-evident' as stated by the reviewer given the 'good' or 'satisfactory' state of preservation of the enamel samples. As requested by the reviewer, we now provide more details on the state of preservation of the enamel samples on the basis of Montgomery (2002) classification – please see pertinent reply below.
Additional revisions carried out that emphasize the groundwater alteration aspect are the following:
- The first paragraph of the introduction section 1.1 of the original manuscript, which emphasized the anthropological aspects of the study, has been deleted and section rename accordingly;

- We now discuss in detail Kamenov et al.'s (2018) MTC (maximum threshold concentration) index for anthropological samples, which highlights the preferential behavior of the trace elements analyzed here (lines 82 to 88, lines 330-335, and lines 444-446).
- We have included a new Figure 3, which illustrates the Kamenov et al. (2018) C/MTC normalized patterns for the samples investigated here; the diagram clearly shows that the contents of U, Fe, and Nd are elevated compared to modern-day (in vivo) human enamel samples, and these are consistent with groundwater alteration (now discussed in lines 330 to 335).
- The timing of the groundwater alteration has to clearly be post mortem (i.e., within the last 600 years), especially given the radiogenic signatures of the Pb isotope ratios for several samples; i.e., time is required to accrue radiogenic Pb from the decay of U). This is now clearly stated in lines 449 to 451.

The paper starts with a discussion of evidence for post mortem diagenetic alteration in tooth enamel. Cautioning against the problems of such alteration of Sr in ancient skeletal remains and noting the use of Sr ppm range of 100-250 as guidance for un-altered enamel. Such generalization should be treated with caution as diet and climate can affect Sr concentrations (Evans et al 2012).

- Reference to the Evans et al. (2012) study in relation to Sr abundances in relation to diet and climate is now made in lines 72 to 75. However, low C/MTC values (<<1) for Sr (new Figure 3) clearly show that Sr has not been perturbed by groundwater alteration; this is now stated in lines 368-369.

Sr isotopes have been used in tooth enamel for many years now and Pb is increasing used eg Samulsen and Potra 2020. Where Pb is present, at low concentrations, it is obvious that it is more susceptible to contamination via the laws of mixing and there are several papers, as noted by the authors, warning of this. Of course, in the spectrum of preservation between modern teeth and fossilized teeth, diagenesis will occur.

- The Samulsen and Potra (2020) study is now cited in line 137.

The important question for archaeological studies is how to detect and monitor this and the most important starting point is to use robust samples: A good guide to sample preservation is given in Montgomery 2002. Table 5.1, p120. It is essential that the method of preparation and sampling to the materials for analysis need to be described.

- Agreed – As requested, we provide more details in relation to the nature and state of the samples investigated here in lines 221 to 233. We now refer to Montgomery's (2002) Enamel Preservation Classification Score, and scores for our enamel samples rank between 3 and 4 indicating that all tooth preservation was graded as 'good' or 'satisfactory' in lines 223-224.

This study makes it clear that it has chosen poor quality skeletal material in order to study this process of diagenesis so why then try to discuss this with respect to preserved biogenic signatures of Sr?

The skeletal material may have been poor, but this was not the material analyzed and reported here. As stated above, the preservation state of our enamel samples was good to satisfactory. As we point out in lines 226 to 229, "Despite the presence of such damages and moderate to severe occlusal attrition in almost all adult teeth, the enamel of the selected teeth was generally hard, glossy, and milky-white with only some small areas of discoloration. Some teeth were previously harvested of dentine for ancient DNA analysis in a clean lab." Thus, this is the main reason why we discuss the preserved biogenic signatures of Sr in the manuscript.

Why did the authors not use Kamenov geochemical index of alteration as it clear picks up the elevated REE content of their samples- a good sign of geogenic alteration.

- As stated and detailed above, the Kamenov et al. (2018) MTC index for sample preservation is now discussed in detail and presented in new Figure 3.

The definition of anthropogenic expose is unclear to me. The authors contrast geogenic (exposure to soil bedrock) to anthropogenic (exposure to ores used in making Kohl and glazes). I would argue that anthropogenic exposure is related to exposure of EXTRACTED ore used for human purposes. So this need clarifying. Neolithic populations, living close to an orebody, but predating mining activity, would not have anthropogenic exposure to the ore.

- Agreed- we have clarified the meaning of anthropogenic exposure in lines 14, 261 and lines 393-394.

Why would you expect Pb ppm to correlate with 87Sr/86Sr ratios? (P20)

- The reviewer admits in one of their preceding comments that because of the low Pb abundances in human enamel, then it is obviously more susceptible to contamination via the laws of mixing. Therefore, the reviewer's question is somewhat odd; i.e., one would expect a correlation between Pb concentrations (ppm) and 87Sr/86Sr ratios if indeed the latter were also impacted by the groundwater alteration, which they are not……

Reviewer #2 (numbered points are from reviewer):

The authors measured Sr and Pb stable isotope ratios of human tooth enamel for 18 individuals, recovered from a Christian cemetery near the Nile River in Sudan. They used the two isotope systems to investigate diagenetic changes in the teeth. Samples with "acceptable" Sr concentrations but unusual 87Sr/86Sr ratios were interpreted as individuals originating from other regions. Prior flooding of the cemetery likely impacted Pb isotopic compositions.

The text was concise and clear. With that said, I would suggest minor revisions to the text. In addition, I believe some sample labels have been mismatched with data in the tables and figures as patterns described in the text do not fit what I can "see" in my review of numbers; more details are given in #10 below. This potential problem must be addressed before the paper is accepted for publication.

I hope the authors find the following questions and recommendations useful:

I would suggest using the term "ratios" as opposed to "values" when presenting Sr or Pb results (i.e., Line 37, 382, etc.).

- Agreed – we have made this change throughout the text.

In Section 1.3, what are "incompatible elements" (Line 116) and how does this impact Pb concentrations/isotope ratios?

- The definition of an incompatible element is now provided in lines 118-120, and it is pertinent given that both Pb and U belong to this group of elements; obviously, the U/Pb ratio is one parameter that controls the Pb isotope compositions of samples.

In Section 2.3, the standard notation for "radiocarbon" is 14C, not C14. Please correct.

- *Corrected as requested (lines 210 and 212).*

In Line 213, the authors note that "not all 27 individuals uncovered were examined/sampled" but the reader must look at Table 1 to see how many WERE examined/sampled. As part of Section 2.3, I would recommend specifying that teeth from 18 of 27 individuals are included in the current study.

- As requested, this information has been added to the revised manuscript (line 204).

In Section 3.1, I believe the references to Table 1 should instead be references to Table 2.

- References to Table 2 have been made in Section 3.1.

Please be consistent in the shorthand used to describe solutions. The terminology is not currently standardized – for example: DD (16N) HNO3 (Line 226) 2.5N DD HCl (Line 244) 0.8 N DD HBr (Line 261)

- As requested, the shorthand is now consistent throughout this section.

Check the solutions listed for separation and purification of Sr in Section 3.2. It appears the same solution of 2.5N HCl was used to load the columns and also elute the Sr? I do not believe that's correct.

- We are slightly confused here by the reviewer's query. It is standard procedure to use the same high quality, double-distilled 2.5N HCl throughout the ion exchange chromatography in order to ensure lowest blank levels. Obviously, it is not exactly the same solution that is used, i.e., different aliquots are involved, one contains the sample, the other is simply acid. We have tried to clarify this point (lines 278 - 280).

[8] How many "analytical sessions" (Line 253) were used for measuring Sr isotope ratios? If SRM 987 was analyzed 4 times, does that represent the number of analytical sessions? Similarly, how many analytical sessions were used for measuring Pb isotope ratios? Line 277 mentions "the analytical session" although 2□ for SRM 981 was apparently calculated from 3 measurements.

- Data was collected during 2 analytical sessions; this information has now been added in line 288 for Sr isotope measurements and line 314 for Pb isotope analyses.

[9] Check the "certified value" of SRM 987 (Line 254) and the 2005 citation for the number given in the text. The certificate available online from NIST.gov is dated 19 June 2007 and gives the following: 87Sr/86Sr = 0.710 34 ± 0.000 26

- This is somewhat of an odd query and it's the first time I've been asked this question during the past 30 years of isotope geochemistry research. It is a well-known and established fact that the accepted value for the NIST SRM 987 Sr standard is 0.71025; one has to merely type in this number with the standard name in a Google search and you will be inundated with scholarly papers that cite this isotope ratio. In any event, we now provide a citation to Faure and Mensing's (2005) Principles of Isotope Geology textbook (line 290) since in Chapter 5, page 78, it states that the NBS 987 Sr isotope standard has a certified value of 0.71025.

In addition, please add a source for the "certified values" of SRM 981. The certificate available online from NIST.gov only provides numbers for 204Pb/206Pb, 207Pb/206Pb, and 208Pb/206Pb.

- We have inserted the paper by Baker et al. (2004) in line 317, which provides a robust compilation and comparison of NIST SRM 981 values, including values obtained by triple-spike method.

[10] In Section 4, the authors note 6 samples (3, 7, 12, 14, 15, and 16) had "elevated Sr abundances" (Lines 288-289). However, it appears that KUR-9 also falls outside the shaded box in Figure 3. Yet KUR-9 has a Sr concentration of 106 ppm in Table 2, which would place the sample inside the shaded box. In fact, the samples noted as having elevated abundances in the text and Figure 3 aren't all supported by the data in Table 2. For example –

KUR-3 = 343 ppm (Table 2), outside shaded box in Figure 3 KUR-4 = 398 ppm (Table 2), inside shaded box in Figure 3
Am I not correctly reading the data in the table and cross-referencing it to the figure? Were some lines in the table sorted incorrectly? Were some the labels in the figure jumbled?
If there has been a mismatch in data and sample identifiers (as I suspect there has been), it would explain why the only sample with an EF >20 is KUR-11… and not KUR-6 as currently stated in the text (Line 318). Please check the sample identifiers are correctly aligned with results and address this potential mismatch.

- Agreed – the mismatch issue was related to the concentrations solely listed in Table 2 and not in the figures; the data in the latter were accurately illustrated. We have now fixed the elemental concentrations in Table 2 so that they accurately record the data shown in the various trace element and isotope plots.

[11] If correlations are mentioned (Line 292), I would suggest providing the Pearson's r (or other statistic).

- R2 value for this regression is now provided in line 328.

[12] Is the content of both U and Pb expected to be in vivo <1 ppm? It's unclear in Line 296. What is the "expected" content for Mn (Line 299)? In other words, how did the authors know Mn content was elevated in the study samples?

- Yes, the elevated contents of Mn and other elements are in relation to 'in vivo' samples. This is now discussed in more detail in lines 330 to 335.

[13] How exactly were the 7 samples flagged in red in Figure 3 identified? It appears to be a combination of elevated Sr concentration (i.e., the shaded box) with higher 87Sr/86Sr ratio (>0.7072?) – but why was that ratio limit selected/used? Did the authors simply look for a natural "break" in the measured ratios of the samples? Please clarify.

- Based on the distribution of the data in now Figure 4 (old figure 3), it is clear that there are 2 groups of 87Sr/86Sr ratios given a similar range of Sr contents, which are considered non-altered or overlap in vivo modern-day human enamel (100 to 250 ppm; shaded region).

On a related note, it would be useful if the authors could provide 87Sr/86Sr ratios of the local El- Kurru geology. Although the local geology is described in Section 2.1, I did not find a measurements of soil/rocks from the region. (In contrast, some geologic references were provided for Pb isotope ratios – i.e., green symbols in Figure 6.)

- Agreed – Although we had reported a range of Sr isotope compositions for metamorphic rocks belonging to the SMC and ANS in the discussion section of the original version of the manuscript

(now again in lines 477 to 482), we have now nonetheless included a new paragraph with this information (lines 339 to 343).

[14] Please label KUR-4 in Figure 6 if it's called out in the text as being a distinctive endmember (Line 374). Likewise, KUR-3, -12, -16, and -18 (Line 421) should be labeled in the appropriate figures if they are called out as plotting "closest to the natural Pb endmember component."

- Labels for samples KUR-3, -12, -16, and -18 have been inserted in new Fig. 7 (old Fig. 6). However, the Pb isotope composition for sample KUR-4 is not illustrated for scaling reasons; i.e., its ratios are extremely radiogenic and would significantly compress all of the data if added. This exclusion is now stated in the accompanying figure caption.

[15] This study did not demonstrate that analysis of "small amounts of sample material" was reliable… unless there was a method validation component to Section 3 that was not emphasized enough for me to recognize the effort? For example, were samples or reference measured repeatedly at a variety of starting weights/concentration?
At present, I would recommend deleting the 3rd concluding point.

- Agreed, although not entirely an accurate statement, this conclusion point has been deleted

Finally, please check that the samples called out in the last concluding point are the correct samples based on the potential mismatch in data and sample identifiers (see #10).

- Again and as stated above, the sample numbers listed are the correct ones since the mismatch issue was related to Table 2 and not in any of the figures.

Tables:
Please use consistent sample identifiers between tables and text. Should it be KUR-# or Kur-#?
- Agreed- These have been made consistent throughout the text and tables.

Table 1 – The Methods text should be referenced for the explanation of EF (enrichment factors).
- Agreed – this description was previously in the Discussion section of the original manuscript, and is now in the Methods section (lines 258 to 274).

Table 2 – What exactly is different about KUR-4? It's not the only sample with two digits provided for uncertainty (see also KUR-1, KUR-15).

- The reason for the lesser significant figures is because of the significantly higher, absolute ratios associated with sample KUR-4; i.e., it doesn't make sense to list additional significant figures after the decimal place when the uncertainty is already significant in the first decimal place!

Figures:
Figure 1 – Please include an overview map of northern Africa, for orientation.
- As requested, an inset map of Africa has been added to Figure 1 for orientation purposes.

Figure 3 – The shaded box is very faint when printed.
- Shading of box has been made less transparent (now Figure 4).

Figure 4 – Use the shorthand from Figure 1 (SMC, ANS). The shaded regions are very faint when printed.
- As requested, acronyms have been added to Figure 4 (now Figure 5) and shaded regions have been made less transparent.

Figure 6 – Consider using gray dots for El-Kurru enamel (this study) as red dots were used in previous figures to "flag" samples. Also, "el" should be capitalized in the legend.
- As suggested, dots have been made gray and "el" has been capitalized in the legend (now Figure 7).

References:
The Geologic Map of Sudan cited in Line 171 is not included in the list of References. Also check the format of that in-text citation.
- Reference has been added to citation list.

Grammatical –
Line 40: Sentence subject "use of…" is singular and "have" should be "has" - *corrected*
Line 72: Closing parenthesis missing – "…(e.g., brushite…" - *corrected*
Line 76: "… is the predominant process" of diagenesis? *- corrected*
Line 86: REE is not defined – *now defined*
Line 131: Sentence subject "reporting" is singular and "are" should be "is" in Line 134 - *corrected*
Line 239: Check formatting of standard solution concentration – *this had been verified*
Line 325: Abbreviate Stacey and Kramers evolution curve as S/K to match figure Line 364: Capitalize 87sr – *S/K abbreviation has been inserted and Sr capitalized as requested.*

Should you require additional information, then please don't hesitate to contact me.

We look forward to hearing from you soon with a final decision on the publication of our manuscript in Applied Geochemistry.

Best regards,

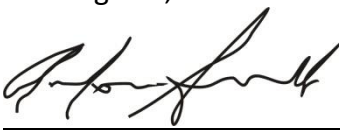

Dr. Antonio Simonetti

- Pb and Sr isotope data for tooth enamel from El-Kurru Medieval burial site, Sudan
- Elevated trace element signatures (Pb, U) indicate natural (geogenic) source
- Pb isotope data reveals post mortem diagenesis involving groundwater alteration
- Sr isotope compositions indicate individuals from different geographic regions

Trace element and Pb and Sr isotope investigation of tooth enamel from archaeological remains at El-Kurru, Sudan: Evaluating the role of groundwater-related diagenetic alteration

Antonio Simonetti[a*], Michele R. Buzon[b], Loretta Corcoran[a], Abagail M. Breidenstein[c], Geoff Emberling[d]

a: Department of Civil and Environmental Engineering and Earth Sciences, University of Notre Dame, Notre Dame, Indiana 46556, USA

b: Department of Anthropology, Purdue University, West Lafayette, Indiana 47907, USA

c: Institut für Evolutionäre Medizin, Universität Zürich, Winterthurerstrasse 190, 8057 Zürich, Switzerland

d: Kelsey Museum of Archaeology, University of Michigan, 434 South State Street, Ann Arbor, Michigan 48109-1390, USA

*: corresponding author: simonetti.3@nd.edu

KEY WORDS: tooth enamel, Pb and Sr isotope ratios, El-Kurru, ICP-MS, groundwater alteration, provenance

ABSTRACT

This study reports new trace element and Pb and Sr isotope compositions of tooth enamel from archaeological remains at a Medieval (Christian) cemetery located adjacent to the Kushite royal cemetery of El-Kurru, Sudan. The archaeological site of El-Kurru is located along the Nile River on the southern edge of the Nubian Plateau; the bedrock geology consists of Neoproterozoic crystalline basement and is overlain by fluvial sandstones and mudstones of Cretaceous age. El-Kurru is situated between two well-developed drainage basins, and in the past has been subjected to periodic (wadi-related) flooding as a result of intense local precipitation events. Enamel samples were taken from 18 individuals of varying ages and both sexes. Trace element abundances for a significant number of samples record elevated concentrations relative to modern ("in-vivo") enamel, including Pb and U; however, the abundances for both elements do not correlate significantly with the contents of the remaining trace elements (Ba, Fe, Mg, Mn, Nd, Sr) investigated here. The calculated enrichment factors for all trace elements studied here relative to average crustal values are not consistent with exposure to Pb ores for human purposes, which is corroborated by the Pb isotope results. The Sr isotope compositions define 2 main groups that yield $^{87}Sr/^{86}Sr$ ratios that are either higher or lower than 0.7072 with similar Sr abundances (range between ~100 and ~400 ppm). The Pb isotope compositions are extremely variable and correlate well with their corresponding U/Pb ratios; the former overlap Pb isotope ratios for proximal Neoproterozoic rocks belonging to the Saharan Metacraton and Arabian Nubian Shield tectonic provinces. The combined trace element abundances and Sr and Pb isotope compositions for the enamel samples located within the Christian cemetery at El-Kurru are best interpreted to record interaction with groundwater that occurred post-mortem during flooding events. As reported in previous anthropological studies of a similar nature, the Pb

isotope results reported here are particularly sensitive to monitoring post mortem diagenetic alteration given their extremely low abundances in non-altered tooth enamel. In contrast, the $^{87}Sr/^{86}Sr$ ratios have been minimally perturbed by post mortem alteration, and therefore most likely represent individuals with distinct Sr isotopic signatures inherited from different geographic regions.

1. INTRODUCTION

1.1. $^{87}Sr/^{86}Sr$ ratios as provenance indicator and evaluating post mortem diagenesis in human tooth enamel

The use of strontium isotope ($^{87}Sr/^{86}Sr$) compositions has made an important contribution to understanding the provenance of materials in archaeology and interactions and migrations of ancient civilizations throughout the globe; such examples include Roman mobility in Europe (e.g., Schweissing and Grupe, 2003; Evans et al., 2006; Chenery et al., 2010) and the movements of the Wari, Inca, and Tiwanaku in South America (e.g., Knudson, 2008; Andrushko et al., 2009; Slovak et al., 2009; Turner et al., 2009; Buzon et al., 2012). On Earth, the $^{87}Sr/^{86}Sr$ ratios of biological and geological materials vary as a function of the geological provinces, which are dependent on their age, and mineralogical make-up. Areas that are characterized by older bedrock with a higher proportion of minerals containing high Rb/Sr, such as micas (e.g., biotite, muscovite, alkali feldspar), will yield higher $^{87}Sr/^{86}Sr$ ratios compared to regions that contain younger rocks with lower Rb/Sr ratios. The reason being that the parent nuclide, ^{87}Rb, decays to the stable daughter isotope, ^{87}Sr, via beta decay (half-life of ~50 billion years). The $^{87}Sr/^{86}Sr$ ratios are then transferred into the hydrosphere and ecosphere through weathering. Animals record the $^{87}Sr/^{86}Sr$ compositions from their environment and diet and this signature is subsequently incorporated into their organic and skeletal tissues. Organic tissues that grow continuously, such as hair, teeth, bones, and tusks, may record temporal variations in the $^{87}Sr/^{86}Sr$ ratios, which can then be used to decipher migration patterns of individuals or groups from ancient civilizations. For example, Buzon et al. (2016) have effectively used the Sr isotope compositions of dental remains and faunal samples from archaeological sites of interest in Egypt's Nile Valley to distinguish between local (autochthonous) and non-local (allochthonous)

52 populations. Of importance and as outlined in Bataille et al. (2018), $^{87}Sr/^{86}Sr$ ratios display a high
53 resolution but predictable scalar spatial pattern that follow geological regimes and limited
54 temporal variability. Therefore, spatiotemporal patterns of $^{87}Sr/^{86}Sr$ ratios in the geosphere,
55 ecosphere and hydrosphere may provide precise and unique geolocation potential for provenance
56 studies.

57 Caution must be exerted, however, when employing the Sr isotope compositions for the purposes
58 of provenance determination as diagenetic modification by cumulative physical, chemical and/or
59 biological alteration can perturb the original Sr isotopic signatures incorporated within ancient
60 skeletal remains (e.g., Retzmann et al., 2019). Subsequent burial, Sr from the soil and/or
61 groundwater of the entombment environment may accumulate in teeth. The predominant
62 hydroxyapatite lattice of the latter may recrystallize and even form secondary minerals (e.g.,
63 brushite ($CaHPO_4 \cdot 2H_2O$) or carbonate ($CaCO_3$)) in micro-cracks, pores and vacancies (Nelson et
64 al., 1986; Kohn et al., 1999; Nielsen-Marsh and Hedges, 2000; Prohaska et al., 2002; Hoppe et
65 al., 2003), which may then alter the original, biogenic Sr isotope signature/fingerprint of the
66 sample. In arid environments such as the Nile River valley, crystallization of secondary phases
67 is the predominant process of diagenesis rather than bacterial alteration (Maurer et al., 2014;
68 Dudás et al., 2016). Thus, several chemical indices are reported in order to evaluate the potential
69 diagenetic alteration in studies of large populations for provenance identification. For example,
70 elevated (> 250 ppm) and depleted (< 100 ppm) Sr contents in human enamel have been
71 considered as indications of diagenetic changes (e.g., Dudás et al., 2016), which is also a
72 function of the repository conditions (e.g., Sponheimer and Lee-Thorp, 2006). However, on the
73 basis of Sr abundances (yielded a median value of 84 ppm) in fossilized human tooth enamel
74 from 74 archaeological sites in Britain, the study by Evans et al. (2012) indicates these may

reflect both diet and climate. Additionally, previous investigations of human and animal skeletal remains have shown that other indicators of diagenetic alteration include Ca/P (mass fraction) ratios above the theoretical value (2.16) of biogenic hydroxyapatite (Sillen, 1986), the presence of increased contents of elements, such as Al, Si, Ba, V, Fe and Mn, and/or the presence of elevated contents of ultra-trace elements (mainly REEs (rare earth elements), Y, Hf, Th, U; in vivo < 1 ppm; e.g., Kohn et al., 1999; Trueman et al., 2008; Koenig et al., 2009; Benson et al., 2013; Kohn and Moses, 2013; Willmes et al., 2016; Kamenov et al., 2018; Retzmann et al., 2019). Specifically, Kamenov et al. (2018) developed the maximum threshold concentrations (MTC) index as a means to evaluate post mortem addition of elements into preserved tooth enamel; MTC is calculated (in ppm) by taking the maximum concentration of an element established in pristine (non-altered) modern human tooth enamel and adding 2 times its documented standard deviation (STDEV). Thus, calculated C/MTC values of >1 when comparing elemental abundances for fossilized samples (C) to corresponding MTC values indicate post mortem addition (Kamenov et al., 2018).

Recently, Retzmann et al. (2019) developed a novel method for evaluating the degree of diagenetic alteration based on the comparison of the Sr abundances and isotope compositions of enamel and corresponding dentine; the latter exhibits a higher porosity, smaller crystallites, and a much higher organic content (~30%) relative to enamel and is therefore more susceptible to diagenetic alteration. However, the general consensus is that tooth enamel is not significantly affected by diagenesis due to its compact structure with very little pore space and a minor amount of organic content (~ 2 %). Hence, tooth enamel is expected to preserve its original, biogenic Sr isotopic value and represents reliable sample material for investigating mobility and population migration studies (e.g., Kyle, 1986; Lee-Thorp and Sponheimer, 2003; Bentley, 2006;

98 Buzon et al., 2007; Buzon and Simonetti, 2013; Montgomery, 2010; Slovak and Paytan, 2012;
99 Szostek et al., 2015: Buzon et al., 2016; Schrader et al., 2019).

100 The comparative method outlined by Retzmann et al. (2019) obviously necessitates the analysis
101 of both enamel and corresponding dentine (or bone) from the same individual in order to assess
102 the degree of post-deposition diagenetic alteration. However, this approach may not always be
103 feasible due to sampling issues. In this study, we propose an alternative approach which involves
104 investigating the lead (Pb) isotope signatures in conjunction with the corresponding Sr isotope
105 and trace elemental compositions of tooth enamel.

106

107 *1.2. Pb isotopes as an environmental tracer*

108 The lead and strontium isotopic compositions of an individual's hard tissues (tooth, bone) will
109 reflect their diet (Ericson, 1985). Both elements may readily substitute for calcium in the
110 hydroxyapatite matrix of teeth and bone (Nelson et al., 1986; Simons, 1986; Bercovitz and
111 Laufer, 1990; Bowen, 2001; Simpson et al., 2021). Tooth enamel of permanent adult teeth forms
112 during early childhood (typically during first 12 years of life) and is considered a dead tissue
113 because it is not penetrated by any organic structures (Steele and Bramblett, 1988). Therefore,
114 tooth enamel will reflect the isotope compositions of the (geologic) environment in which a
115 person lived while the tooth was forming. This consists primarily of the bedrock geology
116 associated with exposed land surfaces (top veneer) on Earth, which is the continental crust.

117 The continental crust makes up only ~0.6% by mass of the silicate Earth, but it does contain a
118 very large proportion (20-70%; Rudnick and Fountain, 1995) of incompatible elements; the latter
119 are preferentially incorporated in Earth's crust and not the upper mantle due to incompatible size

and/or charge in predominant mantle minerals, which include uranium (U) and lead (Pb). Lead has 4 isotopes: ^{204}Pb, ^{206}Pb, ^{207}Pb, and ^{208}Pb, and the latter three are the stable daughter products from the radiogenic decay of long-lived isotopes ^{238}U, ^{235}U, and ^{232}Th, respectively, in addition to their primordial abundances present at the time of solar system/Earth formation. In contrast, ^{204}Pb is the only non-radiogenic isotope of Pb, and its abundance is thus constant in nature. Therefore, the present-day Pb isotope composition of any geological sample is a function of its Pb isotope composition at the time of its formation, the U−Pb-Th ratios, and its age. Due to the large variations in the geochemical behavior of U, Th, and Pb, the Pb isotopic composition of rocks, minerals (e.g., galena – PbS), and ores display a significant natural variation, which can be used as an isotopic "fingerprint." As such, this fingerprint may be employed to link Pb ores and the industrial (anthropogenic) materials produced from them (Brill and Wampler, 1967; Iñañez et al., 2010; Sangster et al., 2000). Moreover, ancient civilizations have extracted Pb from ore deposits over thousands of years for a variety of purposes (metallurgical, medicinal, and industrial), hence, rendering Pb one of the most heavily utilized metals during human history. Previous investigations have demonstrated that reporting the Pb isotope compositions of archaeological materials, such as kohls and glass (e.g., Shortland, 2006) and pottery glazes (e.g., Iñañez et al., 2010; Schurr et al., 2018), the mineral galena (PbS) (e.g., Shortland, 2006; Mirnejad et al., 2011, 2015), and ancient human and prehistoric animal teeth (e.g., Samuelsen and Potra, 2020) is effective for shedding light on transport and trade practices of metals and ores in ancient civilizations and source attribution purposes in crustal environments.

Numerous previous human epidemiological investigations indicate that Pb abundances in hard tissues such as bone and tooth typically represent a longer-term indicator of several years (e.g., Gulson, 1996; Johnston et al., 2019). Unlike the relatively high concentrations of Sr (hundreds of

ppm) in tooth enamel and dentine, the range of Pb abundances in teeth is in general an order of magnitude lower (i.e., ~1 to 10s of ppm; Gulson, 1996; Purchase and Fergusson, 1986; Wychowanski and Malkiewicz, 2017; Johnston et al., 2019). Higher Pb contents in hard tissue may be indicative of exposure to elevated levels of this metal in the environment, whether it is of natural (geogenic) or anthropogenic (human activity-related) origin. However, it is only through the combined investigation of both the Pb abundances and their corresponding isotopic compositions can an accurate assessment or interpretation be rendered in relation to source attribution purposes.

In this study, the Sr and Pb isotope compositions and trace element abundances of tooth enamel are reported for human remains buried at El-Kurru, Sudan (Fig.1; Emberling et al., 2013; Emberling et al., 2015; Dann et al., 2016). The burials were part of a Medieval (Christian) walled settlement (ca. 600-1400 CE) located on the edge of the Nile floodplain. The Kushite royal cemetery for which El-Kurru is known is located some 400 m to the northwest, on the edge of the desert plateau. This site was chosen for investigation because of the overall poor preservation of the skeletal remains and its unique location in relation to several well-developed drainage systems along the Nile River at El-Kurru. Evidences obtained from taphonomy and observed diagenetic changes in skeletal remains indicate that the site has experienced periodic flooding, and therefore, these events may have impacted the isotopic and trace elemental abundances preserved in tooth enamel for individuals at this site.

2. LOCAL GEOLOGY, HYDROLOGY and SAMPLES

2.1. Local Geology

El-Kurru is located along the Nile River on the southern edge of the Nubian Plateau, which consists of a Neoproterozoic bedrock core that is overlain by horizontal sedimentary rocks (Fig. 1; Dann et al., 2016). The site of El-Kurru is situated proximal to the suture between the Arabian Nubian Shield (ANS) and Saharan Metacraton (SMC) in the Bayuda Desert (Fig. 1). The crystalline basement rocks within the ANS are interpreted as juvenile (newly formed) Neoproterozoic crust and represent dismembered ophiolite (e.g., Abdel-Rahman, 1993; Abdelsalam et al., 1998), whereas those from the SMC represent older cratonic crust that was deformed during the Neoproterozoic (between ~1000 and ~550 Ma), and consist of polymetamorphic amphibolite from magmatic arc environments (e.g., Küster and Liégeois, 2001). The bedrock at the site consists of overlying fluvial sandstones and siltstones of probable Cretaceous age (Geological Research Authority of the Sudan, 1988, Geologic Map of Sudan). At El-Kurru, the Nile has carved into the Neoproterozoic crystalline basement and there is localized floodplain development (Dann et al., 2016).

Within the royal cemetery, the rock exposures in the staircases and chambers consist of a sequence of Cretaceous sandstones, siltstones, and mudstones >5 m thick (Dann et al., 2016). The lowest unit comprises alternating layers of sandstone, siltstone, and mudstone (with thicknesses ~1.5 to ~2 m) that represent either channel (sandstone) or floodplain deposits of ancient rivers (Dann et al., 2016). Moreover, the top of the lowermost sandstone unit is overlain by a paleosol, which consists of thin layers of hard, Fe-cemented, typically fine-grained sediments that represent buried soil horizons; therefore, these may be referred to as ferricretes (Dann et al., 2016). These Cretaceous-aged rock units are overlain unconformably by a thin layer of sandy Quaternary gravels.

2.2. Hydrology

188 The site of El-Kurru is situated between two large, well-developed drainage basins, but the area
189 itself is drained by a smaller and less developed drainage system (Dann et al., 2016). Large-scale
190 flooding events along the Nile are related primarily to the humid climate present at the southern
191 headwaters' region, and three such episodes were recorded in 1946, 1988, and 1994 (Dann et al.,
192 2016). In contrast, the flooding of the wadi draining the site at El-Kurru is attributed to intense
193 local precipitation events, which in a typical year can occur two to three times and results in
194 strong, channelized, knee-deep (at best) flow for about one hour (Dann et al., 2016). Recent
195 excavations revealed that the late mortuary temple located next to the wadi was flooded and
196 ~500 mm of sediment was deposited (Emberling et al., 2015); it is postulated that overland flow
197 from areas surrounding the temple likely contributed to this depositional event. Taphonomy and
198 diagenetic changes have most likely been impacted by water damage that has affected the
199 cemetery for centuries. This cemetery was located at an opening fan of a seasonal wadi and close
200 to the banks of the Nile; it is in close proximity to flooded irrigated palm groves and other
201 agricultural land still in use. Therefore, it is very likely that the cemetery and skeletons have
202 incurred water damage over the centuries.

203 *2.3. Samples*

204 Excavations in 2014 to 2016 uncovered 27 individuals in the Christian cemetery, of which 18
205 were examined in this study. A Christian date for these graves was suggested based on the
206 scarcity of grave goods as well as approximate west-east orientation (relative to the Nile River)
207 and treatment of the bodies; heads of all individuals were oriented cardinally in the northwestern
208 direction, their feet in the southeast, with either their arms or ankles crossed (Dann et al., 2016;
209 Welsby, 2002). Radiocarbon dating of the El-Kurru skeletons has proven difficult due to the poor
210 preservation of collagen. Thus, date estimations are based on the ^{14}C dating of the fortification

211 wall, the mortuary archaeology, and stratigraphy of the skeletal remains. Organics from the wall
212 were ^{14}C dated to *ca*. 600-1000 CE (Dann et al., 2016). Additionally, pottery sherds and
213 decoration motifs date the fills to Classic (*ca*. 800-1100 CE) or Late Christian (*ca*. 1100-1450
214 CE) and one Islamic glass bead was found in an unusual context, but still indicate these burials
215 date at *ca*. 1450 CE. Lastly, the stratigraphy of the cemetery indicates that these burials represent
216 the last phase of occupation in this area. Table 1 lists the approximate ages, sex and burial depths
217 associated with the type of tooth enamel sample investigated in this study. Of note, not all 27
218 individuals uncovered were examined/sampled due to either extremely poor preservation of the
219 tissue leading to not enough material to sample, teeth not recovered from an individual (e.g.,
220 adult KU216 was edentulous), and/or that some subadults did not have enough mineralized
221 material for testing. For this study, sample selection included intact teeth whenever possible and
222 those with enamel that was macroscopically in good condition. Generally, all tooth preservation
223 was graded as good or satisfactory (Enamel Preservation Classification Score of between 3 and
224 4; Montgomery, 2002). Most crowns were fully intact (i.e., not too fragmented) with some thin
225 cracks, some superficial soil concretions or evidence of plant abrasion, and in some cases
226 separation from the underlaying dentine. Despite the presence of such damages and moderate to
227 severe occlusal attrition in almost all adult teeth, the enamel of the selected teeth was generally
228 hard, glossy, and milky-white with only some small areas of discoloration. Some teeth were
229 previously harvested of dentine for ancient DNA analysis in a clean lab. When sampled, the
230 crown was removed from the root with a thin sectioning blade for access to the inner dentine for
231 sampling, leaving the crown enamel intact for further processing. Enamel samples were
232 mechanically cleaned and abraded before chemical purification to reduce post-depositional

233 contamination.

234

235 **3. ANALYTICAL METHODS**

236 *3.1. Trace element geochemistry*

237 Samples of tooth enamel were processed in two steps. In the first step, between ~70 and ~300 mg
238 of enamel was placed in a 15 mL Savillex® Teflon beaker and ~4 ml of concentrated 16N,
239 double-distilled (DD) HNO_3 was added, followed by heating on a hotplate at 110° C for 24h.
240 After the heating, samples were removed from the hotplate and cooled for one hour. After
241 rinsing the sample residues adhered to the sides of the beakers with 18 MΩ cm^{-2} water, samples
242 were placed back on the hotplate to achieve complete dryness. In the second cycle, all conditions
243 were kept the same, except the amount of 16N DD HNO_3 acid was decreased from 4 to 1 mL.
244 After the last drying step, 5 mL of 16N DD HNO_3 acid was added into the beaker and the
245 solution diluted with 18 MΩ cm^{-2} water until a final total volume of ~100 mL was achieved.
246 Appropriate sample volume aliquots for trace element and Sr and Pb isotope analyses were taken
247 from the 100 mL solution. The concentrations of the trace elements (Table 2) were determined
248 by a standard/spike addition method (Jenner et al., 1990), which includes correction for matrix
249 effects and instrumental drift.

250 The trace element abundances (Table 2) for all samples were determined using an Attom (Nu
251 Instruments Ltd., Wales, UK) high resolution inductively coupled plasma mass spectrometer
252 (HR-ICP-MS) in medium mass resolution mode ($M/\Delta M \approx 3000$). Samples were processed using
253 a wet plasma, solution mode introduction system that consists of a cyclonic spray chamber
254 (housed within a Peltier cooling device @7° C) and Meinhard nebulizer (aspiration rate of 0.1

mL/min). Before each analytical session, the Attom instrument was tuned and calibrated using a multi-elemental (Li, B, Na, Si, Sc, Co, Ga, Y, Rh, In, Ba, Lu, Tl, U) 1 ppb (ng g-1) standard solution.

Enrichment factors (EF) have been calculated for each sample for several of the trace elements (e.g., Mn, Sr, Pb, U) with elevated contents (relative to in vivo, modern day human enamel), and these are listed in Table 2. The EFs evaluate the relative contribution from either natural (i.e., soil, bedrock) vs. anthropogenic sources (e.g., ores used for kohl or ceramic glaze production) of a given element in the tooth enamel. $EF_{ELEMENT}$ is defined as the concentration ratio of a given element to that of Mg in this case (or any other element thought to be derived exclusively from a crustal source, such as Si, Al) normalized to the same concentration ratio characteristic of the upper continental crust (e.g., Rudnick and Gao, 2014). In this study, Mg was chosen for this normalization since it is typically an element of natural origin and may substitute for Ca in tooth enamel (LeGeros, 1991); in addition, Mg contents do not correlate with any of the other trace elements investigated here (not shown). For example, the enrichment factor for Pb is thus: $(EF)_{Pb} = [Pb/Mg]_{sample}/[Pb/Mg]_{crust}$. However, given the large natural variations in the composition of crustal materials exposed to surface erosion and the diversity of biogeochemical processes affecting soil development at a global scale, enrichment factors within ±10 times the mean crustal abundances (i.e., EF values between 0.1 to 10) most likely indicate elements derived from continental crust (Duce et al., 1976). Conversely, any $(EF)_{element} > 10$ suggests contributions from other sources, such as human activities.

3.2. Sr isotope compositions

Separation and purification of Sr for subsequent Sr isotope analysis involved ion exchange chromatography, which employed columns containing 1.7 mL of 200-400 mesh AG50W-X8

resin. Sample aliquots (containing ~300 ng total Sr) in 0.25 mL of 2.5N DD HCl were loaded onto the resin beds; this was followed by several additional wash steps totaling ~15 ml of 2.5N DD HCl acid, and the Sr was subsequently eluted with 4 mL of 2.5N DD HCl. After the ion exchange chemistry, Sr-bearing aliquots were dried, dissolved in 2% HNO_3 solution (~2 mL) and aspirated into the ICP torch using a desolvating nebulizing system (DSN-100 from Nu Instruments Ltd.). Strontium isotope measurements were conducted using a NuPlasma II MC-ICP-MS (multi-collector inductively coupled plasma mass spectrometer; Nu Instruments Ltd.) instrument according to the protocol outlined in Balboni et al. (2016). Strontium isotope data was acquired in static, multi-collection mode using 5 Faraday collectors for a total of 400 s, consisting of 40 scans of 10 s integrations. The analytical protocol's accuracy and reproducibility were verified by analyzing the NIST SRM 987 strontium isotope standard during two analytical sessions, which yielded an average value of 0.710235 ± 0.000044 (2σ; n=4), in agreement with the certified value of 0.71025 (Faure and Mensing, 2005).

3.3. Pb isotope compositions

The Pb separation method is adapted from Manhes et al. (1980) and a brief summary is provided here (after Koeman et al., 2015). The Pb ion exchange micro-columns consist of approximately 20 µL of clean AG1-X8 resin (75−150 mesh) placed into a polypropylene tube combined with a polystyrene frit. The resin volume is cleaned using 0.15 mL of ultrapure (18 MΩ cm^{-2}) H_2O, and further conditioned with 0.15 mL of 0.8 N DD HBr. The sample solution was loaded with 0.6 mL of 0.8 N DD HBr, washed twice with 0.15 mL of 0.8 N DD HBr, and last eluted with 0.7 mL of 6 N DD HCl acid. After the eluted Pb is dried down, the ion exchange procedure is repeated with fresh resin in order to further purify the Pb aliquot. Following the last elution procedure, the

300 Pb aliquot is dried down and dissolved again in 2% HNO_3 for solution mode MC-ICP-MS
301 analysis.

302 Pb isotope compositions of the sample solutions were determined using the same procedure
303 outlined in Simonetti et al. (2004). After the purification steps, the aliquot of Pb was spiked with
304 a NIST SRM 997 Thallium standard solution (2.5 ppb). Seven Faraday cups on the Nu Plasma II
305 MC-ICPMS instrument were employed to simultaneously measure the Pb and Tl isotopes and
306 ^{202}Hg. The instrumental mass bias (exponential law; ^{205}Tl/^{203}Tl = 2.3887) is determined by
307 measuring the ^{205}Tl/^{203}Tl, and ^{202}Hg is monitored to correct for the interference of ^{204}Hg on ^{204}Pb.
308 Prior to the aspiration of the samples into the plasma, ion signals for the gas and acid blanks
309 ("on-peak-zeros") were recorded for 30 s to determine baseline values. For each analysis, data
310 acquisition involved 2 blocks of 25 scans (each scan has a 10 s integration time). A 25-ppb
311 solution of the NIST SRM 981 Pb standard (spiked with 6 ppb NIST SRM 997 Tl standard) was
312 measured periodically during the analytical session in order to validate the Pb isotope results.
313 The average Pb isotope ratios and associated 2σ standard deviations obtained on 3 measurements
314 of the NIST SRM 981 Pb isotope standard for two analytical sessions are as follows:
315 ^{206}Pb/^{204}Pb= 16.939 ±0.007, ^{207}Pb/^{204}Pb= 15.493 ±0.007, ^{208}Pb/^{204}Pb= 36.699 ±0.008,
316 ^{208}Pb/^{206}Pb= 2.1666 ±0.0002, and ^{207}Pb/^{206}Pb= 0.91464 ±0.00004, which overlap with certified
317 values for this standard (Baker et al., 2004).
318

319 **4. RESULTS**

320 Tables 2 and 3 list the trace element abundances and Sr and Pb isotope compositions for the 18
321 samples of tooth enamel from El-Kurru investigated here, respectively; these data are also
322 illustrated in Figures 2 to 8. The Sr abundances for the tooth enamel vary between 106 and 425

ppm (Table 2; Fig. 2), and a majority fall within the range considered to represent diagenetically unaltered material (between 100 and 250 ppm; Dudás et al., 2016). Six samples (KUR-3, -7, -12, -14, -15, -16) contain elevated Sr abundances (>250 ppm and up to 425 ppm; Table 2). Figure 2 plots the concentrations of Sr versus those for several trace elements, Mg, Ba, and U; Mg abundances do not exhibit any correlation with Sr contents (Fig. 2a), whereas Ba and U show a fairly good positive correlation (R^2 correlation coefficient ≈ 0.74), respectively (Fig. 2b, c). The contents of Mn and Pb versus those of U are also illustrated in Figures 2d-f, and these in general all correlate positively. Of note, the contents of U, Nd, and Fe reported here for all samples exceed C/MTC normalized values >1 (Figure 3); a C/MTC value ≤1 is considered to be representative of non-altered samples and equivalent to modern-day tooth enamel (i.e., *in vivo;* Kamenov et al., 2018). In Figure 3, the normalized C/MTC values for the remaining elements are all <1 with the exception of Mn and Ba, which fluctuate slightly on either side of unity. Overall, the C/MTC patterns shown in Figure 3 are not consistent for all of the samples investigated. Lastly, the vast majority of the enrichment factors (EFs) listed for Mn, Pb, Sr, and U in Table 2 vary between 1 (or <1) and 10, with the exception of tooth enamel sample KUR-11 that records a EF_{Pb} of ~21.

The Sr isotope compositions for the KUR enamel samples investigated here define two groups relative to their corresponding Sr contents (Fig. 4; Table 2), and these overlap primarily the range of variable, present-day $^{87}Sr/^{86}Sr$ ratios for metamorphic rocks from the SMC (~0.7030 to ~0.7089) and not with the less radiogenic signatures (~0.7030 to ~0.7053) for the metamorphic rocks from the ANS tectonic province (Evuk et al., 2017).

As discussed earlier, assessing the Pb isotope compositions of geological, environmental, or industrial samples provide an effective means for provenance determination. Table 3 lists the Pb

346 isotope compositions for the tooth enamel samples investigated here, and these are illustrated in
347 Figures 5 to 7. In Fig. 5, the Pb isotope data for the tooth enamel samples are compared to those
348 for rocks belonging to both the neighboring SMC and ANS tectonic provinces (Evuk et al.,
349 2017), which indicate a substantive degree of overlap, in particular with those from the SMC. In
350 addition, Fig. 5 also contains the Stacey and Kramers (1975) evolution curve, which represents
351 the time-integrated Pb isotope composition of average continental crust over the past 3.7 billion
352 years. The Pb isotope compositions for the El-Kurru enamel samples mainly plot above and to
353 the right of the Stacey and Kramers (1975) Pb evolution curve (S/K), and define well constrained
354 linear arrays. In the $^{206}Pb/^{204}Pb$ versus $^{207}Pb/^{204}Pb$ plot, the best-fit regression line defines a slope
355 of 0.0629, which corresponds to a Neoproterozoic $^{207}Pb/^{206}Pb$ age of approximately 705 million
356 years old; the latter corresponds to the age of the crystalline basement in the region (e.g., Evuk et
357 al., 2017). Typically, any linear array on a Pb-Pb isotope plot is considered to represent either
358 binary mixing between two distinct end-member components (i.e., resulting from open system
359 behavior), or may simply reflect the addition of radiogenic Pb resulting from the decay of U over
360 geologic time. Both of these hypotheses will be evaluated and discussed in the following section.

361

362 **5. DISCUSSION**

363 Figure 4 plots the Sr abundances versus their corresponding $^{87}Sr/^{86}Sr$ ratios for the tooth enamel
364 samples from El-Kurru examined here. Hypothetically, enamel for individuals that lived or
365 originated from the same geologic area and have not been affected by post mortem diagenesis
366 should define a restricted field; in particular, the range in Sr contents should ideally be restricted
367 between 100 and 250 ppm for non-diagenetically altered samples (e.g., Dudás et al., 2016).
368 Moreover, the C/MTC values for Sr for the enamel samples studied here are all <1 (Fig. 3),

369 which indicates that Sr abundances have not been impacted by groundwater alteration. Overall, a
370 majority of the enamel samples from El-Kurru plot within this range of Sr abundances (100 to
371 250 ppm; Fig. 4) and define two groups in relation to their Sr isotope compositions. The group of
372 samples with lower $^{87}Sr/^{86}Sr$ ratios (<0.7072) define a relatively restricted range (~0.7066 to
373 ~0.7070) and do not correlate with their corresponding Sr contents; whereas the second group
374 with more radiogenic Sr isotope compositions record more variable (~0.7074 to ~0.7083) ratios
375 and seem to correlate positively with their Sr abundances (Fig. 4). Thus, the bimodal distribution
376 in the Sr isotope results reported here, in particular for enamel samples with Sr abundances
377 between 100 and 250 ppm (as outlined in Fig. 4), can be interpreted to either represent
378 individuals originating from different regions (i.e., local vs. immigrant), or less likely reflect
379 different degrees of diagenetic alteration.

380 In order to better evaluate the post mortem alteration hypothesis, Figure 6 illustrates the $^{87}Sr/^{86}Sr$
381 ratios versus their corresponding U/Pb values for the El-Kurru enamel samples studied here since
382 the latter parameter may be used to evaluate the degree of diagenetic alteration (e.g., Kohn et al.,
383 1999; Trueman et al., 2008; Koenig et al., 2009; Benson et al., 2013; Kohn and Moses, 2013;
384 Willmes et al., 2016; Kamenov et al., 2018). The group of enamel samples characterized by the
385 lower Sr isotope compositions record a larger range of U/Pb ratios (~0 to ~1.5) compared to
386 those for the radiogenic (higher) group of enamel samples (~0 to ~0.3; except for sample KUR-
387 1), with the latter defining a positive trend (Fig. 6a). Moreover, the U/Pb values are in general
388 positively correlated with their Pb isotope compositions (Fig. 6b), which indicate that these
389 record the addition of radiogenic in-growth of Pb originating from the time-integrated decay of
390 U. On the basis of solely the U/Pb ratios reported here, it is difficult to discern exactly which

391 enamel samples record non-diagenetically altered $^{87}Sr/^{86}Sr$ ratios since both groups exhibit trends
392 that may be attributed to the addition of U post-mortem (Fig. 6).

393 An alternative approach is to compare the Pb isotope ratios for the enamel samples reported here
394 to those for pertinent atmospheric, geological, and anthropogenic (i.e., exposure to extracted Pb
395 ores for human purposes; e.g., pottery glazes, kohls) samples reported within the region of the
396 Nile River Valley. Given the unique geochemical nature of the U-Pb radiogenic isotope system,
397 Pb-Pb isotope plots (e.g., Fig. 7) are an effective tool in assessing open-system behavior or
398 mixing of Pb from multiple sources. If a suite of samples has indeed been affected by either of
399 the latter processes, then the result is that the Pb isotope data will be define linear arrays and plot
400 between the two end-member compositions. In Fig. 7, the Pb isotope compositions for the
401 enamel samples from El-Kurru define well-constrained linear arrays with enamel sample KUR-4
402 recording the most distinct and elevated Pb isotope ratios (Table 3). The results reported here
403 from El-Kurru are compared to those from the studies of Stós-Gale and Gale (1981), Hassan and
404 Hassan (1981), and Shortland et al. (2006), which examined the compositions for a variety of
405 archaeological samples (lead ores, kohls, lead metal, copper alloys, glass, glaze and pigment)
406 within Egypt, which also define a well-constrained linear array (Fig. 7), but with a completely
407 different slope. Both plots in Figure 7 clearly indicate that the linear arrays defined by the El-
408 Kurru samples are unique when compared to existing data for various environmental and
409 anthropogenic samples within the Nile River Valley. The two linear arrays appear to converge at
410 higher $^{207}Pb/^{206}Pb$ ratios (Fig. 7). Also shown in Fig. 7 are the Pb isotope compositions for
411 modern-day atmospheric aerosols sampled within the Middle Eastern region (Bollhofer and
412 Rossman, 2000); these plot at much higher $^{207}Pb/^{206}Pb$ ratios and do not appear to involve the
413 same end-member (natural and anthropogenic) components as those required to explain the data

414 from either El-Kurru, or other archaeological samples from within the Nile River Valley. Figure
415 7 also displays the Pb isotope composition of present-day, average continental crust (Stacey and
416 Kramers, 1975) and the average signatures for Neoproterozoic metamorphic rocks belonging to
417 the SMC and more juvenile samples from the ANS (from Evuk et al., 2017; shown in Fig. 5);
418 these data also plot close to the point of convergence for the Pb-Pb mixing arrays defined by the
419 El-Kurru and Egyptian archaeological samples. Therefore, we postulate that Pb derived from
420 regional bedrock (crust) is one end-member of the El-Kurru mixing line. The second end-
421 member for the El-Kurru requires a component that is U-rich or characterized by a high U/Pb
422 ratio.

423 Lead present in natural samples that have not been impacted by the addition of U subsequent
424 their time of formation are characterized by Pb isotope compositions that are a function of their
425 age (and their original U/Pb ratio) and these define a relatively restricted range in nature (e.g.,
426 $^{207}Pb/^{206}Pb$: ~0.83 to ~1.1 for samples between 0 and 3,000 million years old). In contrast, Pb
427 present in natural samples that was derived solely from radiogenic sources, i.e., it is the result of
428 U decay with no other Pb present at the time of formation is also age dependent and will be
429 characterized by much lower Pb isotope ratios (e.g., $^{207}Pb/^{206}Pb$: ~0.04 to ~0.4). For example, as
430 stated earlier, the best fit linear regression in Figure 4a defined by the tooth enamel samples from
431 El-Kurru has a slope ~0.0629, which corresponds to Neoproterozoic $^{207}Pb/^{206}Pb$ secondary
432 isochron age. Hence, a sample containing a mixture of natural (geogenic) Pb from its initial time
433 of formation and possibly radiogenic Pb accumulating from a U-rich endmember will record a
434 mixed Pb isotopic signature. Therefore, the Pb-Pb isotope arrays defined by the enamel samples
435 from El-Kurru (Fig. 7) most likely represent mixing between background, crustal Pb and
436 radiogenic Pb accumulated from U-bearing groundwater. Typically, dissolved U is found in most

surface water and groundwater at very low concentrations (ppb or ng g^{-1} range), and at much higher values when associated with highly mineralized, thermal and brine waters (Kumar et al., 2011). During bedrock and soil interaction with groundwater, radionuclides may transfer by dissolution, desorption, and erosion (Vongunten and Benes, 1995). The transport of U and other radionuclides in groundwater is dependent on the presence of fractures or faults and their interconnectivity within the bedrock. Moreover, the transport (movement) of U within groundwater depends on multiple factors including diffusion, emanation, and permeability of the rocks (Lopez et al., 2002). The combined elevated abundances of Fe, Nd and U for all the El-Kurru enamel samples as shown by corresponding C/MTC values (Fig. 3) are consistent with post mortem diagenetic alteration (Kamenov et al., 2018). The source of U and the radiogenic Pb incorporated into the samples of tooth enamel most likely emanates from the surrounding Neoproterozoic sandstones and mudstones, which are most likely characterized by U contents of 1 to 10 ppm (i.e., average continental crust; Rudnick and Gao, 2014). Thus, given the radiogenic nature of the Pb isotope compositions for several enamel samples (KUR-1, -4, -15; Table 2 and Figs. 5 to 7), the post mortem diagenetic alteration occurred in the recent past so as to provide time to accrue radiogenic Pb from the radioactive decay of U.

Given the elemental abundances and Pb isotope compositions reported here (Tables 2 and 3; Figs. 2 to 7), tooth enamel samples KUR-3, -12, -16, and -18 contain relatively similar Pb isotope compositions and plot closest to the natural Pb endmember component (Fig. 7); these samples also record elevated contents of Pb (between ~3 and ~23 ppm) and higher corresponding EFs (relative to the remaining samples; Table 2), which suggest these samples have been significantly impacted by groundwater diagenetic alteration. In general, the Pb isotope compositions for most samples correlate with their corresponding U/Pb values (Fig. 6b), and

460 therefore, the Pb-Pb isotope arrays defined by the El-Kurru enamel samples and illustrated in
461 Fig. 7 are interpreted to represent diagenetic alteration by groundwater with variable U/Pb ratios.
462 Of particular importance, these 4 enamel samples (KUR-3, -12, -16, and -18) belong to both
463 groups of Sr isotope compositions (Fig. 4), and their Pb concentrations don't correlate with their
464 corresponding $^{87}Sr/^{86}Sr$ ratios; for example, samples KUR-1, -2, and -11 record similar, higher
465 $^{87}Sr/^{86}Sr$ ratios (range from 0.70748 to 0.70772; Fig. 4; Table 2) but contain extremely variable
466 Pb contents of 0.16, 1.28 and 61.95 ppm (Table 2), respectively. Moreover, Pb contents and Sr
467 isotope compositions of tooth enamel reported here are not a function of their location within the
468 burial site. Figure 8 illustrates the locations of the skeletal remains at the El-Kurru burial site for
469 the individuals investigated here, and the enamel samples with the highest Pb concentrations and
470 least radiogenic Pb isotope compositions appear to be concentrated into 2 areas. Within these
471 areas, enamel samples are characterized by a wide range of $^{87}Sr/^{86}Sr$ ratios (from both groups;
472 Fig. 8), and therefore, this feature may be explained in two ways. The first being that the Sr
473 isotope compositions do indeed reflect differing provenance and their $^{87}Sr/^{86}Sr$ ratios were
474 buffered, or not affected by diagenetic alteration because of the much higher contents of Sr in
475 tooth enamel versus that found in groundwater. The fact that there is no correlation between the
476 Sr and Pb isotope compositions (or between Pb contents and Sr isotope ratios) for the tooth
477 enamel samples investigated here lends support to this interpretation. An alternative explanation
478 is that the groundwater entering the shallow burial pits was characterized by variable Sr isotopic
479 compositions, which reflects the Sr isotopic heterogeneity ($^{87}Sr/^{86}Sr$ ratios range between
480 ~0.7032 and ~0.7089) for the surrounding Neoproterozoic basement rocks; these consist of a
481 variety of metamorphic rocks (metagabbro, amphibole schist, granulitic amphibolite) within the
482 surrounding Saharan Metacraton (Evuk et al., 2017). However, there is only an approximate

maximum difference of 1.25 m in burial depth elevations for the individuals investigated here (Table 1); therefore, it seems unlikely that the varying Sr isotope compositions reflect a variable hydrological regime that is controlled by the local bedrock geology since the host Cretaceous mudstones, siltstone, and sandstone units are in general of greater thickness than the variation in burial depth (Dann et al., 2016). Moreover, there are no correlations exhibited (not shown) between burial depth elevation of the individuals examined here (Table 1) and any elemental (Table 2) or isotope signatures (Table 3). Thus, our preferred interpretation is that the variable Sr isotope compositions for samples with restricted Sr contents (100 to 250 ppm; Fig. 4) represent original and non-diagenetically altered signatures that reflect individuals originating from different areas within this region of Sudan.

6. CONCLUSIONS

Based on the trace elemental abundances and Sr and Pb isotope results reported in this study, the main conclusions and interpretations are as follows:

- The elevated trace element concentrations, in particular for those of Pb and U, cannot be attributed to human/anthropogenic activities as evidenced by the low EFs (<10) and corresponding Pb isotope compositions. Hence, it is important to note that the Pb isotope results for the tooth enamel samples from El-Kurru are critical in establishing that the extremely radiogenic (high) ratios originate from natural (geogenic) sources;

- The Pb isotope compositions and accompanying Fe, Nd, U and Pb contents (U/Pb ratios) indicate that the Christian-age skeletal remains and samples of tooth enamel from El-Kurru have

been impacted by recent groundwater alteration due to the burial site's proximal location to several wadis that have rendered it prone to flooding events in the past;

- Based on the combined trace element results and Pb and Sr isotope compositions reported here, it is most likely that several individuals (e.g., KUR-1, -2, -8, and -11 *vs*. those characterized by lower Sr isotope ratios; Fig. 4) present within the Christian burial site originated from different geographic regions of Sudan. Assessment of their exact geographic origins are beyond the scope of this present study and will be the focus of future investigation.

ACKNOWLEDGEMENTS

This work was funded by the National Science Foundation (BCS grant #1916718) to A. Simonetti and M.R. Buzon. We thank two anonymous reviewers for their comments and valuable input on an earlier version of the manuscript.

REFERENCES

Abdel-Rahman, E.M., 1993. Geochemical and geotectonic controls of the metallogenic evolution of selected ophiolite complexes from the Sudan. *Berl Geowiss Abh, Reihe A* **145**, 175 pp.

Abdelsalam, M.G., Stern, R.J., Copeland, P., Elfaki, E., Elhur, B., Ibrahim, F.M., 1998. The Neoproterozoic Keraf suture in NE Sudan: sinistral transpression along the eastern margin of west Gondwana. *J. Geol.* **106**, 133-148.

Andrushko, V.A., Buzon, M.R., Simonetti, A., Creaser, R.A., 2009. Strontium isotope evidence for prehistoric migration at Chokepukio, Valley of Cuzco, Peru. *Lat. Am. Antiq.* **20**, 57-75.

Baker, J.A., Peat, D., Waight, T., Meyzen, C., 2004. Pb isotopic analysis of standards and samples using a ^{207}Pb–^{204}Pb double spike and thallium to correct for mass bias with a double-focusing MC-ICP-MS. *Chem. Geol*. **211**, 275–303.

Balboni, E., Jones, N., Spano, T., Simonetti, A., Burns P.C., 2016. Chemical and Sr isotopic characterization of North America uranium ores: nuclear forensic applications. *Appl. Geochem.* **74**, 24-32.

Bataille, C.P., von Holstein, I.C.C., Willmes, J.E., Liu, X-M., Davies, G.R., 2018. A bioavailable strontium isoscape for Western Europe: A machine learning approach. *PLoS ONE* **13**, e0197386. doi.org/10.1371/journal.pone.0197386.

Benson, A., Kinsley, L., Willmes, M., Defleur, A., Kokkonen, H., Mussi, M., Grün, R., 2013. Laser Ablation Depth Profiling of U-series and Sr Isotopes in Human Fossils. *J. Archaeol. Sci.* **40**, 2991–3000.

539 Bentley, A.R., 2006. Strontium Isotopes from the Earth to the Archaeological Skeleton: A
540 Review. *J. Archaeol. Method Theory* **13**, 135–187.

541 Bercovitz, K., Laufer D., 1990. Tooth type as indicator of exposure to lead of adults and
542 children. *Arch. Oral Biol*. **35**, 895-897.

543 Bollhöfer, A., Rosman, K.J.R., 2000. Isotopic source signatures for atmospheric lead: The
544 Southern Hemisphere. *Geochim. Cosmochim. Acta* **64**, 3251–3262.

545 Bowen, W.H., 2001. Exposure to metal ions and susceptibility to dental caries. *J. Dent. Educ.*
546 **65**, 1046-1053.

547 Brill, R.H., Wampler J.M., 1967. Isotope studies of ancient lead. *Am. J. Archaeol*. **71**, 63-77.

548 Buzon, M.R., Conlee, C.A., Simonetti, A., Bowen, G.J., 2012. The consequences of Wari
549 contact in the Nasca region during the Middle Horizon: archaeological, skeletal, and isotopic
550 evidence. *J. Archaeol. Sci*. **39**, 2627-2636.

551 Buzon, M.R., Simonetti, A., 2013. Strontium isotope ($^{87}Sr/^{86}Sr$) variability in the Nile Valley:
552 Identifying residential mobility during ancient Egyptian and Nubian sociopolitical changes in
553 the New Kingdom and Napatan Periods. *Am. J. Phys. Anthropol*. **151**, 1-9.

554 Buzon, M.R., Simonetti, A., Creaser, R.A., 2007. Migration in the Nile Valley during the New
555 Kingdom period: a preliminary strontium isotope study. *J. Archaeol. Sci*. **34**, 1391-1401.

556 Buzon, M.R., Stuart, T.S., Simonetti, A., 2016. Entanglement and the Formation of the Ancient
557 Nubian Napatan State. *Am. Anthropol*. **118**, 284-300.

558 Chenery, C., Müldner, G., Evans, J., Eckardt, H., Lewis, M., 2010. Strontium and stable isotope
559 evidence for diet and mobility in Roman Gloucester, UK. *J. Archaeol. Sci.* **37**, 150-163.

560 Dann, R.J., Emberling, G., Stearns, C., Antis, S., Skuldbol, T., Uildriks, M., Rose, K., Phillips,
561 J., Breidenstein, A., Miller, N.F., 2016. El Kurru 2015-16 Preliminary Report. *Sudan and*
562 *Nubia* **20**, 35-49.

563 Duce, R.A., Hoffman, G.L., Ray, B.J., Fletcher, I.S., Fletcher, W.G.T., Fasching, J.L.,
564 Piotrowicz, S.R., Walsh, P.R., Hoffman, E.J., Miller, J.M., Heffter, J.L., 1976. Trace metals
565 in the marine atmosphere: Sources and fluxes, in: Windom, H.L., Duce, R.A. (Eds.), Marine
566 Pollution Transfer, Lexington Books, Blue Ridge Summit, pp. 77–119.

567 Dudás, F.Ö., LeBlanc, S.A., Carter, S.W., Bowring, S.A., 2016. Pb and Sr Concentrations and
568 Isotopic Compositions in Prehistoric North American Teeth: A Methodological Study, *Chem.*
569 *Geol.* **429**, 21–32.

570 Emberling, G., Dann, R.J., Abdelwahab Mohamed-Ali, M., Skuldbøl, T., Boaz, B., Cheng, J.,
571 Blinkhorn, E., 2013. New Excavations at El Kurru: Beyond the Napatan Royal Cemetery.
572 *Sudan and Nubia* **17**, 42-60.

573 Emberling, G., Dann, R.J., Mohamed-Ali, A.S., et al., 2015. In a Royal Cemetery of Kush:
574 Archaeological Investigations at El Kurru, Northern Sudan, 2014-15. *Sudan and Nubia* **19**,
575 54-70.

576 Ericson, J.E., 1985. Strontium isotope characterization in the study of prehistoric human
577 ecology. *J. Hum. Evol.* **14**, 503-514.

578 Evans, J.A., Chenery, C.A., Montgomery, J., 2012. A summary of strontium and oxygen isotope
579 variation in archaeological human tooth enamel excavated from Britain. *J. Anal. At.*
580 *Spectrom*. **27**, 754–764.

581 Evans, J., Stoodley, N., Chenery, C., 2006. A strontium and oxygen isotope assessment of a
582 possible fourth century immigrant population in a Hampshire cemetery, southern England. *J.*
583 *Archaeol. Sci.* **33**, 265-272.

584 Evuk, D., Lucassen, F., Franz, G., 2017. Lead isotope evolution across the Neoproterozoic
585 boundary between craton and juvenile crust, Bayuda Desert, Sudan. *J. Afr. Earth Sci.* **135**,
586 72-81.

587 Faure, G., Mensing, T.M., 2005. Isotopes: principles and applications (3rd edition). John Wiley
588 and Sons, Inc., Hoboken, New Jersey.

589 Geological Research Authority of the Sudan, 1988. Geologic Map of Sudan. Ministry of Energy
590 & Mines, Geological & Mineral Resources Department, Khartoum.

591 Gulson, B.L., 1996. Tooth Analyses of Sources and Intensity of Lead Exposure in Children.
592 *Environ. Health Perspect.* **104**, 306-312.

593 Hassan, A.A., Hassan F.A., 1981. Source of galena in predynastic Egypt at Nagada.
594 *Archaeometry* **23**, 77-82.

595 Hoppe, K.A., Koch, P.L., Furutani, T.T., 2003. Assessing the Preservation of Biogenic
596 Strontium in Fossil Bones and Tooth Enamel. *Int. J. Osteoarchaeol.* **13**, 20–28.

597 Iñañez, J.G., Bellucci, J.J., Rodríguez-Alegría, E., Ash, R., McDonough, W., Speakman, R.J.,
598 2010. Romita pottery revisited: a reassessment of the provenance of ceramics from Colonial
599 Mexico by LA-MC-ICP-MS. *J. Archaeol. Sci*. **37**, 2698-2704.

600 Jenner, G.A., Longerich, H.P., Jackson, S.E., Fryer, B.J., 1990. ICP-MS - a powerful tool for
601 high-precision trace-element analysis in Earth sciences: evidence from analysis of selected
602 U.S.G.S. reference samples. *Chem. Geol.* **83**, 133-148.

603 Johnston, J.E., Franklin, M., Roh, H., Austin, C., Arora, M., 2019. Lead and Arsenic in Shed
604 Deciduous Teeth of Children Living Near a Lead-Acid Battery Smelter. *Environ. Sci. Tech*.
605 **53**, 6000−6006.

606 Kamenov, G.D., Lofaro, E.M., Goad, G., Krigbaum, J., 2018. Trace Elements in Modern and
607 Archaeological Human Teeth: Implications for Human Metal Exposure and Enamel
608 Diagenetic Changes. *J. Archaeol. Sci*. **99**, 27–34.

609 Knudson, K.J., 2008. Tiwanaku influence in the South Central Andes: strontium isotope
610 analysis and Middle Horizon migration. *Lat. Am. Antiq*. **19**, 3-23.

611 Koeman, E.C., Simonetti, A., Burns, P.C., 2015. Sourcing of Copper and Lead within Red
612 Inclusions from Trinitite Postdetonation Material. *Anal. Chem.* **87**, 5380−5386.

613 Koenig, E., Rogers, R.R., Trueman, C.N., 2009. Visualizing Fossilization Using Laser
614 Ablation–Inductively Coupled Plasma–Mass Spectrometry Maps of Trace Elements in Late
615 Cretaceous Bones. *Geology* **37**, 511–515.

616 Kohn, M.J., Moses, R.J., 2013. Trace Element Diffusivities in Bone Rule Out Simple Diffusive
617 Uptake During Fossilization but Explain In Vivo Uptake and Release. *Proc. Natl. Acad. Sci.*
618 *U.S.A.* **110**, 419–424.

619 Kohn, M.J., Schoeninger, M.J., Barker, W.W., 1999. Altered States: Effects of Diagenesis on
620 Fossil Tooth Chemistry. *Geochim. Cosmochim. Acta* **63**, 2737–2747.

621 Kumar, A., Rout, S., Narayanan, U., Mishra, M.K., Tripathi, R.M., Singh, J., Kumar, S.,
622 Kushwaha, H.S., 2011. Geochemical modelling of uranium speciation in the subsurface
623 aquatic environment of Punjab State in India. *J. Geol. Min. Res.* **3**, 137–146.

624 Küster, D., Liégeois, J.P., 2001. Sr, Nd isotopes and geochemistry of the Bayuda Desert high-
625 grade metamorphic-basement (Sudan): an early Pan-African oceanic convergent margin, not
626 the edge of the East Saharan ghost craton. *Precambrian Res.* **109**, 1-23.

627 Kyle, J.H., 1986. Effect of Post-burial Contamination on the Concentrations of Major and Minor
628 Elements in Human Bones and Teeth – the Implications for Palaeodietary Research. *J.*
629 *Archaeol. Sci*. **13**, 403–416.

630 Lee-Thorp, J., Sponheimer, M., 2003. Three Case Studies Used to Reassess the Reliability of
631 Fossil Bone and Enamel Isotope Signals for Paleodietary Studies. *J. Anthropol. Archaeol.* **22**,
632 208–216.

633 LeGeros, R., 1991. Calcium phosphates in enamel, dentine and bone. in: Myres, H, (Ed.),
634 Calcium Phosphates in Oral Biology. 15th ed. Basel: Karger, pp. 108–129.

635 Lopez, R.N., Segovia, N., Cisiega, M.G., Lopez, M.B.E., Armienta, M.A., Seidel, J.L., Pena, P.,
636 Godinez, L., Tamez, E., 2002. Determination of radon, major and trace elements in water
637 samples from springs and wells of northern Mexico State, Mexico. *Geofis. Int*. **41**, 407–414.

638 Manhes, G., Allègre, C.J., Dupré, B., Hamelin, B., 1980. Lead isotope study of basic ultrabasic
639 layered complexes: Speculations about the age of the Earth and primitive mantle
640 characteristics. *Earth Planet. Sci. Lett.* **47**, 370–382.

641 Maurer, A. F., Person, A., Tütken, T., Amblard-Pison, S., Ségalen L., 2014. Bone Diagenesis in
642 Arid Environments: An Intraskeletal Approach. *Palaeogeogr. Palaeoclimatol. Palaeoecol.*
643 **416**, 17–29.

644 Mirnejad, H., Simonetti, A., Molasalehi F., 2011. Pb isotopic compositions of some Zn–Pb
645 deposits and occurrences from Urumieh–Dokhtar and Sanandaj–Sirjan zones in Iran: *Ore*
646 *Geol. Rev.* **39**, 181–187.

647 Mirnejad, H., Simonetti A., Molasalehi F., 2015. Origin and formational history of some Pb-Zn
648 deposits from Alborz and Central Iran: Pb isotope constraints. *Int. Geol. Rev.* **57**, 463–471.

649 Montgomery, J., 2002. Lead and strontium isotope compositions of human dental tissues as an
650 indicator of ancient exposure and population dynamics. PhD, University of Bradford, UK,
651 382 pp. https://doi.org/10.5284/1000249

652 Montgomery, J., 2010. Passports from the Past: Investigating Human Dispersals Using
653 Strontium Isotope Analysis of Tooth Enamel. *Ann. Hum. Biol.* **37**, 325–346.

654 Nelson, B.K., Deniro, M.J., Schoeninger, M.J., DePaolo, D.J., Hare, P.E., 1986. Effects of
655 diagenesis on strontium, carbon, nitrogen, and oxygen concentration and isotopic
656 concentration of bone. *Geochim. Cosmochim. Acta* **50**, 1941-1949.

657 Nielsen-Marsh, C.M., Hedges, R.E.M., 2000. Patterns of Diagenesis in Bone I: The Effects of
658 Site Environments. *J. Archaeol. Sci*. **27**, 1139–1150.

659 Prohaska, T., Latkoczy, C., Schultheis, G., Teschler-Nicola, M., Stingeder, G., 2002.
660 Investigation of Sr Isotope Ratios in Prehistoric Human Bones and Teeth Using Laser
661 Ablation ICPMS and ICP-MS after Rb/Sr Separation. *J. Anal. At. Spectrom.* **17**, 887–891.

662 Purchase, N.G., Fergusson, J.E., 1986. Lead in teeth: The influence of the tooth type and the
663 sample within a tooth on lead levels. *Sci. Total Environ.* **52**, 239-250.

664 Retzmann, A., Budka, J., Sattmann, H., Irrgeher, J., Prohaska, T., 2019. The New kingdom
665 population on Sai Island: application of Sr isotopes to investigate cultural entanglement in
666 Ancient Nubia. *Ägypten und Levante/Egypt and the Levant* **29**, 355–380.

667 Rudnick, R.L., Fountain, D.M., 1995. Nature and composition of the continental crust: A lower
668 crustal perspective. *Rev. Geophys*. **33**, 267–309.

669 Rudnick, R.L., Gao S., 2014. Composition of the Continental Crust. Treatise on Geochemistry
670 (2nd edition). *Reference Module in Earth Systems and Environmental Sciences* **4**, 1-51.

671 Samuelsen, J.R., Potra, A., 2020. Biologically available Pb: A method for ancient human
672 sourcing using Pb isotopes from prehistoric animal tooth enamel. *J. Archaeol. Sci.* **115**,
673 105079. https://doi.org/10.1016/j.jas.2020.105079

674 Sangster, D.F., Outridge, P.M., Davis, W.J., 2000. Stable lead isotope characteristics of lead ore
675 deposits of environmental significance. *Environ. Rev.* **8**, 115–147.

676 Schrader, S.A., Buzon, M.R., Corcoran, L., Simonetti, A., 2019. Intraregional $^{87}Sr/^{86}Sr$
677 Variation in Nubia: New Insights from the Third Cataract. *J. Archaeol. Sci.: Rep.* **24**, 373–
678 379.

679 Schurr, M.R., Donohue, P.H., Simonetti, A., Dawson, E.L., 2018. Multi-element and lead
680 isotope characterization of early nineteenth century pottery sherds from Native American and
681 Euro-American sites. *J. Archaeol. Science: Rep*. **20**, 390–399.

682 Schweissing, M.M., Grupe, G., 2003. Stable strontium isotopes in human teeth and bone: a key
683 to migration events of the late Roman period in Bavaria. *J. Archaeol. Sci.* **30**, 1373-1383.

684 Shortland, A.J., 2006. Application of lead isotope analysis to a wide range of Late Bronze age
685 Egyptian Materials. *Archaeometry* **48**, 657–669.

686 Sillen, A., 1986. Biogenic and Diagenetic Sr/Ca in Plio-Pleistocene Fossils of the Omo
687 Shungura Formation. *Paleobiology* **12**, 311–323.

688 Simonetti, A., Gariepy, C., Banic, C., Tanabe, R., Wong, H., 2004. Pb isotopic investigation of
689 aircraft-sampled emissions from the Horne smelter (Rouyn, Quebec): implications for
690 atmospheric pollution in northeastern North America. *Geochim. Cosmochim. Acta* **68**, 3285–
691 3294.

692 Simons, T.J., 1986. Cellular interactions between lead and calcium. *Br. Med. Bull.* **42**, 431-434.

693 Simpson, R., Cooper, D.M.L., Swanston, T., Coulthard, I., Varney, T.L., 2021. Historical
694 overview and new directions in bioarchaeological trace element analysis: a review. *Archaeol.*
695 *Anthropol. Sci*., https://doi.org/10.1007/s12520-020-01262-4.

696 Slovak, N.M., Paytan, A., 2012. Applications of Sr Isotopes in Archaeology, 743–768, in:
697 Baskaran, M. (Ed.), Handbook of Environmental Isotope Geochemistry, Vol. I, Berlin,
698 Heidelberg.

699 Slovak, N.M., Paytan, A., Wiegand, B.A., 2009. Reconstructing Middle Horizon mobility
700 patterns on the coast of Peru through strontium isotope analysis. *J. Archaeol. Sci.* **36**, 157-
701 165.

Sponheimer, M., Lee-Thorp, J.A., 2006. Enamel Diagenesis at South African Australopith Sites: Implications for Paleoecological Reconstruction with Trace Elements. *Geochim. Cosmochim. Acta* **70**, 1644–1654.

Stacey, J.S., Kramers, J.D., 1975. Approximation of terrestrial lead isotope evolution by a two-stage model. *Earth Planet. Sci. Lett.* **26**, 207-22.

Steele, D.G., Bramblett, C.A., 1988. The Anatomy and Biology of the Human Skeleton. Texas A&M University, College Station, TX.

Stós-Gale, Z.A., Gale, N.H., 1981. Sources of Galena, lead and silver in predynastic Egypt. In: Revue d'Archéométrie, n°1, 1981. Actes du XXe symposium international d'archéométrie, Paris 26-29 mars 1980 Volume III, 285-296.

Szostek, K., Mądrzyk, K., Cienkosz-Stepańczak, B., 2015. Strontium Isotopes as an Indicator of Human Migration– Easy Questions, Difficult Answers. *Anthropol. Rev*. **78**, 133–156.

Trueman, C.N., Palmer, M.R., Field, J., Privat, K., Ludgate, N., Chavagnac, V., Eberth, D.A., Cifelli, R., Rogers, R.R., 2008. Comparing Rates of Recrystallisation and the Potential for Preservation of Biomolecules from the Distribution of Trace Elements in Fossil Bones. *C. R. Palevol* **7**, 145–158.

Turner, B.L., Kamenov, G.D., Kingston, J.D., Armelagos, G.J., 2009. Insights into immigration and social class at Machu Picchu, Peru based on oxygen, strontium, and lead isotopic analysis. *J. Archaeol. Sci.* **36**, 317-332.

Vongunten, H.R., Benes P., 1995. Speciation of radionuclides in the environment. *Radiochim. Acta* **69**, 1–29.

723 Welsby, D.A., 2002. The medieval kingdoms of Nubia: pagans, Christians and Muslims along
724 the Middle Nile. London: British Museum Press.

725 Willmes, M., Kinsley, L., Moncel, M.H., Armstrong, R.A., Aubert, M., Eggins, S., Grün, R.,
726 2016. Improvement of Laser Ablation In Situ Micro-analysis to Identify Diagenetic
727 Alteration and Measure Strontium Isotope Ratios in Fossil Human Teeth. *J. Archaeol. Sci.*
728 **70**, 102–116.

729 Wychowanski, P., Malkiewicz, K., 2017. Evaluation of Metal Ion Concentration in Hard
730 Tissues of Teeth in Residents of Central Poland. *BioMed Res. Int. 2017,* 6419709.
731 https://doi.org/10.1155/2017/6419709

732

FIGURE CAPTIONS

Fig. 1. Inset shows location of study area (red rectangle) within continental Africa. Main diagram is a map illustrating the regional geology of northeastern Sudan, which outlines the cratonic crust with Neoproterozoic deformation referred to as the Saharan Metacraton (SMC, red areas), and Neoproterozoic juvenile crust of the Arabian Nubian Shield (ANS, green area). Also shown are the locations of burial site at El-Kurru (present study) and the archaeological site of Tombos, both along the Nile River. Dashed line labeled KKSS = Keraf Kabus Sekerr Suture zone between ANS and SMC crustal provinces. Map is modified after Evuk et al. (2017).

Fig. 2. Bivariate plots displaying the concentrations (all expressed in ppm) of Sr versus those for (A) Mg, (B) Ba, and (C) U, and U compared to those for (D) Mn, (E) Ba, and (F) Pb for samples of tooth enamel from El-Kurru examined in this study. Red and black solid circles represent samples of tooth enamel with high and low $^{87}Sr/^{86}Sr$ as defined in Fig. 4 and detailed in text.

Fig. 3. Trace element abundances for El-Kurru human enamel samples investigated here (Table 2) normalized to those established by maximum threshold concentration (MTC) index after Kamenov et al. (2018). C/MTC= Concentration (C) of trace element (ppm) divided by corresponding MTC value. The red arrows indicate samples characterized by high $^{87}Sr/^{86}Sr$ ratios (Fig. 4). Dashed horizontal line at unity (C/MTC value= 1.0) separates elements/samples affected by post mortem diagenetic alteration (>1.0) versus non-altered (<1.0).

Fig. 4. Diagram illustrates the Sr contents (ppm) versus their corresponding Sr isotope compositions for the samples of tooth enamel from El-Kurru investigated here. The samples

define two groups relative to their $^{87}Sr/^{86}Sr$ ratios, those with higher (red) compared to those with lower (black) signatures. The shaded region represents the range of Sr abundances considered to represent unaltered, pristine tooth enamel (100 to 250 ppm; Dudás et al. 2016). Numbers adjacent to data points refer to corresponding sample numbers (Tables 1, 2 and 3). Associated uncertainties for both Sr contents and isotope compositions are within the size of the symbol.

Fig. 5. Plots of $^{206}Pb/^{204}Pb$ versus (A) $^{207}Pb/^{204}Pb$ and (B) $^{208}Pb/^{204}Pb$ for samples of tooth enamel from El-Kurru examined here (with the exception of sample KUR-4 in order to maximize scaling). These are compared to Pb isotope compositions (from Evuk et al., 2017) for samples of juvenile Neoproterozoic crust from the neighboring Arabian Nubian Shield (+, green field) and the Neoproterozoic Saharan Metacraton (*, red field; areas shown in Fig. 1). Also shown is the Pb isotopic evolution curve for average continental crust (S/K; Stacey and Kramers, 1975). Red and black solid circles refer to group designation based on their corresponding Sr isotope compositions (Fig. 4). In (A) El-Kurru samples define a best-fit linear regression line with a slope that corresponds to a secondary isochron age of approximately 700 million years (Ma), which is similar to the age of the surrounding basement rocks of the ANS and SMC. Associated uncertainties are within the size of the symbol.

Fig. 6. Diagrams illustrate U/Pb ratios versus (A) $^{87}Sr/^{86}Sr$ and (B) $^{206}Pb/^{204}Pb$ for samples of tooth enamel from El-Kurru examined here. Red and black solid circles refer to group designation based on their corresponding Sr isotope compositions (Fig. 4) and numbers refer to sample numbers (Tables 1, 2 and 3). The data point corresponding to sample KUR-4 is not

778 shown for scaling purposes due to its extremely radiogenic Pb isotope composition
779 ($^{206}Pb/^{204}Pb$ = 56.351; Table 3). Associated uncertainties are within the size of the symbol.

780 **Fig. 7.** Plots of $^{207}Pb/^{206}Pb$ versus (A) $^{208}Pb/^{206}Pb$ and (B) $^{208}Pb/^{207}Pb$ for samples of tooth
781 enamel from El-Kurru examined here (solid red circles). These are compared to the Pb isotope
782 compositions for a variety of archaeological samples (lead ores, kohls, lead metal, copper
783 alloys, glass, glaze and pigment) within Egypt (Stós-Gale and Gale, 1981; Hassan and
784 Hassan, 1981; Shortland et al., 2006), and those modern-day atmospheric aerosols (**X**= Cairo;
785 += Israel, Lebanon) sampled within the Middle Eastern region (Bollhofer and Rossman,
786 2000). Solid green square represents the present-day (0 million years, Ma) Pb isotope
787 composition of average continental crust (Stacey and Kramers, 1975). Solid green circle and
788 diamond = average Pb isotope compositions of Neoproterozoic metamorphic rocks from SMC
789 and ANS (shown in Fig. 5), respectively; both are calculated using data from Evuk et al.
790 (2017). Of note, the Pb isotope compositions for sample KUR-4, which are significantly more
791 radiogenic signatures (Table 3), are not illustrated for scaling purposes. Abbreviation
792 Precamb. = Precambrian period (older than 541 million years) and Miocene epoch = 23.03 to
793 5.3 million years ago. Associated uncertainties are within the size of the symbol.

794 **Fig. 8.** Plan of the Medieval cemetery at El-Kurru archaeological site showing its position
795 relative to the modern irrigation channel, the brick wall gateway, and later mud-brick
796 domestic architecture adjacent to it (after Dann et al. 2016). The numbers adjacent to red and
797 black solid circles (based on Sr isotope compositions), which indicate position of skeletal
798 remains within cemetery, correspond to sample numbers (Tables 1, 2 and 3). Also shown are
799 their Pb contents (ppm, purple text). Empty circles represent locations of skeletal remains not
800 investigated here.

Trace element and Pb and Sr isotope investigation of tooth enamel from archaeological remains at El-Kurru, Sudan: Evaluating the role of groundwater-related diagenetic alteration

Antonio Simonetti[a*], Michele R. Buzon[b], Loretta Corcoran[a], Abagail M. Breidenstein[c], Geoff Emberling[d]

a: Department of Civil and Environmental Engineering and Earth Sciences, University of Notre Dame, Notre Dame, Indiana 46556, USA

b: Department of Anthropology, Purdue University, West Lafayette, Indiana 47907, USA

c: Institut für Evolutionäre Medizin, Universität Zürich, Winterthurerstrasse 190, 8057 Zürich, Switzerland

d: Kelsey Museum of Archaeology, University of Michigan, 434 South State Street, Ann Arbor, Michigan 48109-1390, USA

*: corresponding author: simonetti.3@nd.edu

KEY WORDS: tooth enamel, Pb and Sr isotope ratios, El-Kurru, ICP-MS, groundwater alteration, provenance

ABSTRACT

This study reports new trace element and Pb and Sr isotope compositions of tooth enamel from archaeological remains at a Medieval (Christian) cemetery located adjacent to the Kushite royal cemetery of El-Kurru, Sudan. The archaeological site of El-Kurru is located along the Nile River on the southern edge of the Nubian Plateau; the bedrock geology consists of Neoproterozoic crystalline basement and is overlain by fluvial sandstones and mudstones of Cretaceous age. El-Kurru is situated between two well-developed drainage basins, and in the past has been subjected to periodic (wadi-related) flooding as a result of intense local precipitation events. Enamel samples were taken from 18 individuals of varying ages and both sexes. Trace element abundances for a significant number of samples record elevated ~~(>>1 ppm)~~ concentrations relative to modern ("in-vivo") enamel, including Pb and U; however, the abundances for both elements do not correlate significantly with the contents of the remaining trace elements (~~Sr,~~ Ba, Fe,~~Mn,~~ Mg, Mn, Nd, Sr) investigated here. The calculated enrichment factors for all trace elements studied here relative to average crustal values are not consistent with anthropogenic addition, which is corroborated by the Pb isotope results. The Sr isotope compositions define 2 main groups that yield $^{87}Sr/^{86}Sr$ ratios that are either higher or lower than 0.7072 with similar Sr abundances (range between ~100 and ~400 ppm). The Pb isotope compositions are extremely variable and correlate well with their corresponding U/Pb ratios; the former overlap Pb isotope ratios~~values~~ for proximal Neoproterozoic rocks belonging to the Saharan Metacraton and Arabian Nubian Shield tectonic provinces. The combined trace element abundances and Sr and Pb isotope compositions for the enamel samples located within the Christian cemetery at El-Kurru are best interpreted to record interaction with ~~Pb- and U-bearing~~ groundwater that occurred post-mortem during flooding events. ~~The results reported here indicate that~~As reported

in previous anthropological studies of a similar nature, the Pb isotope results reported here~~systematics~~ are particularly sensitive to monitoring post mortem diagenetic alteration given their extremely low abundances in non-altered tooth enamel. In contrast, ~~the Sr isotope compositions do not correlate either with their corresponding Pb isotope results, or with their U/Pb ratios (or Pb or U abundances independently). This suggests that~~ the $^{87}Sr/^{86}Sr$ ratios have been minimally perturbed by post mortem alteration, and therefore most likely represent individuals with distinct Sr isotopic signatures inherited from different geographic regions.

1. INTRODUCTION

1.1. ~~Ancient population migration and use of~~ $^{87}Sr/^{86}Sr$ ratios as provenance indicator and evaluating post mortem diagenesis in human tooth enamel

~~The Nile River Valley has been viewed as an 'interactive cultural highway' (Graves, 2018) in northeast Africa since the drying of the Sahara led to early settlement along the river beginning in about 5000 BCE (Smith 2018). Buzon et al. (2016) adopted a multi-dimensional approach to examine population dynamics and cultural transformations in the frontier zone of ancient Nubia and Egypt during a period of rapid governmental transition from Egyptian colony to independent Nubian Napatan state (*ca.* 1400 – 650 BCE), in particular based on excavations at the site of Tombos (Fig. 1). Buzon et al. (2016) combined strontium isotope analysis ($^{87}Sr/^{86}Sr$ values) of residential mobility with mortuary and craniometric analyses to evaluate the circumstances that contributed to the transformations in identity.~~

The use of strontium isotope ($^{87}Sr/^{86}Sr$) compositions has~~ve~~ made an important contribution to understanding the provenance of materials in archaeology and interactions and migrations of ancient civilizations throughout the globe; such examples include Roman mobility in Europe (e.g., Schweissing and Grupe, 2003; Evans et al., 2006; Chenery et al., 2010) and the movements of the Wari, Inca, and Tiwanaku in South America (e.g., Knudson, 2008; Andrushko et al., 2009; Slovak et al., 2009; Turner et al., 2009; Buzon et al., 2012). On Earth, the $^{87}Sr/^{86}Sr$ ratios of biological and geological materials vary as a function of the geological provinces, which are dependent on their age, and mineralogical make-up. Areas that are characterized by older bedrock with a higher proportion of minerals containing high Rb/Sr, such as micas (e.g., biotite, muscovite, alkali feldspar), will yield higher $^{87}Sr/^{86}Sr$ ratios compared to regions that contain younger rocks with lower Rb/Sr ratios. The reason being that the parent nuclide, ^{87}Rb, decays to

the stable daughter isotope, ^{87}Sr, via beta decay (half-life of ~50 billion years). The $^{87}Sr/^{86}Sr$ ratios are then transferred into the hydrosphere and ecosphere through weathering. Animals record the $^{87}Sr/^{86}Sr$ compositions from their environment and diet and this signature is subsequently incorporated into their organic and skeletal tissues. Organic tissues that grow continuously, such as hair, teeth, bones, and tusks, may record temporal variations in the $^{87}Sr/^{86}Sr$ ratios, which can then be used to decipher migration patterns of individuals or groups from ancient civilizations. For example, Buzon et al. (2016) have effectively used the Sr isotope compositions of dental remains and faunal samples from archaeological sites of interest in Egypt's Nile Valley to distinguish between local (autochthonous) and non-local (allochthonous) populations. Of importance and as outlined in Bataille et al. (2018), $^{87}Sr/^{86}Sr$ ratios display a high resolution but predictable scalar spatial pattern that follow geological regimes and limited temporal variability. Therefore, spatiotemporal patterns of $^{87}Sr/^{86}Sr$ ratios in the geosphere, ecosphere and hydrosphere may provide precise and unique geolocation potential for provenance studies.

~~*1.2. Evaluating post mortem diagenesis*~~

Caution must be exerted, however, when employing the Sr isotope compositions for the purposes of provenance determination as diagenetic modification by cumulative physical, chemical and/or biological alteration can perturb the original Sr isotopic signatures incorporated within ancient skeletal remains (e.g., Retzmann et al., 2019). Subsequent burial, Sr from the soil and/or groundwater of the entombment environment may accumulate in teeth. The predominant hydroxyapatite lattice of the latter may recrystallize and even form secondary minerals (e.g., brushite ($CaHPO_4 \cdot 2H_2O$) or carbonate ($CaCO_3$)) in micro-cracks, pores and vacancies (Nelson et al., 1986; Kohn et al., 1999; Nielsen-Marsh and Hedges, 2000; Prohaska et al., 2002; Hoppe et

al., 2003), which may then alter the original, biogenic Sr isotope signature/fingerprint of the sample. In arid environments such as the Nile River valley, crystallization of secondary phases is the predominant process of diagensis rather than bacterial alteration (Maurer et al., 2014; Dudás et al., 2016). Thus, several chemical indices are reported in order to evaluate the potential diagenetic alteration in studies of large populations for provenance identification. For example, elevated (> 250 ppm) and depleted (< 100 ppm) Sr contents in human enamel have been considered as indications of diagenetic changes (e.g., Dudás et al., 2016), which is also a function of the repository conditions (e.g., Sponheimer and Lee-Thorp, 2006). However, the study by Evans et al. (2012) indicate that Sr abundances in fossilized human tooth enamel based on a compilation of 74 archaeological sites in Britain, which yield a median value of 84 ppm, may reflect both diet and climate. Additionally, previous investigations of human and animal skeletal remains have shown that other indicators of diagenetic alteration include Ca/P (mass fraction) ratios above the theoretical value (2.16) of biogenic hydroxyapatite (Sillen, 1986), the presence of increased contents of elements, such as Al, Si, Ba, V, Fe and Mn, and/or the presence of elevated contents of ultra-trace elements (mainly REEs (rare earth elements~~s~~), Y, Hf, Th, U; in vivo < 1 ppm; e.g., Kohn et al., 1999; Trueman et al., 2008; Koenig et al., 2009; Benson et al., 2013; Kohn and Moses, 2013; Willmes et al., 2016; Kamenov et al., 2018; Retzmann et al., 2019). Specifically, Kamenov et al. (2018) developed the maximum threshold concentrations (MTC) index as a means to evaluate post mortem addition of elements into preserved tooth enamel; MTC is calculated (in ppm) by taking the maximum concentration of an element established in pristine (non-altered) modern human tooth enamel and adding 2 times its documented standard deviation (STDEV). Thus, calculated, normalized values of >1 when

comparing elemental abundances for samples to corresponding MTC values indicate post mortem addition (Kamenov et al., 2018).

Recently, Retzmann et al. (2019) developed a novel method for evaluating the degree of diagenetic alteration based on the comparison of the Sr abundances and isotope compositions of enamel and corresponding dentine; the latter exhibits a higher porosity, smaller crystallites, and a much higher organic content (~30%) relative to enamel and is therefore more susceptible to diagenetic alteration. However, the general consensus is that tooth enamel is not significantly affected by diagenesis due to its compact structure with very little pore space and a minor amount of organic content (~ 2 %). Hence, tooth enamel is expected to preserve its original, biogenic Sr isotopic value and represents reliable sample material for investigating mobility and population migration studies (e.g., Kyle, 1986; Lee-Thorp and Sponheimer, 2003; Bentley, 2006; Buzon et al., 2007; Buzon and Simonetti, 2013; Montgomery, 2010; Slovak and Paytan, 2012; Szostek et al., 2015: Buzon et al., 2016; Schrader et al., 2019).

The comparative method outlined by Retzmann et al. (2019) obviously necessitates the analysis of both enamel and corresponding dentine (or bone) from the same individual in order to assess the degree of post-deposition diagenetic alteration. However, this approach may not always be feasible due to sampling issues. In this study, we propose an alternative approach which involves investigating the lead (Pb) isotope signatures in conjunction with the corresponding Sr isotope and trace elemental compositions of tooth enamel.

1.2~~3~~. Pb isotopes as an environmental tracer

The lead and strontium isotopic compositions of an individual's hard tissues (tooth, bone) will reflect their diet (Ericson, 1985). Both elements may readily substitute for calcium in the

hydroxyapatite matrix of teeth and bone (Nelson et al., 1986; Simons, 1986; Bercovitz and Laufer, 1990; Bowen, 2001; Simpson et al., 2021). Tooth enamel of permanent adult teeth forms during early childhood (typically during first 12 years of life) and is considered a dead tissue because it is not penetrated by any organic structures (Steele and Bramblett, 1988). Therefore, tooth enamel will reflect the isotope compositions of the (geologic) environment in which a person lived while the tooth was forming. This consists primarily of the bedrock geology associated with exposed land surfaces (top veneer) on Earth, which is the continental crust.

The continental crust makes up only ~0.6% by mass of the silicate Earth, but it does contain a very large proportion (20-70%; Rudnick and Fountain, 1995) of incompatible elements; ~~(~~ the latter are preferentially incorporated in Earth's crust and not the upper mantle due to incompatible size and/or charge in predominant mantle minerals~~20–70%, depending on element)~~, which includ~~e~~ing uranium (U) and lead (Pb). Lead has 4 isotopes: ^{204}Pb, ^{206}Pb, ^{207}Pb, and ^{208}Pb, and the latter three are the stable daughter products from the radiogenic decay of long-lived isotopes ^{238}U, ^{235}U, and ^{232}Th, respectively, in addition to their primordial abundances present at the time of solar system/Earth formation. In contrast, ^{204}Pb is the only non-radiogenic isotope of Pb, and its abundance is thus constant in nature. Therefore, the present-day Pb isotope composition of any geological sample is a function of its Pb isotope composition at the time of its formation, the U−Pb-Th ratios, and its age. Due to the large variations in the geochemical behavior of U, Th, and Pb, the Pb isotopic composition of rocks, minerals (e.g., galena – PbS), and ores display a significant natural variation, which can be used as an isotopic "fingerprint." As such, this fingerprint may be employed to link Pb ores and the industrial (anthropogenic) materials produced from them (Brill and Wampler, 1967; Iñañez et al., 2010; Sangster et al., 2000). Moreover, ancient civilizations have extracted Pb from ore deposits over thousands of

years for a variety of purposes (metallurgical, medicinal, and industrial), hence, rendering Pb one of the most heavily utilized metals during human history. Previous investigations have demonstrated that reporting the Pb isotope compositions of archaeological materials, such as kohls and glass (e.g., Shortland, 2006) and pottery glazes (e.g., Iñañez et al., 2010; Schurr et al., 2018), ~~and~~ the mineral galena (PbS) (e.g., Shortland, 2006; Mirnejad et al., 2011, 2015), and ancient human and prehistoric animal teeth (Samuelsen and Potra, 2020) is~~are~~ effective for shedding light on transport and trade practices of metals and ores in ancient civilizations and source attribution purposes in crustal environments.

Numerous previous human epidemiological investigations indicate that Pb abundances in hard tissues such as bone and tooth typically represent a longer-term indicator of several years (e.g., Gulson, 1996; Johnston et al., 2019). Unlike the relatively high concentrations of Sr (hundreds of ppm) in tooth enamel and dentine, the range of Pb abundances in teeth is in general an order of magnitude lower (i.e., ~1 to 10s of ppm; Gulson, 1996; Purchase and Fergusson, 1986; Wychowanski and Malkiewicz, 2017; Johnston et al., 2019). Higher Pb contents in hard tissue may be indicative of exposure to elevated levels of this metal in the environment, whether it is of natural (geogenic) or anthropogenic (human-related) origin. However, it is only through the combined investigation of both the Pb abundances and their corresponding isotopic compositions can an accurate assessment or interpretation be rendered in relation to source attribution purposes.

In this study, the Sr and Pb isotope compositions and trace element abundances of tooth enamel are reported for human remains buried at El-Kurru, Sudan (Fig.1; Emberling et al., 2013; Emberling et al., 2015; Dann et al., 2016). The burials were part of a Medieval (Christian) walled settlement (ca. 600-1400 CE) located on the edge of the Nile floodplain. The Kushite royal

cemetery for which El-Kurru is known is located some 400 m to the northwest, on the edge of the desert plateau. This site was chosen for investigation because of the overall poor preservation of the skeletal remains and its unique location in relation to several well-developed drainage systems along the Nile River at El-Kurru. Evidences obtained from taphonomy and observed diagenetic changes in skeletal remains indicate that the site has experienced periodic flooding, and therefore, these events may have impacted the isotopic and trace elemental abundances preserved in tooth enamel for individuals at this site.

2. LOCAL GEOLOGY, HYDROLOGY and SAMPLES

2.1. Local Geology

El-Kurru is located along the Nile River on the southern edge of the Nubian Plateau, which consists of a Neoproterozoic bedrock core that is overlain by horizontal sedimentary rocks (Fig. 1; Dann et al., 2016). The site of El-Kurru is situated proximal to the suture between the Arabian Nubian Shield (ANS) and Saharan Metacraton (SMC) in the Bayuda Desert (Fig. 1). The crystalline basement rocks within the ANS are interpreted as juvenile (newly formed) Neoproterozoic crust and represent dismembered ophiolite (e.g., Abdel-Rahman, 1993; Abdelsalam et al., 1998), whereas those from the SMC represent older cratonic crust that was deformed during the Neoproterozoic (between ~1000 and ~550 Ma), and consist of polymetamorphic amphibolite from magmatic arc environments (e.g., Küster and Liégeois, 2001). The bedrock at the site consists of overlying fluvial sandstones and siltstones of probable Cretaceous age (Geological Research Authority of the Sudan, 1988, Geologic Map of Sudan). At

El-Kurru, the Nile has carved into the Neoproterozoic crystalline basement and there is localized floodplain development (Dann et al., 2016).

Within the royal cemetery, the rock exposures in the staircases and chambers consist of a sequence of Cretaceous sandstones, siltstones, and mudstones >5 m thick (Dann et al., 2016). The lowest unit comprises alternating layers of sandstone, siltstone, and mudstone (with thicknesses ~1.5 to ~2 m) that represent either channel (sandstone) or floodplain deposits of ancient rivers (Dann et al., 2016). Moreover, the top of the lowermost sandstone unit is overlain by a paleosol, which consists of thin layers of hard, Fe-cemented, typically fine-grained sediments that represent buried soil horizons; therefore, these may be referred to as ferricretes (Dann et al., 2016). These Cretaceous-aged rock units are overlain unconformably by a thin layer of sandy Quaternary gravels.

2.2. Hydrology

The site of El-Kurru is situated between two large, well-developed drainage basins, but the area itself is drained by a smaller and less developed drainage system (Dann et al., 2016). Large-scale flooding events along the Nile are related primarily to the humid climate present at the southern headwaters' region, and three such episodes were recorded in 1946, 1988, and 1994 (Dann et al., 2016). In contrast, the flooding of the wadi draining the site at El-Kurru is attributed to intense local precipitation events, which in a typical year can occur two to three times and results in strong, channelized, knee-deep (at best) flow for about one hour (Dann et al., 2016). Recent excavations revealed that the late mortuary temple located next to the wadi was flooded and ~500 mm of sediment was deposited (Emberling et al., 2015); it is postulated that overland flow from areas surrounding the temple likely contributed to this depositional event. Taphonomy and diagenetic changes have most likely been impacted by water damage that has affected the

cemetery for centuries. This cemetery was located at an opening fan of a seasonal wadi and close to the banks of the Nile; it is in close proximity to flooded irrigated palm groves and other agricultural land still in use. Therefore, it is very likely that the cemetery and skeletons have incurred water damage over the centuries.

2.3. Samples

Excavations in 2014 to 2016 uncovered 27 individuals in the Christian cemetery, of which 18 were examined in this study. ~~and a~~A Christian date for these graves was suggested based on the scarcity of grave goods as well as approximate west-east orientation (relative to the Nile River) and treatment of the bodies; heads of all individuals were oriented cardinally in the northwestern direction, their feet in the southeast, with either their arms or ankles crossed (Dann et al., 2016; Welsby, 2002). Radiocarbon dating of the El-Kurru skeletons has proven difficult due to the poor preservation of collagen. Thus, date estimations are based on the ^{14}C dating of the fortification wall, the mortuary archaeology, and stratigraphy of the skeletal remains. Organics from the wall were C^{14} dated to *ca*. 600-1000 CE (Dann et al., 2016). Additionally, pottery sherds and decoration motifs date the fills to Classic (*ca*. 800-1100 CE) or Late Christian (*ca*. 1100-1450 CE) and one Islamic glass bead was found in an unusual context, but still indicate these burials date at *ca*. 1450 CE. Lastly, the stratigraphy of the cemetery indicates that these burials represent the last phase of occupation in this area. Table 1 lists the approximate ages, sex and burial depths associated with the type of tooth enamel sample investigated in this study. Of note, not all 27 individuals uncovered were examined/sampled due to either extremely poor preservation of the tissue leading to not enough material to sample, teeth not recovered from an individual (e.g., adult KU216 was edentulous), and/or that some subadults did not have enough mineralized material for testing. For this study, sample selection included intact teeth whenever possible and

Formatted: Superscript

those with enamel that was macroscopically in good condition. Generally, all tooth preservation was graded as good or satisfactory (Enamel Preservation Classification Score of between 3 and 4; Montgomery, 2002). Most crowns were fully intact (i.e., not too fragmented) with some thin cracks, some superficial soil concretions or evidence of plant abrasion, and in some cases separation from the underlaying dentine. Despite the presence of such damages and moderate to severe occlusal attrition in almost all adult teeth, the enamel of the selected teeth was generally hard, glossy, and milky-white with only some small areas of discoloration. Some teeth were previously harvested of dentine for ancient DNA analysis in a clean lab. When sampled, the crown was removed from the root with a thin sectioning blade for access to the inner dentine for sampling, leaving the crown enamel intact for further processing. Enamel samples were mechanically cleaned and abraded before chemical purification to reduce post-depositional contamination.

3. ANALYTICAL METHODS

3.1. Trace element geochemistry

Samples of tooth enamel were processed in two steps. In the first step, between ~70 and ~300 mg of enamel was placed in a 15 mL Savillex® Teflon beaker and ~4 ml of concentrated 16N, double-distilled (DD)~~, concentrated (16N)~~ HNO_3 was added, followed by heating on a hotplate at 110° C for 24h. After the heating, samples were removed from the hotplate and cooled for one hour. After rinsing the sample residues adhered to the sides of the beakers with 18 MΩ cm^{-2} water, samples were placed back on the hotplate to achieve complete dryness. In the second cycle, all conditions were kept the same, except the amount of ~~DD (~~16N~~)~~ DD HNO_3 acid was decreased from 4 to 1 mL. After the last drying step, 5 mL of ~~DD (~~16N~~)~~ DD HNO_3 acid was

added into the beaker and the solution diluted with 18 MΩ cm^{-2} water until a final total volume of ~100 mL was achieved. Appropriate sample volume aliquots for trace element and Sr and Pb isotope analyses were taken from the 100 mL solution. The concentrations of the trace elements (Table ~~1~~2) were determined by a standard/spike addition method (Jenner et al., 1990), which includes correction for matrix effects and instrumental drift.

The trace element abundances (Table ~~1~~2) for all samples were determined using an Attom (Nu Instruments Ltd., Wales, UK) high resolution inductively coupled plasma mass spectrometer (HR-ICP-MS) in medium mass resolution mode (M/ΔM ≈ 3000). Samples were processed using a wet plasma, solution mode introduction system that consists of a cyclonic spray chamber (housed within a Peltier cooling device @7° C) and Meinhard nebulizer (aspiration rate of 0.1 mL/min). Before each analytical session, the Attom instrument was tuned and calibrated using a multi-elemental (Li, B, Na, Si, Sc, Co, Ga, Y, Rh, In, Ba, Lu, Tl, U) 1 ppb (ng g-1) standard solution.

~~For this purpose, e~~Enrichment factors (EF) have been calculated for each sample for ~~each of these elements~~ several of the trace elements (e.g., Mn, Sr, Pb, U) with elevated contents (relative to in vivo, modern day human enamel), ~~-~~and these are listed in Table 2. The EFs evaluate the relative contribution from either natural (i.e., soil, bedrock) vs. anthropogenic sources (e.g., ores used for kohl or ceramic glaze production) of a given element in the tooth enamel. $EF_{ELEMENT}$ is defined as the concentration ratio of a given element to that of Mg in this case (or any other element thought to be derived exclusively from a crustal source, such as Si, Al) normalized to the same concentration ratio characteristic of the upper continental crust (e.g., Rudnick and Gao, 2014). In this study, Mg was chosen for this normalization since it is typically an element of natural origin and may substitute for Ca in tooth enamel (LeGeros, 1991); in addition, Mg

contents do not correlate with any of the other trace elements investigated here (not shown). For example, the enrichment factor for Pb is thus: $(EF)_{Pb} = [Pb/Mg]_{sample}/[Pb/Mg]_{crust}$. However, given the large natural variations in the composition of crustal materials exposed to surface erosion and the diversity of biogeochemical processes affecting soil development at a global scale, enrichment factors within ±10 times the mean crustal abundances (i.e., EF values between 0.1 to 10) most likely indicate elements derived from continental crust (Duce et al., 1976). Conversely, any $(EF)_{element} > 10$ suggests contributions from other sources, such as human activities.

3.2. Sr isotope compositions

Separation and purification of Sr for subsequent Sr isotope analysis involved ion exchange chromatography, which employed columns containing 1.7 mL of 200-400 mesh AG50W-X8 resin. Sample aliquots (containing ~300 ng total Sr) in 0.25 mL of 2.5N DD HCl were loaded onto the resin beds~~;~~ this was followed by several additional wash steps totaling ~15 ml of 2.5N DD HCl acid, and the Sr was subsequently eluted with 4 mL of 2.5N DD HCl. After the ion exchange chemistry, Sr-bearing aliquots were dried, dissolved in 2% HNO_3 solution (~2 mL) and aspirated into the ICP torch using a desolvating nebulizing system (DSN-100 from Nu Instruments Ltd.). Strontium isotope measurements were conducted using a NuPlasma II MC-ICP-MS (multi-collector inductively coupled plasma mass spectrometer; Nu Instruments Ltd.) instrument according to the protocol outlined in Balboni et al. (2016). Strontium isotope data was acquired in static, multi-collection mode using 5 Faraday collectors for a total of 400 s, consisting of 40 scans of 10 s integrations. The analytical protocol's accuracy and reproducibility were verified by analyzing the NIST SRM 987 strontium isotope standard during two~~the~~

analytical sessions, which yielded an average value of 0.710235 ± 0.000044 (2σ; n=4), in agreement with the certified value of 0.710245 (Faure and Mensing, 2005).

3.3. Pb isotope compositions

The Pb separation method is adapted from Manhes et al. (1980) and a brief summary is provided here (after Koeman et al., 2015). The Pb ion exchange micro-columns consist of approximately 20 µL of clean AG1-X8 resin (75−150 mesh) placed into a polypropylene tube combined with a polystyrene frit. The resin volume is cleaned using 0.15 mL of ultrapure (18 MΩ cm^{-2}) H_2O, and further conditioned with 0.15 mL of 0.8 N DD HBr. The sample solution was loaded with 0.6 mL of 0.8 N DD HBr, washed twice with 0.15 mL of 0.8 N DD HBr, and last eluted with 0.7 mL of 6 N DD HCl acid. After the eluted Pb is dried down, the ion exchange procedure is repeated with fresh resin in order to further purify the Pb aliquot. Following the last elution procedure, the Pb aliquot is dried down and dissolved again in 2% HNO_3 for solution mode MC-ICP-MS analysis.

Pb isotope compositions of the sample solutions were determined using the same procedure outlined in Simonetti et al. (2004). After the purification steps, the aliquot of Pb was spiked with a NIST SRM 997 Thallium standard solution (2.5 ppb). Seven Faraday cups on the Nu Plasma II MC-ICPMS instrument were employed to simultaneously measure the Pb and Tl isotopes and ^{202}Hg. The instrumental mass bias (exponential law; $^{205}Tl/^{203}Tl = 2.3887$) is determined by measuring the $^{205}Tl/^{203}Tl$, and ^{202}Hg is monitored to correct for the interference of ^{204}Hg on ^{204}Pb. Prior to the aspiration of the samples into the plasma, ion signals for the gas and acid blanks ("on-peak-zeros") were recorded for 30 s to determine baseline values. For each analysis, data acquisition involved 2 blocks of 25 scans (each scan has a 10 s integration time). A 25-ppb solution of the NIST SRM 981 Pb standard (spiked with 6 ppb NIST SRM 997 Tl standard) was

measured periodically during the analytical session in order to validate the Pb isotope results. The average Pb isotope ratios and associated 2σ standard deviations obtained on 3 measurements of the NIST SRM 981 Pb isotope standard for two analytical sessions are as follows: $^{206}Pb/^{204}Pb$= 16.939 ±0.007, $^{207}Pb/^{204}Pb$= 15.493 ±0.007, $^{208}Pb/^{204}Pb$= 36.699 ±0.008, $^{208}Pb/^{206}Pb$= 2.1666 ±0.0002, and $^{207}Pb/^{206}Pb$= 0.91464 ±0.00004, which overlap with certified values for this standard.

4. RESULTS

Tables 2 and 3 list the trace element abundances and Sr and Pb isotope compositions for the 18 samples of tooth enamel from El-Kurru investigated here, respectively; these data are also illustrated in Figures 2 to 6. The Sr abundances for the tooth enamel vary between 106 and 425 ppm (Table 2; Fig. 2), and a majority fall within the range considered to represent diagenetically unaltered material (between 100 and 250 ppm; Dudás et al., 2016). Six samples (KUR-3, -7, -12, -14, -15, -16) contain elevated Sr abundances (>250 ppm and up to 425 ppm; Table 2; Fig. 3). Figure 2 plots the concentrations of Sr versus those for several trace elements, Mg, Ba, and U; Mg abundances do not exhibit any correlation with Sr contents (Fig. 2a), whereas Ba and U show either fairly good positive or weak correlations (R^2 correlation coefficient ≈ 0.74), respectively (Fig. 2b, c). The contents of Mn, Ba, and Pb versus those of U are also illustrated in Figures 2d-f, and these in general all correlate positively. Of particular note, the contents of U, Nd, and Fe ~~and Pb~~ reported here for all ~~several~~ samples ~~, which range from <1 to 1.40 ppm and <1 to ~62 ppm, respectively (Table 2)~~, exceed MTC normalized values >1 (Figure 3), which are ~~those~~ considered to represent pristine samples of modern-day tooth enamel (i.e., *in vivo*; ~~<1 ppm; e.g., Kohn et al., 1999; Trueman et al., 2008; Koenig et al., 2009; Benson et al., 2013; Kohn and Moses, 2013;~~

Formatted: Superscript

~~Willmes et al., 2016;~~ Kamenov et al., 2018). In Figure 3, the normalized MTC values for the remaining elements are all <1 with the exception of Mn and Ba, which fluctuate slightly on either side of unity. Overall, the normalized MTC patterns shown in Figure 3 are not consistent for the samples investigated. Lastly, the vast majority of the enrichment factors (EFs) listed for Mn, Pb, Sr, and U in Table 2 vary between 1 (or <1) and 10, with the exception of tooth enamel sample KUR-11 that records a EF_{Pb} of ~21.

~~Given the elevated contents for several of the trace elements (Mn, Sr, Pb, U), it is therefore important to determine the source of their enrichment, i.e., whether it is natural (geogenic) or anthropogenic (human-related) in origin. For this purpose, enrichment factors (EF) have been calculated for each sample for each of these elements and these are listed in Table 2. The EFs evaluate the relative contribution from either natural (i.e., soil, bedrock) vs. anthropogenic sources (e.g., ores used for kohl or ceramic glaze production) of a given element in the tooth enamel. $EF_{ELEMENT}$ is defined as the concentration ratio of a given element to that of Mg in this case (or any other element thought to be derived exclusively from a crustal source, such as Si, Al) normalized to the same concentration ratio characteristic of the upper continental crust (e.g., Rudnick and Gao, 2014). In this study, Mg was chosen for this normalization since it is typically an element of natural origin and may substitute for Ca in tooth enamel (LeGeros, 1991); in addition, Mg contents do not correlate with any of the other trace elements investigated here (not shown). For example, the enrichment factor for Pb is thus: $(EF)_{Pb} = [Pb/Mg]_{sample}/[Pb/Mg]_{crust}$. However, given the large natural variations in the composition of crustal materials exposed to surface erosion and the diversity of biogeochemical processes affecting soil development at a global scale, enrichment factors within ±10 times the mean crustal abundances (i.e., EF values between 0.1 to 10) most likely indicate elements derived from continental crust (Duce et al.,~~

~~1976). Conversely, any $(EF)_{element}$ >10 suggests contributions from other sources, such as human activities. The vast majority of the EFs listed for Mn, Pb, Sr, and U in Table 2 vary between 1 (or <1) and 10, with the exception of tooth enamel sample Kur-11 that records a EF_{Pb} of ~21.~~

The Sr isotope compositions for the KUR enamel samples investigated here define two groups relative to their corresponding Sr contents (Fig. 3; Table 2), and these overlap primarily the range of variable, present-day $^{87}Sr/^{86}Sr$ ratios for metamorphic rocks from the SMC (~0.7030 to ~0.7089) and not the less radiogenic signatures for rocks from the ANS (~0.7030 to ~0.7053) tectonic province (Evuk et al., 2017).

As discussed earlier, assessing the Pb isotope compositions of geological, environmental, or industrial samples provide an effective means for provenance determination. Table 3 lists the Pb isotope compositions for the tooth enamel samples investigated here, and these are illustrated in Figures 4 to 6. In Fig. 4, the Pb isotope data for the tooth enamel samples are compared to those for rocks belonging to both the neighboring SMC and ANS tectonic provinces (Evuk et al., 2017), which indicate a substantive degree of overlap, in particular with those from the SMC. In addition, Fig. 4 also contains the Stacey and Kramers (1975) evolution curve, which represents the time-integrated Pb isotope composition of average continental crust over the past 3.7 billion years. The Pb isotope compositions for the El-Kurru enamel samples mainly plot above and to the right of the Stacey and Kramers (1975) Pb evolution curve (S/K), and define well constrained linear arrays. In the $^{206}Pb/^{204}Pb$ versus $^{207}Pb/^{204}Pb$ plot, the best-fit regression line defines a slope of 0.0629, which corresponds to a Neoproterozoic $^{207}Pb/^{206}Pb$ age of approximately 705 million years old; the latter corresponds to the age of the crystalline basement in the region (e.g., Evuk et al., 2017). Typically, any linear array on a Pb-Pb isotope plot is considered to represent either binary mixing between two distinct end-member components (i.e., resulting from open system

Formatted: Superscript

Formatted: Superscript

behavior), or may simply reflect the addition of radiogenic Pb resulting from the decay of U over geologic time. Both of these hypotheses will be evaluated and discussed in the following section.

5. DISCUSSION

Figure 3 plots the Sr abundances versus their corresponding $^{87}Sr/^{86}Sr$ ratios for the tooth enamel samples from El-Kurru examined here. Hypothetically, enamel for individuals that lived or originated from the same geologic area and have not been affected by post mortem diagenesis should define a restricted field; in particular, the range in Sr contents should ideally be restricted between 100 and 250 ppm for non-diagenetically altered samples (e.g., Dudás et al., 2016). Overall, a majority of the enamel samples from El-Kurru plot within this range of Sr abundances (Fig. 3) and define two groups in relation to their Sr isotope compositions. The group of samples with lower $^{87}Sr/^{86}Sr$ ratios (<0.7072) define a relatively restricted range (~0.7066 to ~0.7070) and do not correlate with their corresponding Sr contents; whereas the second group with more radiogenic Sr isotope compositions record more variable (~0.7074 to ~0.7083) ratios~~values~~ and seem to correlate positively with their Sr abundances (Fig. 3). Thus, the bimodal distribution in the Sr isotope results reported here, in particular for enamel samples with Sr abundances between 100 and 250 ppm (as outlined in Fig. 3), can be interpreted to either represent individuals originating from different regions (i.e., local vs. immigrant), or possibly reflect different degrees of diagenetic alteration.

In order to better evaluate the post mortem alteration hypothesis, Figure 5 illustrates the $^{87}Sr/^{86}Sr$ ratios versus their corresponding U/Pb values for the El-Kurru enamel samples studied here since the latter parameter may be used to evaluate the degree of diagenetic alteration (e.g., Kohn et al.,

1999; Trueman et al., 2008; Koenig et al., 2009; Benson et al., 2013; Kohn and Moses, 2013; Willmes et al., 2016; Kamenov et al., 2018). The group of enamel samples characterized by the lower Sr isotope compositions record a larger range of U/Pb ratios (~0 to ~1.5) compared to those for the radiogenic (higher) group of enamel samples (~0 to ~0.3; except for sample KUR-1), with the latter defining a positive trend (Fig. 5a). Moreover, the U/Pb values are in general positively correlated with their Pb isotope compositions (Fig. 5b), which indicate that these record the addition of radiogenic in-growth of Pb originating from the time-integrated decay of U. On the basis of solely the U/Pb ratios reported here, it is difficult to discern exactly which enamel samples record non-diagenetically altered ^{87}~~sr~~/^{87}Sr/^{86}Sr ratios since both groups exhibit trends that may be attributed to the addition of U post-mortem (Fig. 5).

An alternative approach is to compare the Pb isotope ratios for the enamel samples reported here to those for pertinent atmospheric, geological, and anthropogenic (i.e., exposure to extracted Pb ores for human purposes) ~~e.g., Pb-bearing mineral ores,~~ (e.g., pottery glazes, kohls) samples reported within the region of the Nile River Valley. Given the unique geochemical nature of the U-Pb radiogenic isotope system, Pb-Pb isotope plots (e.g., Fig. 6) are an effective tool in assessing open-system behavior or mixing of Pb from multiple sources. If a suite of samples has indeed been affected by either of the latter processes, then the result is that the Pb isotope data will be define linear arrays and plot between the two end-member compositions. In Fig. 6, the Pb isotope compositions for the enamel samples from El-Kurru define well-constrained linear arrays with enamel sample KUR~~ur-~~4 recording the most distinct and elevated Pb isotope ratios (Table 3). The results reported here from El-Kurru are compared to those from the studies of Stós-Gale and Gale (1981), Hassan and Hassan (1981), and Shortland et al. (2006), which examined the compositions for a variety of archaeological samples (lead ores, kohls, lead metal, copper alloys,

glass, glaze and pigment) within Egypt, which also define a well-constrained linear array (Fig. 6), but with a completely different slope. Both plots in Figure 6 clearly indicate that the linear arrays defined by the El-Kurru samples are unique when compared to existing data for various environmental and anthropogenic samples within the Nile River Valley. The two linear arrays appear to converge at higher $^{207}Pb/^{206}Pb$ ratios~~values~~ (Fig. 6). Also shown in Fig. 6 are the Pb isotope compositions for modern-day atmospheric aerosols sampled within the Middle Eastern region (Bollhofer and Rossman, 2000); these plot at much higher $^{207}Pb/^{206}Pb$ ratios and do not appear to involve the same end-member (natural and anthropogenic) components as those required to explain the data from either El-Kurru, or other archaeological samples from within the Nile River Valley. Figure 6 also displays the Pb isotope composition of present-day, average continental crust (Stacey and Kramers, 1975) and the average signatures~~values~~ for Neoproterozoic metamorphic rocks belonging to the SMC and more juvenile samples from the ANS (from Evuk et al., 2017; shown in Fig. 4); these data also plot close to the point of convergence for the Pb-Pb mixing arrays defined by the El-Kurru and Egyptian archaeological samples. Therefore, we postulate that Pb derived from regional bedrock (crust) is one end-member of the El-Kurru mixing line. The second end-member for the El-Kurru requires a component that is U-rich or characterized by a high U/Pb ratio.

Lead present in natural samples that have not been impacted by the addition of U subsequent their time of formation are characterized by Pb isotope compositions that are a function of their age (and their original U/Pb ratio) and these define a relatively restricted range in nature (e.g., $^{207}Pb/^{206}Pb$: ~0.83 to ~1.1 for samples between 0 and 3,000 million years old). In contrast, Pb present in natural samples that was derived solely from radiogenic sources, i.e., it is the result of U decay with no other Pb present at the time of formation is also age dependent and will be

462 characterized by much lower Pb isotope ratios (e.g., $^{207}Pb/^{206}Pb$: ~0.04 to ~0.4). For example, as
463 stated earlier, the best fit linear regression in Figure 4a defined by the tooth enamel samples from
464 El-Kurru has a slope ~0.0629, which corresponds to Neoproterozoic $^{207}Pb/^{206}Pb$ secondary
465 isochron age. Hence, a sample containing a mixture of natural (geogenic) Pb from its initial time
466 of formation and possibly radiogenic Pb accumulating from a U-rich endmember will record a
467 mixed Pb isotopic signature. Therefore, the Pb-Pb isotope arrays defined by the enamel samples
468 from El-Kurru (Fig. 6) most likely represent mixing between background, crustal Pb and
469 radiogenic Pb accumulated from U-bearing groundwater. Typically, dissolved U is found in most
470 surface water and groundwater at very low concentrations (ppb or ng g^{-1} range), and at much
471 higher values when associated with highly mineralized, thermal and brine waters (Kumar et al.,
472 2011). During bedrock and soil interaction with groundwater, radionuclides may transfer by
473 dissolution, desorption, and erosion (Vongunten and Benes, 1995). The transport of U and other
474 radionuclides in groundwater is dependent on the presence of fractures or faults and their
475 interconnectivity within the bedrock. Moreover, the transport (movement) of U within
476 groundwater depends on multiple factors including diffusion, emanation, and permeability of the
477 rocks (Lopez et al., 2002). The source of U and the radiogenic Pb incorporated into the samples
478 of tooth enamel most likely emanates from the surrounding Neoproterozoic sandstones and
479 mudstones, which are most likely characterized by U contents of 1 to 10 ppm (i.e., average
480 continental crust; Rudnick and Gao, 2014). Moreover, given the radiogenic nature of the Pb
481 isotope compositions for several enamel samples (KUR-1, -4, -15; Table 2 and Figs. 5 to 7), the
482 post mortem diagenetic alteration occurred in the recent past so as to provide time to accrue
483 radiogenic Pb from the radioactive decay of U.

Given the elemental abundances and Pb isotope compositions reported here (Tables 2 and 3; Figs. 2 to ~~6~~7), tooth enamel samples KUR~~ur~~-3, -12, -16, and -18 contain relatively similar Pb isotope compositions and plot closest to the natural Pb endmember component (Fig. 6); these samples also record elevated contents of Pb (between ~3 and ~23 ppm) and higher corresponding EFs (relative to the remaining samples; Table 2), which suggest these samples have been significantly impacted by groundwater diagenetic alteration. In general, the Pb isotope compositions for most samples correlate with their corresponding U/Pb values (Fig. 5b), and therefore, the Pb-Pb isotope arrays defined by the El-Kurru enamel samples and illustrated in Fig. 6 are interpreted to represent diagenetic alteration by groundwater with variable U/Pb ratios. Of particular importance, these 4 enamel samples (KUR~~ur~~-3, -12, -16, and -18) belong to both groups of Sr isotope compositions (Fig. 3), and their Pb concentrations don't correlate with their corresponding $^{87}Sr/^{86}Sr$ ratios; for example, samples KUR~~ur~~-1, -2, and -11 record similar, higher $^{87}Sr/^{86}Sr$ ratios (range from 0.70748 to 0.70772; Fig. 3; Table 2) but contain extremely variable Pb contents of 0.16, 1.28 and 61.95 ppm (Table 2), respectively. Moreover, Pb contents and Sr isotope compositions of tooth enamel reported here are not a function of their location within the burial site. Figure 7 illustrates the locations of the skeletal remains at the El-Kurru burial site for the individuals investigated here, and the enamel samples with the highest Pb concentrations and least radiogenic Pb isotope compositions appear to be concentrated into 2 areas. Within these areas, enamel samples are characterized by a wide range of $^{87}Sr/^{86}Sr$ ratios~~values~~ (from both groups; Fig. 7), and therefore, this feature may be explained in two ways. The first being that the Sr isotope compositions do indeed reflect differing provenance and their $^{87}Sr/^{86}Sr$ ratios were buffered, or not affected by diagenetic alteration because of the much higher contents of Sr in tooth enamel versus that found in groundwater. The fact that there is no correlation between the

507 Sr and Pb isotope compositions (or between Pb contents and Sr isotope ratios) for the tooth
508 enamel samples investigated here lends support to this interpretation. An alternative explanation
509 is that the groundwater entering the shallow burial pits was characterized by variable Sr isotopic
510 compositions, which reflects the Sr isotopic heterogeneity ($^{87}Sr/^{86}Sr$ ratios range between
511 ~0.7032 and ~0.7089) for the surrounding Neoproterozoic basement rocks; these consist of a
512 variety of metamorphic rocks (metagabbro, amphibole schist, granulitic amphibolite) within the
513 surrounding Saharan Metacraton (Evuk et al., 2017). However, there is only an approximate
514 maximum difference of 1.25 m in burial depth elevations for the individuals investigated here
515 (Table 1); therefore, it seems unlikely that the varying Sr isotope compositions reflect a variable
516 hydrological regime that is controlled by the local bedrock geology since the host Cretaceous
517 mudstones, siltstone, and sandstone units are in general of greater thickness than the variation in
518 burial depth (Dann et al., 2016). Moreover, there are no correlations exhibited (not shown)
519 between burial depth elevation of the individuals examined here (Table 1) and any elemental
520 (Table 2) or isotope signatures (Table 3). Thus, our preferred interpretation is that the variable Sr
521 isotope compositions for samples with restricted Sr contents (100 to 250 ppm; Fig. 3) represent
522 original and non-diagenetically altered signatures that reflect individuals originating from
523 different areas within this region of Sudan.

524

525 **6. CONCLUSIONS**

526 Based on the trace elemental abundances and Sr and Pb isotope results reported in this study, the
527 main conclusions and interpretations are as follows:

- The elevated trace element concentrations, in particular for those of Pb and U, cannot be attributed to human/anthropogenic activities as evidenced by the low EFs (<10) and corresponding Pb isotope compositions. Hence, it is important to note that the Pb isotope results for the tooth enamel samples from El-Kurru are critical in establishing that the extremely radiogenic (high) ratios~~values~~ originate from natural (geogenic) sources;

- The Pb isotope compositions and accompanying Pb and U contents (U/Pb ratios) indicate that the Christian-age skeletal remains and samples of tooth enamel from El-Kurru have been impacted by groundwater alteration due to the burial site's proximal location to several wadis that have rendered it prone to flooding events in the past;

~~- Mass spectrometric methods such as multi-collector inductively coupled mass spectrometry (MC-ICP-MS) has rendered Pb isotope analysis of small amounts of sample material (100s of picogram (10^{-12}) to nanogram (10^{-9}) levels) reliable, which provides an additional means to better evaluate the pristinity of archaeological materials;~~

- Based on the combined trace element results and Pb and Sr isotope compositions reported here, it is most likely that several individuals (e.g., KUR-1, -2, -8, and -11 *vs*. those characterized by lower Sr isotope ratios; Fig. 3) present within the Christian burial site originated from different geographic regions of Sudan. Assessment of their exact geographic origins are beyond the scope of this present study and will be the focus of future investigation.

ACKNOWLEDGEMENTS

This work was funded by the National Science Foundation (BCS grant #1916718) to A. Simonetti and M.R. Buzon.

550

551

REFERENCES

Abdel-Rahman, E.M., 1993. Geochemical and geotectonic controls of the metallogenic evolution of selected ophiolite complexes from the Sudan. *Berl Geowiss Abh, Reihe A* **145**, 175 pp.

Abdelsalam, M.G., Stern, R.J., Copeland, P., Elfaki, E., Elhur, B., Ibrahim, F.M., 1998. The Neoproterozoic Keraf suture in NE Sudan: sinistral transpression along the eastern margin of west Gondwana. *J. Geol.* **106**, 133-148.

Andrushko, V.A., Buzon, M.R., Simonetti, A., Creaser, R.A., 2009. Strontium isotope evidence for prehistoric migration at Chokepukio, Valley of Cuzco, Peru. *Lat. Am. Antiq.* **20**, 57-75.

Baker J.A., 2004.

Balboni, E., Jones, N., Spano, T., Simonetti, A., Burns P.C., 2016. Chemical and Sr isotopic characterization of North America uranium ores: nuclear forensic applications. *Appl. Geochem.* **74**, 24-32.

Bataille, C.P., von Holstein, I.C.C., Willmes, J.E., Liu, X-M., Davies, G.R., 2018. A bioavailable strontium isoscape for Western Europe: A machine learning approach. *PLoS ONE* **13**, e0197386. doi.org/10.1371/journal.pone.0197386.

Benson, A., Kinsley, L., Willmes, M., Defleur, A., Kokkonen, H., Mussi, M., Grün, R., 2013. Laser Ablation Depth Profiling of U-series and Sr Isotopes in Human Fossils. *J. Archaeol. Sci.* **40**, 2991–3000.

Bentley, A.R., 2006. Strontium Isotopes from the Earth to the Archaeological Skeleton: A Review. *J. Archaeol. Method Theory* **13**, 135–187.

573 Bercovitz, K., Laufer D., 1990. Tooth type as indicator of exposure to lead of adults and
574 children. *Arch. Oral Biol*. **35**, 895-897.

575 Bollhöfer, A., Rosman, K.J.R., 2000. Isotopic source signatures for atmospheric lead: The
576 Southern Hemisphere. *Geochim. Cosmochim. Acta* **64**, 3251–3262.

577 Bowen, W.H., 2001. Exposure to metal ions and susceptibility to dental caries. *J. Dent. Educ.*
578 **65**, 1046-1053.

579 Brill, R.H., Wampler J.M., 1967. Isotope studies of ancient lead. *Am. J. Archaeol*. **71**, 63-77.

580 Buzon, M.R., Conlee, C.A., Simonetti, A., Bowen, G.J., 2012. The consequences of Wari
581 contact in the Nasca region during the Middle Horizon: archaeological, skeletal, and isotopic
582 evidence. *J. Archaeol. Sci*. **39**, 2627-2636.

583 Buzon, M.R., Simonetti, A., 2013. Strontium isotope ($^{87}Sr/^{86}Sr$) variability in the Nile Valley:
584 Identifying residential mobility during ancient Egyptian and Nubian sociopolitical changes in
585 the New Kingdom and Napatan Periods. *Am. J. Phys. Anthropol*. **151**, 1-9.

586 Buzon, M.R., Simonetti, A., Creaser, R.A., 2007. Migration in the Nile Valley during the New
587 Kingdom period: a preliminary strontium isotope study. *J. Archaeol. Sci*. **34**, 1391-1401.

588 Buzon, M.R., Stuart, T.S., Simonetti, A., 2016. Entanglement and the Formation of the Ancient
589 Nubian Napatan State. *Am. Anthropol*. **118**, 284-300.

590 Chenery, C., Müldner, G., Evans, J., Eckardt, H., Lewis, M., 2010. Strontium and stable isotope
591 evidence for diet and mobility in Roman Gloucester, UK. *J. Archaeol. Sci.* **37**, 150-163.

592 Dann, R.J., Emberling, G., Stearns, C., Antis, S., Skuldbol, T., Uildriks, M., Rose, K., Phillips,
593 J., Breidenstein, A., Miller, N.F., 2016. El Kurru 2015-16 Preliminary Report. *Sudan and*
594 *Nubia* **20**, 35-49.

595 Duce, R.A., Hoffman, G.L., Ray, B.J., Fletcher, I.S., Fletcher, W.G.T., Fasching, J.L.,
596 Piotrowicz, S.R., Walsh, P.R., Hoffman, E.J., Miller, J.M., Heffter, J.L., 1976. Trace metals
597 in the marine atmosphere: Sources and fluxes, in: Windom, H.L., Duce, R.A. (Eds.), Marine
598 Pollution Transfer, Lexington Books, Blue Ridge Summit, pp. 77–119.

599 Dudás, F.Ö., LeBlanc, S.A., Carter, S.W., Bowring, S.A., 2016. Pb and Sr Concentrations and
600 Isotopic Compositions in Prehistoric North American Teeth: A Methodological Study, *Chem.*
601 *Geol.* **429**, 21–32.

602 Emberling, G., Dann, R.J., Abdelwahab Mohamed-Ali, M., Skuldbøl, T., Boaz, B., Cheng, J.,
603 Blinkhorn, E., 2013. New Excavations at El Kurru: Beyond the Napatan Royal Cemetery.
604 *Sudan and Nubia* **17**, 42-60.

605 Emberling, G., Dann, R.J., Mohamed-Ali, A.S., et al., 2015. In a Royal Cemetery of Kush:
606 Archaeological Investigations at El Kurru, Northern Sudan, 2014-15. *Sudan and Nubia* **19**,
607 54-70.

608 Ericson, J.E., 1985. Strontium isotope characterization in the study of prehistoric human
609 ecology. *J. Hum. Evol.* **14**, 503-514.

610 Evans, J., Stoodley, N., Chenery, C., 2006. A strontium and oxygen isotope assessment of a
611 possible fourth century immigrant population in a Hampshire cemetery, southern England. *J.*
612 *Archaeol. Sci.* **33**, 265-272.

613 Evuk, D., Lucassen, F., Franz, G., 2017. Lead isotope evolution across the Neoproterozoic
614 boundary between craton and juvenile crust, Bayuda Desert, Sudan. *J. Afr. Earth Sci.* **135**,
615 72-81.

616 Faure, G., Mensing, T.M., 2005. Isotopes: principles and applications (3rd edition). John Wiley
617 and Sons, Inc., Hoboken, New Jersey.

618 Geological Research Authority of the Sudan, 1988. Geologic Map of Sudan. Ministry of Energy
619 & Mines, Geological & Mineral Resources Department, Khartoum.

620 Graves, C., 2018. Intercultural Communication: Egypt and Nubia c. 2543-1076BC.
621 Connections. University of Birmingham online exhibition catalogue.
622 https://www.birmingham.ac.uk/research/activity/connections/Essays/CGraves.aspx (accessed
623 29 October 2018).

624 Gulson, B.L., 1996. Tooth Analyses of Sources and Intensity of Lead Exposure in Children.
625 *Environ. Health Perspect.* **104**, 306-312.

626 Hassan, A.A., Hassan F.A., 1981. Source of galena in predynastic Egypt at Nagada.
627 *Archaeometry* **23**, 77-82.

628 Hoppe, K.A., Koch, P.L., Furutani, T.T., 2003. Assessing the Preservation of Biogenic
629 Strontium in Fossil Bones and Tooth Enamel. *Int. J. Osteoarchaeol.* **13**, 20–28.

630 Iñañez, J.G., Bellucci, J.J., Rodríguez-Alegría, E., Ash, R., McDonough, W., Speakman, R.J.,
631 2010. Romita pottery revisited: a reassessment of the provenance of ceramics from Colonial
632 Mexico by LA-MC-ICP-MS. *J. Archaeol. Sci*. **37**, 2698-2704.

633 Jenner, G.A., Longerich, H.P., Jackson, S.E., Fryer, B.J., 1990. ICP-MS - a powerful tool for
634 high-precision trace-element analysis in Earth sciences: evidence from analysis of selected
635 U.S.G.S. reference samples. *Chem. Geol.* **83**, 133-148.

636 Johnston, J.E., Franklin, M., Roh, H., Austin, C., Arora, M., 2019. Lead and Arsenic in Shed
637 Deciduous Teeth of Children Living Near a Lead-Acid Battery Smelter. *Environ. Sci. Tech*.
638 **53**, 6000−6006.

639 Kamenov, G.D., Lofaro, E.M., Goad, G., Krigbaum, J., 2018. Trace Elements in Modern and
640 Archaeological Human Teeth: Implications for Human Metal Exposure and Enamel
641 Diagenetic Changes. *J. Archaeol. Sci*. **99**, 27–34.

642 Knudson, K.J., 2008. Tiwanaku influence in the South Central Andes: strontium isotope
643 analysis and Middle Horizon migration. *Lat. Am. Antiq*. **19**, 3-23.

644 Koeman, E.C., Simonetti, A., Burns, P.C., 2015. Sourcing of Copper and Lead within Red
645 Inclusions from Trinitite Postdetonation Material. *Anal. Chem.* **87**, 5380−5386.

646 Koenig, E., Rogers, R.R., Trueman, C.N., 2009. Visualizing Fossilization Using Laser
647 Ablation–Inductively Coupled Plasma–Mass Spectrometry Maps of Trace Elements in Late
648 Cretaceous Bones. *Geology* **37**, 511–515.

649 Kohn, M.J., Moses, R.J., 2013. Trace Element Diffusivities in Bone Rule Out Simple Diffusive
650 Uptake During Fossilization but Explain In Vivo Uptake and Release. *Proc. Natl. Acad. Sci.*
651 *U.S.A.* **110**, 419–424.

652 Kohn, M.J., Schoeninger, M.J., Barker, W.W., 1999. Altered States: Effects of Diagenesis on
653 Fossil Tooth Chemistry. *Geochim. Cosmochim. Acta* **63**, 2737–2747.

654 Kumar, A., Rout, S., Narayanan, U., Mishra, M.K., Tripathi, R.M., Singh, J., Kumar, S.,
655 Kushwaha, H.S., 2011. Geochemical modelling of uranium speciation in the subsurface
656 aquatic environment of Punjab State in India. *J. Geol. Min. Res.* **3**, 137–146.

657 Küster, D., Liégeois, J.P., 2001. Sr, Nd isotopes and geochemistry of the Bayuda Desert high-
658 grade metamorphic-basement (Sudan): an early Pan-African oceanic convergent margin, not
659 the edge of the East Saharan ghost craton. *Precambrian Res.* **109**, 1-23.

660 Kyle, J.H., 1986. Effect of Post-burial Contamination on the Concentrations of Major and Minor
661 Elements in Human Bones and Teeth – the Implications for Palaeodietary Research. *J.*
662 *Archaeol. Sci*. **13**, 403–416.

663 Lee-Thorp, J., Sponheimer, M., 2003. Three Case Studies Used to Reassess the Reliability of
664 Fossil Bone and Enamel Isotope Signals for Paleodietary Studies. *J. Anthropol. Archaeol.* **22**,
665 208–216.

666 LeGeros, R., 1991. Calcium phosphates in enamel, dentine and bone. in: Myres, H, (Ed.),
667 Calcium Phosphates in Oral Biology. 15th ed. Basel: Karger, pp. 108–129.

668 Lopez, R.N., Segovia, N., Cisiega, M.G., Lopez, M.B.E., Armienta, M.A., Seidel, J.L., Pena, P.,
669 Godinez, L., Tamez, E., 2002. Determination of radon, major and trace elements in water
670 samples from springs and wells of northern Mexico State, Mexico. *Geofis. Int*. **41**, 407–414.

671 Manhes, G., Allègre, C.J., Dupré, B., Hamelin, B., 1980. Lead isotope study of basic ultrabasic
672 layered complexes: Speculations about the age of the Earth and primitive mantle
673 characteristics. *Earth Planet. Sci. Lett.* **47**, 370–382.

674 Maurer, A. F., Person, A., Tütken, T., Amblard-Pison, S., Ségalen L., 2014. Bone Diagenesis in
675 Arid Environments: An Intraskeletal Approach. *Palaeogeogr. Palaeoclimatol. Palaeoecol.*
676 **416**, 17–29.

677 McArthur J.M., Howarth R.J. and Shield G.A. 2012. Chapter 7: Strontium Isotope Stratigraphy.
678 In: The Geologic Time Scale, 2012. Gredstein FM, Ogg J.G., Schmotz M.D. and Ogg G.M.
679 Elsevier, Vol 1 of 2, 1144 pp.

680 Mirnejad, H., Simonetti, A., Molasalehi F., 2011. Pb isotopic compositions of some Zn–Pb
681 deposits and occurrences from Urumieh–Dokhtar and Sanandaj–Sirjan zones in Iran: *Ore*
682 *Geol. Rev.* **39**, 181–187.

683 Mirnejad, H., Simonetti A., Molasalehi F., 2015. Origin and formational history of some Pb-Zn
684 deposits from Alborz and Central Iran: Pb isotope constraints. *Int. Geol. Rev.* **57**, 463–471.

685 Montgomery, J., 2010. Passports from the Past: Investigating Human Dispersals Using
686 Strontium Isotope Analysis of Tooth Enamel. *Ann. Hum. Biol.* **37**, 325–346.

687 Nelson, B.K., Deniro, M.J., Schoeninger, M.J., DePaolo, D.J., Hare, P.E., 1986. Effects of
688 diagenesis on strontium, carbon, nitrogen, and oxygen concentration and isotopic
689 concentration of bone. *Geochim. Cosmochim. Acta* **50**, 1941-1949.

690 Nielsen-Marsh, C.M., Hedges, R.E.M., 2000. Patterns of Diagenesis in Bone I: The Effects of
691 Site Environments. *J. Archaeol. Sci*. **27**, 1139–1150.

692 Prohaska, T., Latkoczy, C., Schultheis, G., Teschler-Nicola, M., Stingeder, G., 2002.
693 Investigation of Sr Isotope Ratios in Prehistoric Human Bones and Teeth Using Laser
694 Ablation ICPMS and ICP-MS after Rb/Sr Separation. *J. Anal. At. Spectrom.* **17**, 887–891.

695 Purchase, N.G., Fergusson, J.E., 1986. Lead in teeth: The influence of the tooth type and the
696 sample within a tooth on lead levels. *Sci. Total Environ.* **52**, 239-250.

697 Retzmann, A., Budka, J., Sattmann, H., Irrgeher, J., Prohaska, T., 2019. The New kingdom
698 population on Sai Island: application of Sr isotopes to investigate cultural entanglement in
699 Ancient Nubia. *Ägypten und Levante/Egypt and the Levant* **29**, 355–380.

700 Rudnick, R.L., Fountain, D.M., 1995. Nature and composition of the continental crust: A lower
701 crustal perspective. *Rev. Geophys*. **33**, 267–309.

702 Rudnick, R.L., Gao S., 2014. Composition of the Continental Crust. Treatise on Geochemistry
703 (2nd edition). *Reference Module in Earth Systems and Environmental Sciences* **4**, 1-51.

704 Sangster, D.F., Outridge, P.M., Davis, W.J., 2000. Stable lead isotope characteristics of lead ore
705 deposits of environmental significance. *Environ. Rev.* **8**, 115–147.

706 Schrader, S.A., Buzon, M.R., Corcoran, L., Simonetti, A., 2019. Intraregional $^{87}Sr/^{86}Sr$
707 Variation in Nubia: New Insights from the Third Cataract. *J. Archaeol. Sci.: Rep.* **24**, 373–
708 379.

709 Schurr, M.R., Donohue, P.H., Simonetti, A., Dawson, E.L., 2018. Multi-element and lead
710 isotope characterization of early nineteenth century pottery sherds from Native American and
711 Euro-American sites. *J. Archaeol. Science: Rep*. **20**, 390–399.

712 Schweissing, M.M., Grupe, G., 2003. Stable strontium isotopes in human teeth and bone: a key
713 to migration events of the late Roman period in Bavaria. *J. Archaeol. Sci.* **30**, 1373-1383.

714 Shortland, A.J., 2006. Application of lead isotope analysis to a wide range of Late Bronze age
715 Egyptian Materials. *Archaeometry* **48**, 657–669.

716 Sillen, A., 1986. Biogenic and Diagenetic Sr/Ca in Plio-Pleistocene Fossils of the Omo
717 Shungura Formation. *Paleobiology* **12**, 311–323.

718 Simonetti, A., Gariepy, C., Banic, C., Tanabe, R., Wong, H., 2004. Pb isotopic investigation of
719 aircraft-sampled emissions from the Horne smelter (Rouyn, Quebec): implications for
720 atmospheric pollution in northeastern North America. *Geochim. Cosmochim. Acta* **68**, 3285–
721 3294.

722 Simons, T.J., 1986. Cellular interactions between lead and calcium. *Br. Med. Bull.* **42**, 431-434.

723 Simpson, R., Cooper, D.M.L., Swanston, T., Coulthard, I., Varney, T.L., 2021. Historical
724 overview and new directions in bioarchaeological trace element analysis: a review. *Archaeol.*
725 *Anthropol. Sci*., https://doi.org/10.1007/s12520-020-01262-4.

726 Slovak, N.M., Paytan, A., 2012. Applications of Sr Isotopes in Archaeology, 743–768, in:
727 Baskaran, M. (Ed.), Handbook of Environmental Isotope Geochemistry, Vol. I, Berlin,
728 Heidelberg.

729 Slovak, N.M., Paytan, A., Wiegand, B.A., 2009. Reconstructing Middle Horizon mobility
730 patterns on the coast of Peru through strontium isotope analysis. *J. Archaeol. Sci.* **36**, 157-
731 165.

732 Smith, S.T., 2018. Gift of the Nile? Climate change, the origins of Egyptian civilization and its
733 interactions within Northeast Africa. in: Bács, T.A., Bollók, Á., Vida, T. (Eds.), Across the
734 Mediterranean--Along the Nile: Studies in Egyptology, Nubiology and Late Antiquity
735 Dedicated to László Török on the Occasion of His 75th Birthday, v. 1. Budapest: Institute of
736 Archaeology, Research Centre for the Humanities, Hungarian Academy of Sciences and
737 Museum of Fine Arts, pp. 325-345.

738 Sponheimer, M., Lee-Thorp, J.A., 2006. Enamel Diagenesis at South African Australopith Sites:
739 Implications for Paleoecological Reconstruction with Trace Elements. *Geochim. Cosmochim.*
740 *Acta* **70**, 1644–1654.

741 Stacey, J.S., Kramers, J.D., 1975. Approximation of terrestrial lead isotope evolution by a two-
742 stage model. *Earth Planet. Sci. Lett.* **26**, 207-22.

743 Steele, D.G., Bramblett, C.A., 1988. The Anatomy and Biology of the Human Skeleton. Texas
744 A&M University, College Station, TX.

745 Stós-Gale, Z.A., Gale, N.H., 1981. Sources of Galena, lead and silver in predynastic Egypt. In:
746 Revue d'Archéométrie, n°1, 1981. Actes du XXe symposium international d'archéométrie,
747 Paris 26-29 mars 1980 Volume III, 285-296.

748 Szostek, K., Mądrzyk, K., Cienkosz-Stepańczak, B., 2015. Strontium Isotopes as an Indicator of
749 Human Migration– Easy Questions, Difficult Answers. *Anthropol. Rev*. **78**, 133–156.

750 Trueman, C.N., Palmer, M.R., Field, J., Privat, K., Ludgate, N., Chavagnac, V., Eberth, D.A.,
751 Cifelli, R., Rogers, R.R., 2008. Comparing Rates of Recrystallisation and the Potential for
752 Preservation of Biomolecules from the Distribution of Trace Elements in Fossil Bones. *C. R.*
753 *Palevol* **7**, 145–158.

754 Turner, B.L., Kamenov, G.D., Kingston, J.D., Armelagos, G.J., 2009. Insights into immigration
755 and social class at Machu Picchu, Peru based on oxygen, strontium, and lead isotopic
756 analysis. *J. Archaeol. Sci.* **36**, 317-332.

757 Vongunten, H.R., Benes P., 1995. Speciation of radionuclides in the environment. *Radiochim.*
758 *Acta* **69**, 1–29.

759 Welsby, D.A., 2002. The medieval kingdoms of Nubia: pagans, Christians and Muslims along
760 the Middle Nile. London: British Museum Press.

761 Willmes, M., Kinsley, L., Moncel, M.H., Armstrong, R.A., Aubert, M., Eggins, S., Grün, R.,
762 2016. Improvement of Laser Ablation In Situ Micro-analysis to Identify Diagenetic
763 Alteration and Measure Strontium Isotope Ratios in Fossil Human Teeth. *J. Archaeol. Sci.*
764 **70**, 102–116.

765 Wychowanski, P., Malkiewicz, K., 2017. Evaluation of Metal Ion Concentration in Hard
766 Tissues of Teeth in Residents of Central Poland. *BioMed Res. Int. 2017,* 6419709.
767 https://doi.org/10.1155/2017/6419709

768

FIGURE CAPTIONS

Fig. 1. Map illustrating the regional geology of northeastern Sudan, which outlines the cratonic crust with Neoproterozoic deformation referred to as the Saharan Metacraton (SMC, red areas), and Neoproterozoic juvenile crust of the Arabian Nubian Shield (ANS, green area). Also shown are the locations of burial site at El-Kurru (present study) and the archaeological site of Tombos, both along the Nile River. Dashed line labeled KKSS = Keraf Kabus Sekerr Suture zone between ANS and SMC crustal provinces. Map is modified after Evuk et al. (2017).

Fig. 2. Bivariate plots displaying the concentrations (all expressed in ppm) of Sr versus those for (A) Mg, (B) Ba, and (C) U, and U compared to those for (D) Mn, (E) Ba, and (F) Pb for samples of tooth enamel from El-Kurru examined in this study. Red and black solid circles represent samples of tooth enamel with high and low $^{87}Sr/^{86}Sr$ as defined in Fig. 3 and detailed in text.

Fig. 3. Diagram illustrates the Sr contents (ppm) versus their corresponding Sr isotope compositions for the samples of tooth enamel from El-Kurru investigated here. The samples define two groups relative to their $^{87}Sr/^{86}Sr$ ratios, those with higher (red) compared to those with lower (black) signatures~~values~~. The shaded region represents the range of Sr abundances considered to represent unaltered, pristine tooth enamel (100 to 250 ppm; Dudás et al. 2016). Numbers adjacent to data points refer to corresponding sample numbers (Tables 1, 2 and 3). Associated uncertainties for both Sr contents and isotope compositions are within the size of the symbol.

Fig. 4. Plots of $^{206}Pb/^{204}Pb$ versus (A) $^{207}Pb/^{204}Pb$ and (B) $^{208}Pb/^{204}Pb$ for samples of tooth enamel from El-Kurru examined here (with the exception of sample KUR-4 in order to

maximize scaling). These are compared to Pb isotope compositions (from Evuk et al., 2017) for samples of juvenile Neoproterozoic crust from the neighboring Arabian Nubian Shield (+, green field) and the Neoproterozoic Saharan Metacraton (*, red field; areas shown in Fig. 2). Also shown is the Pb isotopic evolution curve for average continental crust (S/K; Stacey and Kramers, 1975). Red and black solid circles refer to group designation based on their corresponding Sr isotope compositions (Fig. 3). In (A) El-Kurru samples define a best-fit linear regression line with a slope that corresponds to a secondary isochron age of approximately 700 million years (Ma), which is similar to the age of the surrounding basement rocks of the ANS and SMC. Associated uncertainties are within the size of the symbol.

Fig. 5. Diagrams illustrate U/Pb ratios versus (A) $^{87}Sr/^{86}Sr$ and (B) $^{206}Pb/^{204}Pb$ for samples of tooth enamel from El-Kurru examined here. Red and black solid circles refer to group designation based on their corresponding Sr isotope compositions (Fig. 3) and numbers refer to sample numbers (Tables 1, 2 and 3). The data point corresponding to sample KURur-4 is not shown for scaling purposes due to its extremely radiogenic Pb isotope composition ($^{206}Pb/^{204}Pb$ = 56.351; Table 3). Associated uncertainties are within the size of the symbol.

Fig. 6. Plots of $^{207}Pb/^{206}Pb$ versus (A) $^{208}Pb/^{206}Pb$ and (B) $^{208}Pb/^{207}Pb$ for samples of tooth enamel from El-Kurru examined here (solid red circles). These are compared to the Pb isotope compositions for a variety of archaeological samples (lead ores, kohls, lead metal, copper alloys, glass, glaze and pigment) within Egypt (Stós-Gale and Gale, 1981; Hassan and Hassan, 1981; Shortland et al., 2006), and those modern-day atmospheric aerosols (**X**= Cairo; += Israel, Lebanon) sampled within the Middle Eastern region (Bollhofer and Rossman, 2000). Solid green square represents the present-day (0 million years, Ma) Pb isotope

composition of average continental crust (Stacey and Kramers, 1975). Solid green circle and diamond = average Pb isotope compositions of Neoproterozoic metamorphic rocks from SMC and ANS (shown in Fig. 4), respectively; both are calculated using data from Evuk et al. (2017). Of note, the Pb isotope compositions for sample KUR-4, which are significantly more radiogenic signatures (Table 3), are not illustrated for scaling purposes. Abbreviation Precamb. = Precambrian period (older than 541 million years) and Miocene epoch = 23.03 to 5.3 million years ago. Associated uncertainties are within the size of the symbol.

Fig. 7. Plan of the Medieval cemetery at El-Kurru archaeological site showing its position relative to the modern irrigation channel, the brick wall gateway, and later mud-brick domestic architecture adjacent to it (after Dann et al. 2016). The numbers adjacent to red and black solid circles (based on Sr isotope compositions), which indicate position of skeletal remains within cemetery, correspond to sample numbers (Tables 1, 2 and 3). Also shown are their Pb contents (ppm, purple text). Empty circles represent locations of skeletal remains not investigated here.

Table 1. Information for tooth enamel samples from El-Kurru investigated here.

Sample #	Tooth	Sex Estimation	Age Estimation (in years)	Median Burial Elevation (meters)
KUR-01	PM	Probable Female	Adolescent (15 +/-3)	248.74
KUR-02	M1	Indeterminate	Child (3 +/-1)	249.35
KUR-03	PM^2	Male	Young Adult (20-35)	248.89
KUR-04	PM_2	Indeterminate	Adolescent (15 +/-3)	248.80
KUR-05	PM	Indeterminate	Middle Adult (36-50)	248.82
KUR-06	PM_1	Indeterminate	Child (7-9)	249.02
KUR-07	PM	Probable Female	Older Adult (50+)	249.06
KUR-08	PM	Male	Young Adult (20-35)	249.10
KUR-09	PM^1	Female	Young Adult (20-35)	248.85
KUR-10	PM_1	Indeterminate	Older Adult (50+)	n.d.
KUR-11	PM_2	Probable Male	Older Adult (50+)	248.85
KUR-12	dm_1	Indeterminate	Child (4.5)	249.39
KUR-13	M^1	Indeterminate	Child (7.5)	249.11
KUR-14	M_3	Probable Female	Middle Adult (36-50)	248.84
KUR-15	PM_x	Male	Older Adult (50+)	249.29
KUR-16	dm_1	Indeterminate	Child (3.5)	249.40
KUR-17	PM_1	Indeterminate	Adolescent (17.5)	248.93
KUR-18	dm_1	Indeterminate	Child (5.5+)	249.31

M=unspecified molar; PM= premolar; M_3= third molar; dm_1= first deciduous molar; PM_1= first premolar; PM_2= second premolar. n.d. = not determined

Table 2. Trace element concentrations (ppm) and enrichments factors for Pb, U, Sr, and Mn for samples of tooth enamel from El-Kurru in this study.

Sample	Mg	Mn	Fe	Sr	Ba	Nd	Pb	U	U/Pb	EF_{Pb}	EF_{U}	EF_{Sr}	EF_{Mn}
KUR-1	2276	3.53	286	188	10	0.07	0.16	0.18	1.12	0.06	0.45	3.85	0.03
KUR-2	2148	21.52	436	245	36	0.19	1.28	0.30	0.23	0.52	0.77	5.33	0.19
KUR-3	2215	34.34	400	343	80	0.38	9.58	1.52	0.16	3.80	3.79	7.24	0.30
KUR-4	2289	2.52	302	172	6	0.13	0.11	0.07	0.58	0.04	0.16	3.51	0.02
KUR-5	973	11.76	141	106	19	0.06	0.23	0.20	0.86	0.21	1.12	5.12	0.23
KUR-6	2627	13.02	325	221	16	0.09	0.71	0.16	0.23	0.24	0.34	3.93	0.10
KUR-7	2942	13.85	565	398	52	0.35	0.85	0.21	0.25	0.25	0.40	6.33	0.09
KUR-8	2513	20.19	352	188	19	1.15	0.33	0.08	0.24	0.11	0.17	3.50	0.16
KUR-9	2605	7.09	338	256	36	0.18	0.43	0.42	0.97	0.15	0.89	4.59	0.05
KUR-10	3181	8.35	391	236	27	0.28	0.97	0.32	0.33	0.27	0.55	3.47	0.05
KUR-11	2629	41.77	509	225	15	0.50	61.95	0.34	0.01	20.7	0.71	4.00	0.31
KUR-12	2675	29.20	368	291	81	0.38	22.47	1.30	0.06	7.4	2.69	5.08	0.21
KUR-13	2507	9.09	317	115	10	0.90	3.17	0.12	0.04	1.11	0.26	2.15	0.07
KUR-14	2485	17.18	369	425	73	0.22	0.63	0.47	0.75	0.22	1.05	7.99	0.13
KUR-15	2695	41.23	393	286	25	0.76	0.29	0.35	1.20	0.10	0.72	4.96	0.30
KUR-16	2537	66.23	440	290	82	0.32	2.89	1.40	0.48	1.00	3.06	5.35	0.50
KUR-17	2621	9.26	278	181	14	0.10	2.60	0.11	0.04	0.87	0.24	3.22	0.07
KUR-18	2256	23.76	322	169	33	0.31	7.73	0.71	0.09	3.01	1.75	3.51	0.20

The 2σ level relative standard deviation (RSD% = standard deviation / average concentration x 2 x 100) is a function of absolute elemental concentration, and thus varies between ~2.5 and ~6.0% for the more abundant elements (Mg, Mn, Fe, Sr, Ba) and between ~15 and ~46% for Nd, Pb, and U (<< 1 ppm).

Table 3. Sr and Pb isotope compositions for samples of tooth enamel from El-Kurru.

Sample #	$^{87}Sr/^{86}Sr$	$^{206}Pb/^{204}Pb$	$^{207}Pb/^{204}Pb$	$^{208}Pb/^{204}Pb$	$^{208}Pb/^{206}Pb$	$^{207}Pb/^{206}Pb$	$^{208}Pb/^{207}Pb$
KUR-1	0.70748(1)	23.081(21)	15.934(2)	38.609(4)	1.6728(16)	0.6904(6)	2.4230(6)
KUR-2	0.70772(2)	19.503(1)	15.741(1)	38.501(2)	1.9741(2)	0.8071(1)	2.4459(1)
KUR-3	0.70799(1)	18.308(1)	15.643(1)	38.384(2)	2.0965(1)	0.8544(1)	2.4537(1)
KUR-4	0.70694(1)	56.351(.98)	18.060(.87)	37.917(.5)	0.6826(.1)	0.3176(.04)	2.0995(.05)
KUR-5	0.70712(1)	19.799(1)	15.757(1)	38.503(1)	1.9448(1)	0.7958(1)	2.4436(1)
KUR-6	0.70668(2)	18.496(1)	15.672(1)	38.477(1)	2.0803(1)	0.8473(1)	2.4551(1)
KUR-7	0.70831(2)	19.056(3)	15.721(1)	38.479(1)	2.0192(4)	0.8250(2)	2.4476(2)
KUR-8	0.70812(1)	19.001(1)	15.693(1)	38.530(2)	2.0278(1)	0.8259(1)	2.4552(1)
KUR-9	0.70670(2)	19.748(2)	15.747(1)	38.516(2)	1.9504(2)	0.7974(1)	2.4460(1)
KUR-10	0.70696(1)	20.503(1)	15.806(1)	38.483(1)	1.8769(1)	0.7709(1)	2.4347(1)
KUR-11	0.70768(1)	18.715(1)	15.704(1)	38.481(2)	2.0561(1)	0.8391(1)	2.4504(1)
KUR-12	0.70772(1)	18.338(1)	15.688(1)	38.538(1)	2.1015(1)	0.8555(1)	2.4566(1)
KUR-13	0.70688(1)	18.812(1)	15.702(1)	38.460(1)	2.0444(1)	0.8347(1)	2.4493(1)
KUR-14	0.70678(1)	19.077(1)	15.715(1)	38.508(2)	2.0186(1)	0.8238(1)	2.4504(1)
KUR-15	0.70663(1)	22.464(15)	15.987(1)	38.531(3)	1.7150(12)	0.7116(4)	2.4102(4)
KUR-16	0.70678(1)	18.369(1)	15.692(1)	38.561(2)	2.0993(1)	0.8543(1)	2.4574(1)
KUR-17	0.70679(1)	18.511(1)	15.664(1)	38.412(2)	2.0751(1)	0.8462(1)	2.4522(1)
KUR-18	0.70677(1)	18.292(1)	15.676(1)	38.443(2)	2.1017(1)	0.8570(1)	2.4523(1)

Number in parenthesis represents uncertainty (2σ level) in the last digits reported except for sample Kur-4.

Figure

Click here to access/download;Figure;Figure_1_v4.jpg

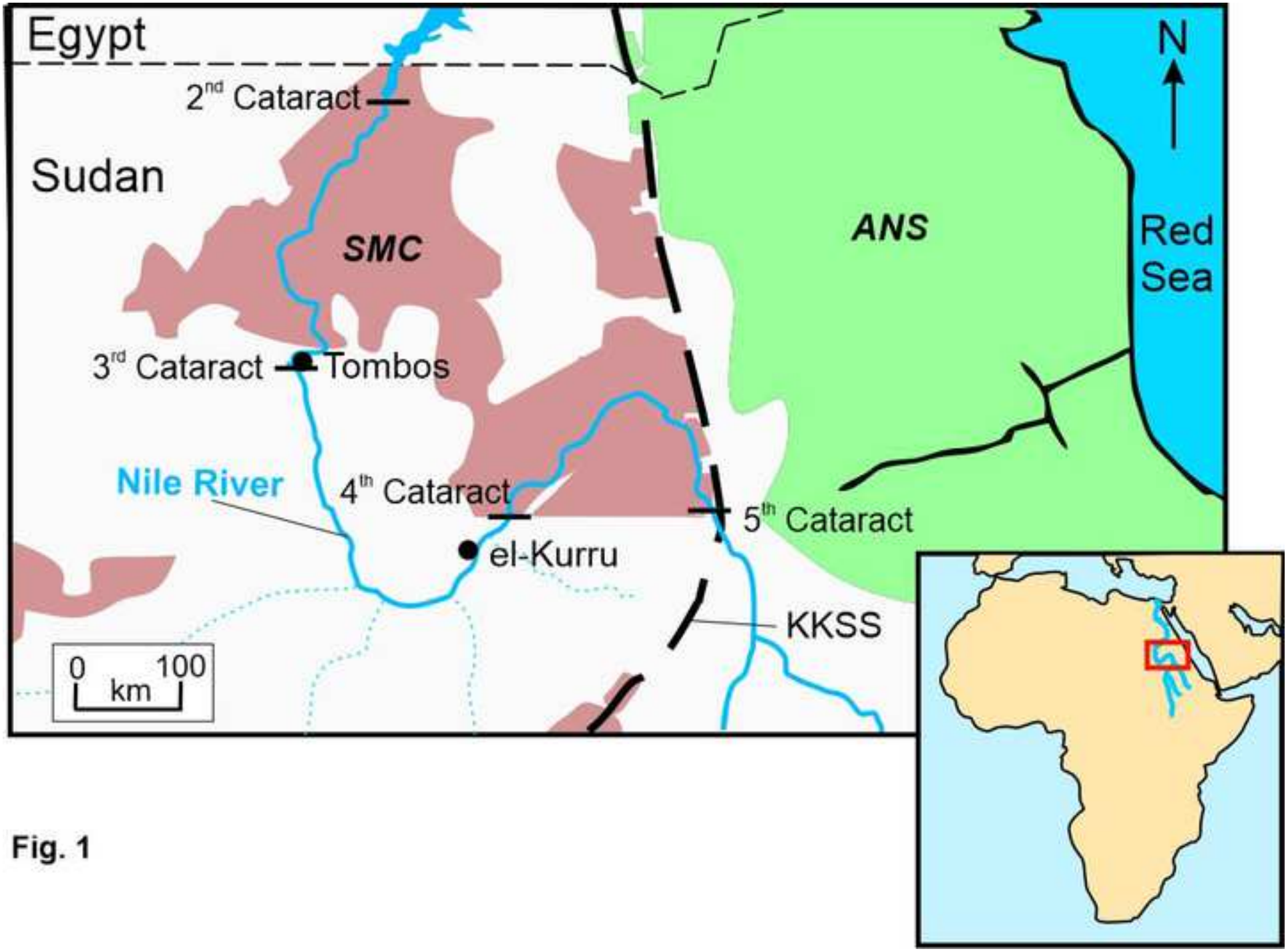

Fig. 1

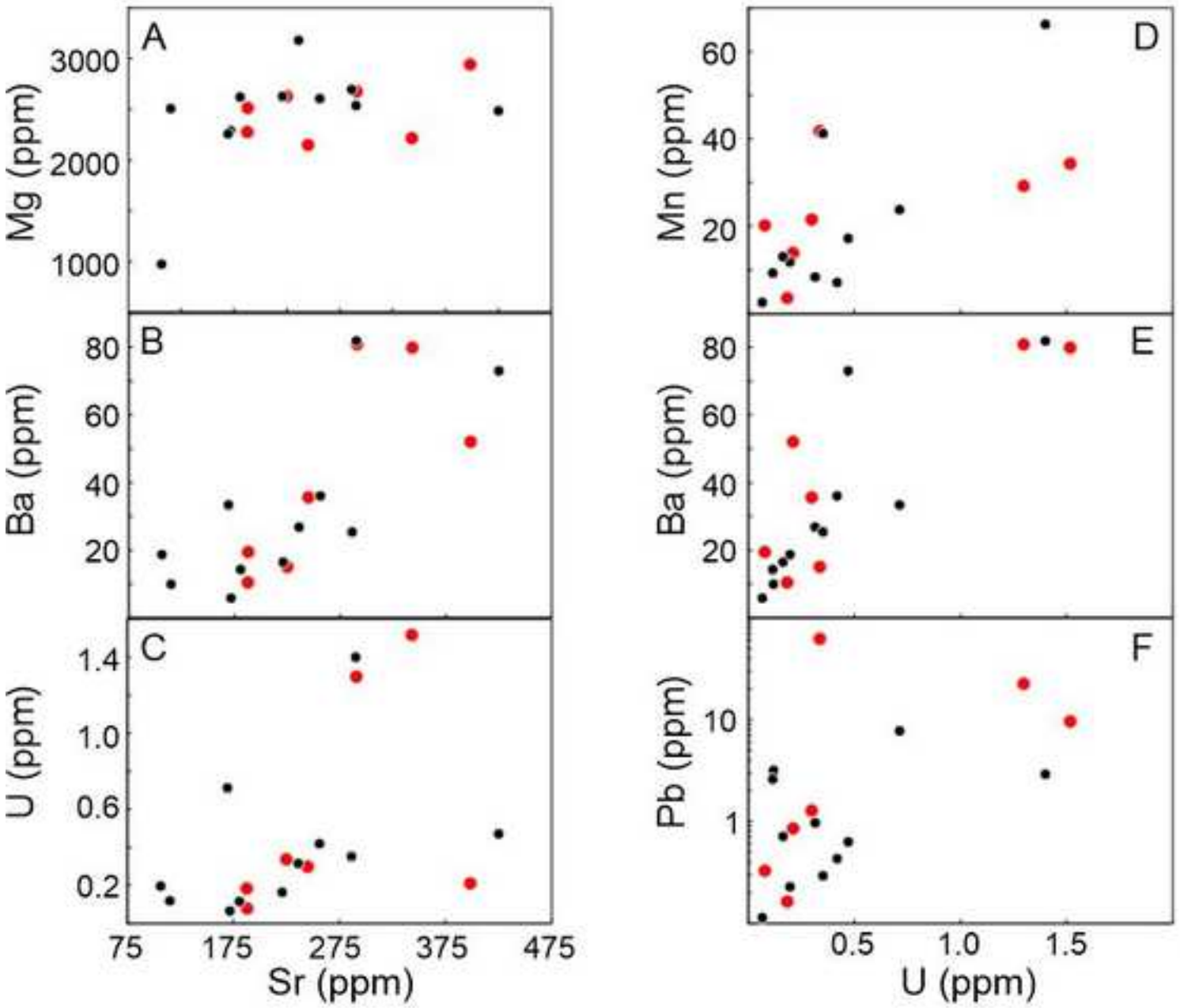

Fig. 2.

Figure

Click here to access/download;Figure;Figure_3_new.jpg

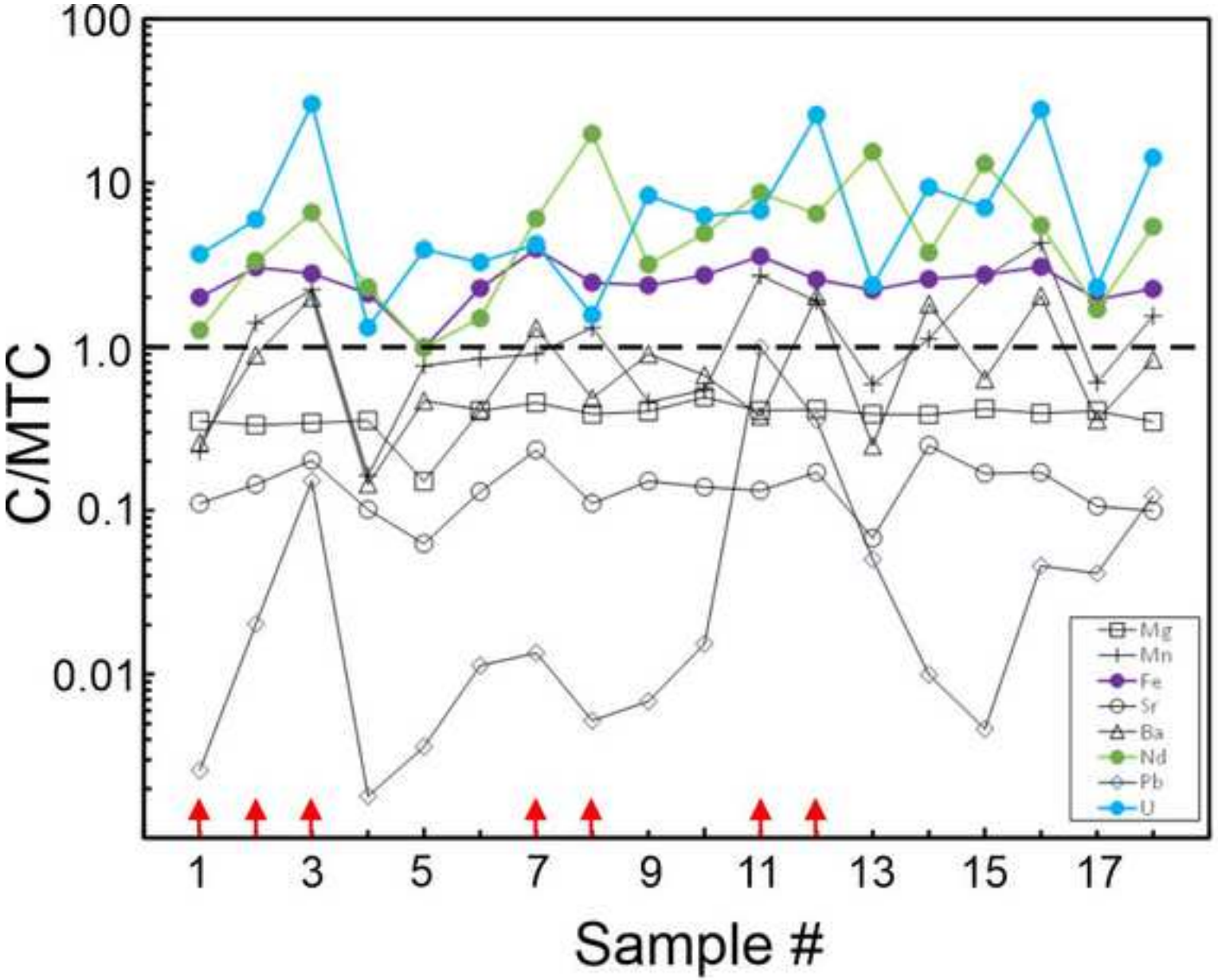

Fig. 3

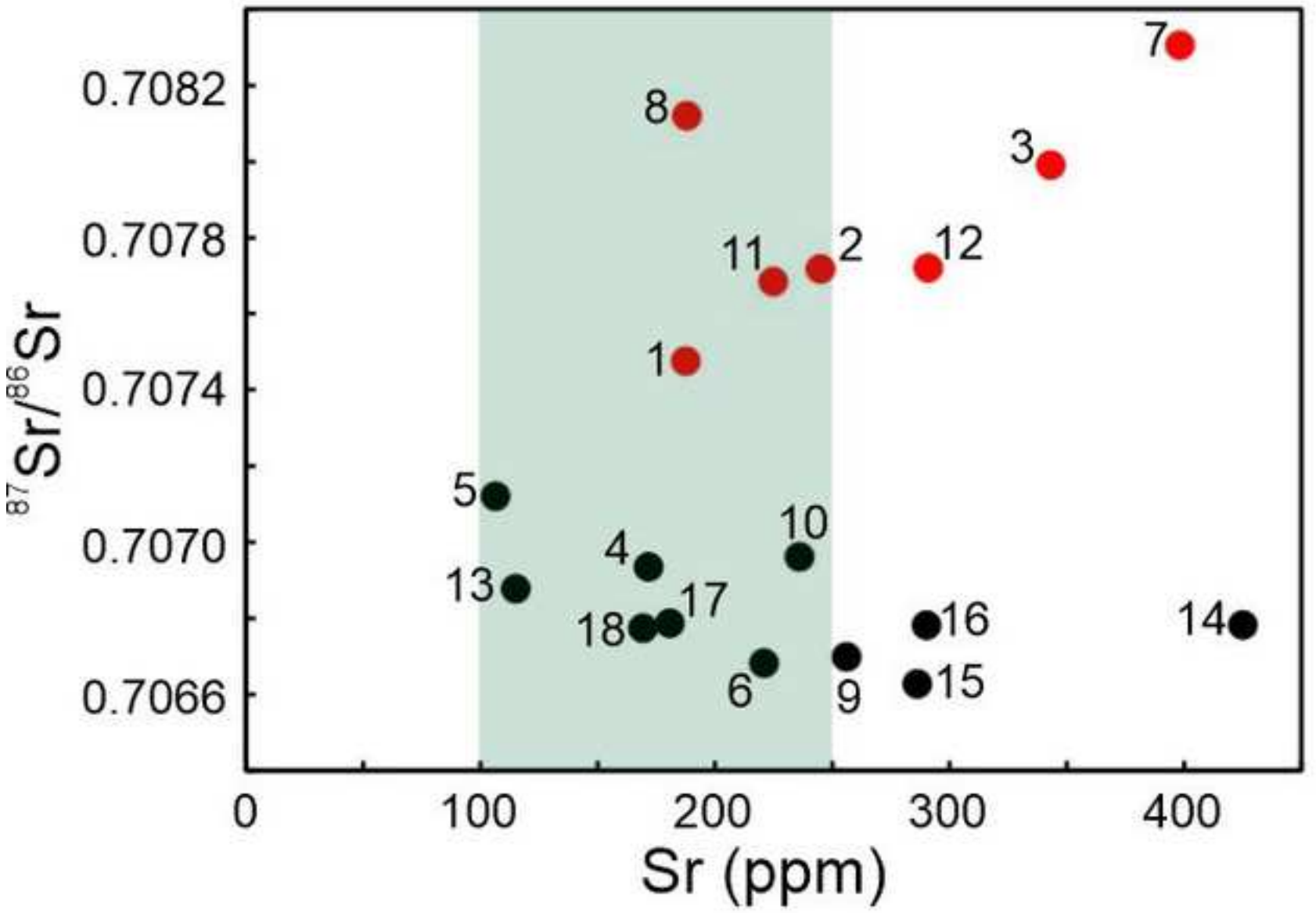

Fig. 4.

Figure

Click here to access/download;Figure;Figure_5_new.jpg

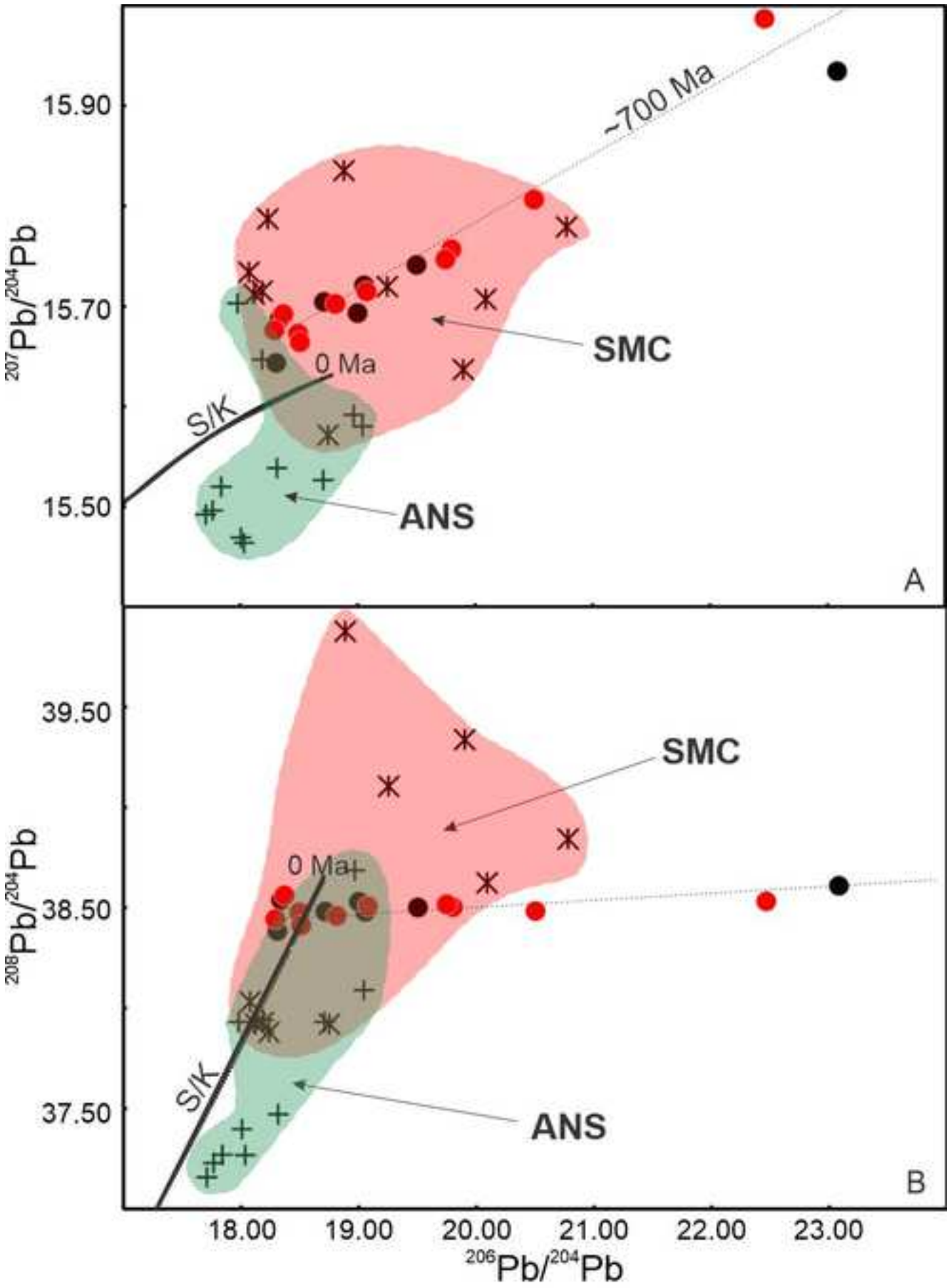

Fig. 5.

Figure

Click here to access/download;Figure;Figure_6_new.jpg

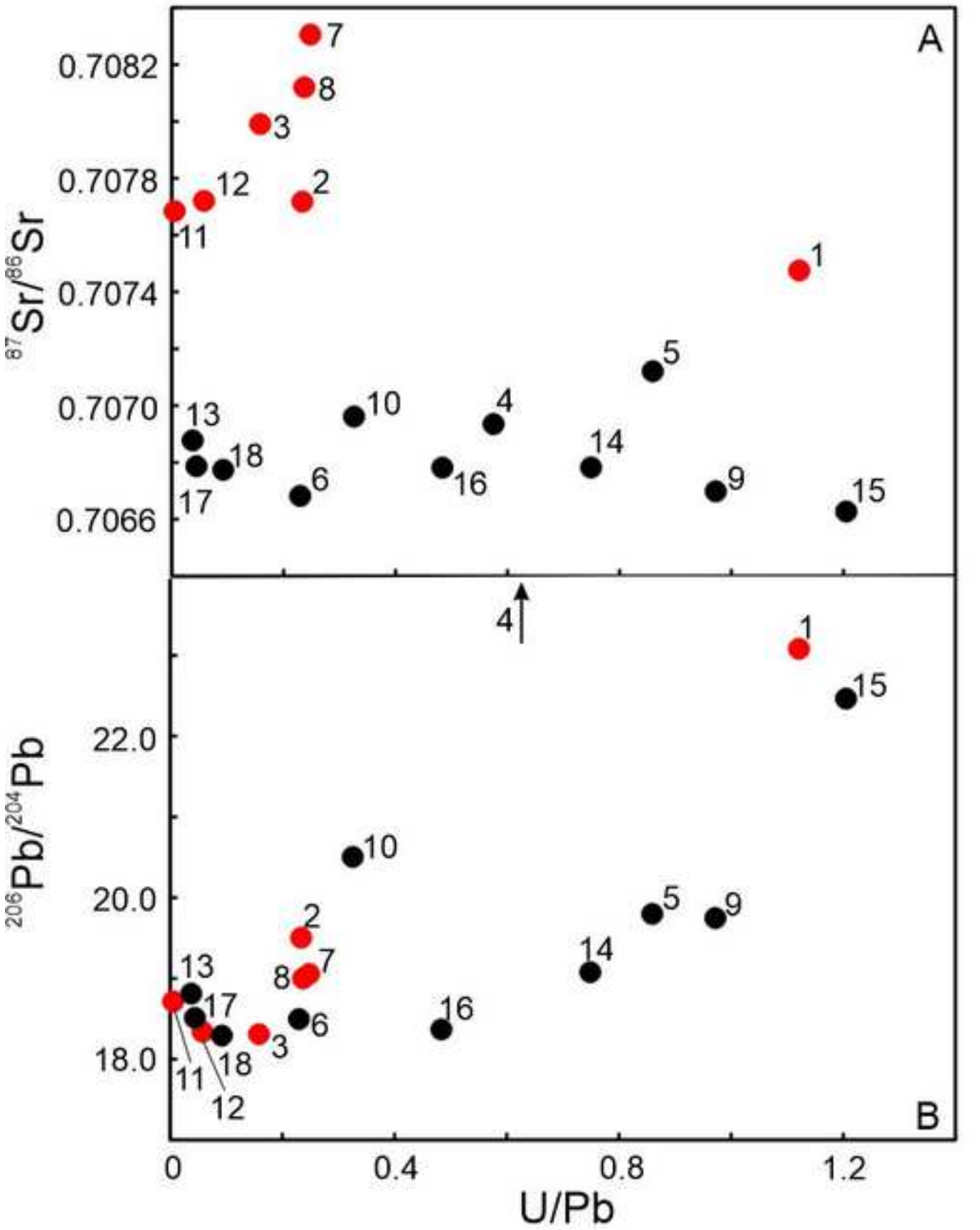

Fig. 6.

Figure

Click here to access/download;Figure;Figure_7_new.jpg

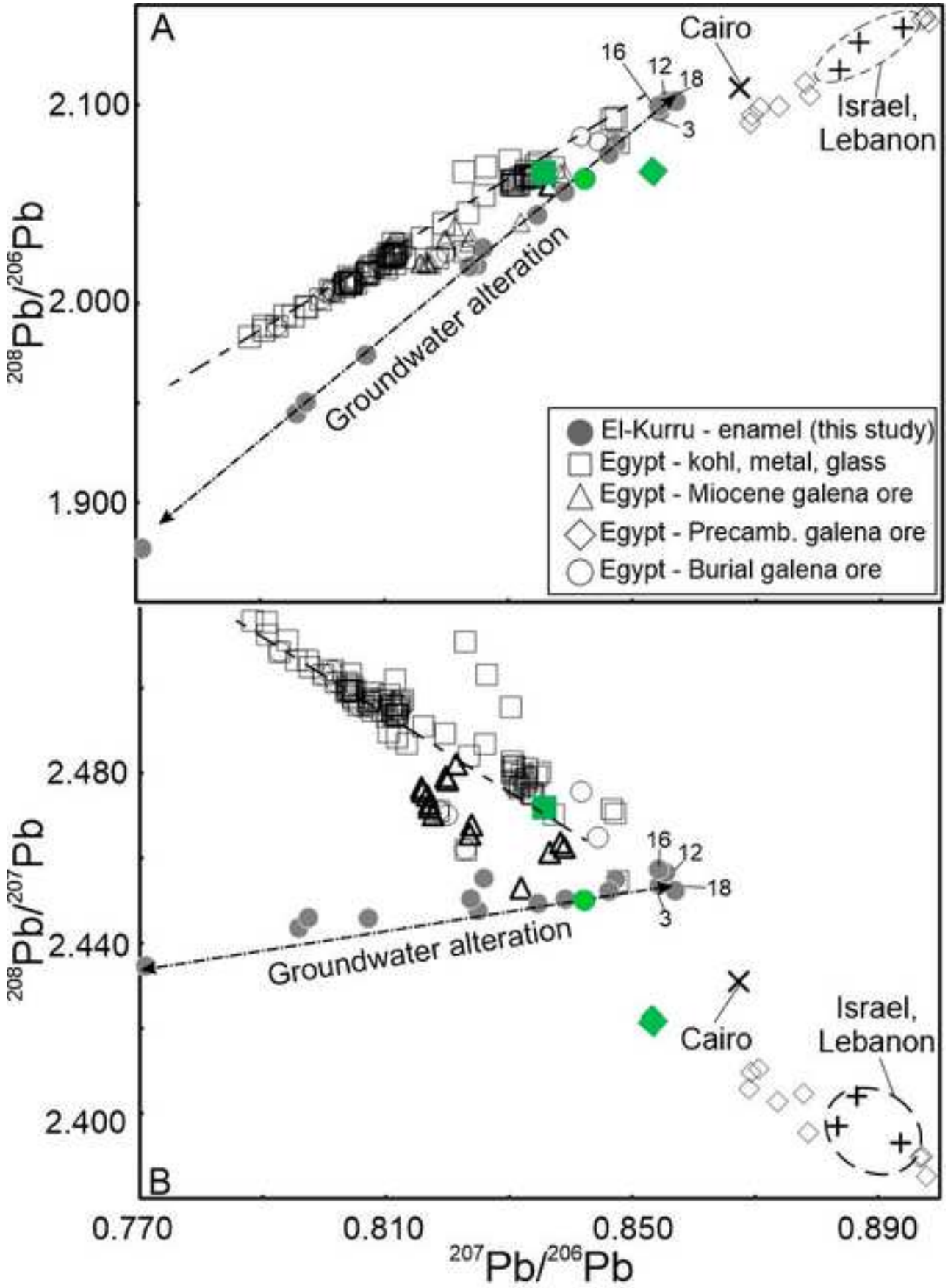

Fig. 7.

Figure

Click here to access/download;Figure;Figure_8_new.jpg

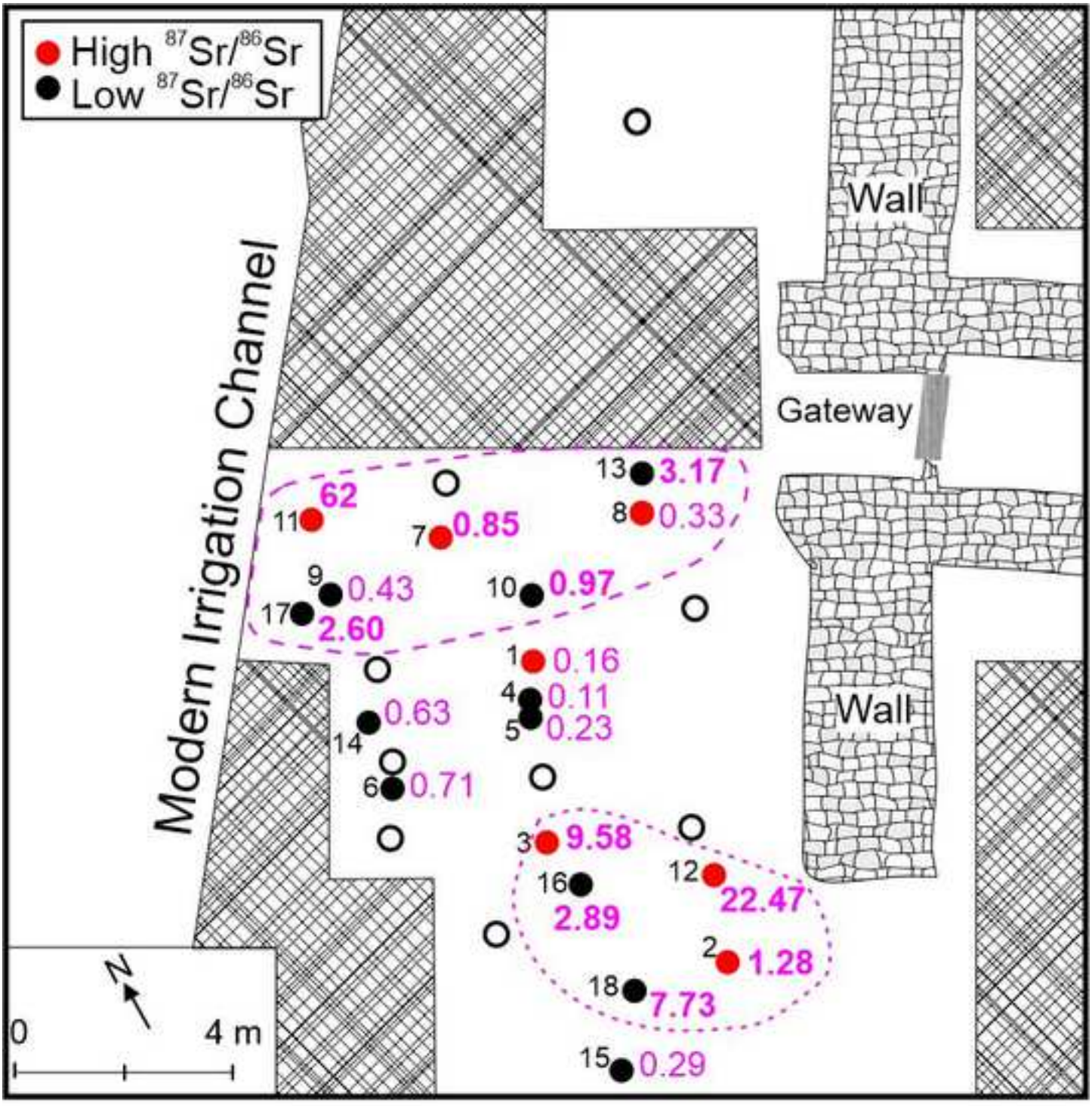

Fig. 8.

Declaration of interests

☒ The authors declare that they have no known competing financial interests or personal relationships that could have appeared to influence the work reported in this paper.

☐The authors declare the following financial interests/personal relationships which may be considered as potential competing interests:
